Rap1 is a main regulator of Adherens junction remodelling in the fly retina

Zile Mubarik Burki

A thesis submitted for the degree of

Doctor of Philosophy

University College London

2017

Supervised by Professor Franck Pichaud

MRC Laboratory for Molecular Cell Biology

University College London

Declaration

I, Mubarik Burki confirm that the work presented in this thesis is my own. Where information has been derived from other sources, I confirm that this has been indicated in the thesis.

Signed……..

Abstract

During epithelial cell polarisation, the conserved apical and lateral polarity proteins set up the position of the *Zonula Adherens (ZA)*, which consists of a circumferential belt of *Adherens Junction (AJ)* material, and thus define the apical and lateral domains of the cell. During my thesis, I have tried to uncover the genes that are involved in the transcriptional control of polarity remodelling and *ZA* morphogenesis during development. To this end, I used the genetically amenable *Drosophila* retina to carry out transcriptional profiling at the onset of photoreceptor polarity remodelling. With this approach, I was able to uncover several genes that seem to be regulated during polarity remodelling, including the zinc finger transcription factor *ovo*, which might regulate photoreceptor morphogenesis through regulation of the actin cytoskeleton. In addition to the transcriptional control of epithelial polarity, I made use of the fly photoreceptor to uncover new cellular and molecular pathways that promote *AJ* morphogenesis during *ZA* assembly. Using a candidate-based approach, I identified the small GTPase protein Rap1 as an important regulator of *AJ* morphogenesis, through stabilisation of DE-Cad at the developing *ZA*. In this context, I found that *rap1* functions with the p21-activated kinase *pak4* to promote *AJ* material accumulation at the developing *ZA*. Finally, in order to discover new genes and mechanisms that might link *rap1* to the epithelial gene network, I made use of *rap1* RNAi, to conduct a large-scale genetic modifier screen. This genetic screen led to the identification of several ubiquitin-related genes that genetically interact with *rap1* and therefore might be involved in *rap1*-dependent polarity remodelling and *ZA* morphogenesis.

Acknowledgements

I would first like to express my gratitude to my supervisor Franck, for all the support, patience and advice he gave me throughout the last three years. Without his exceptional attention to detail, guidance and constant feedback this PhD would not have been possible.

I would like to say thanks to Laura and Evi for their invaluable feedback on my thesis. I am also very grateful to Chiara, who has always been extremely supportive of my work and future plans.

I would also like to say a heartfelt thank you to Abi, Ami and Bhai for always believing in me and encouraging me to follow my dreams and aspirations. And finally to my Husband Janana, who has been by my side throughout this PhD, with whom I have celebrated every little success and complained about every single disappointment.

I stumbled across a quote recently that I feel perfectly explains why I enjoy Science and probably why I joined Franck's lab:

"I am terribly fascinated with things that I don't understand" (Richard Saul Wurman).

Hopefully, I know more about apical-basal polarity than I did three years ago.

Table of Contents

Table of figures

List of tables

Abbreviations

A - Anterior

AJ – Adherens Junction

A/P – Anteroposterior

AEL – After Egg Laying

APF – After Puparium Formation

aPKC – Atypical Protein Kinase C

Arm – Armadillo

Arp2/3 – Actin-Related Proteins 2/3

Baz – Bazooka

Cat – Catenin

Cdc42 – Cell division cycle 42

Cno - Canoe

Crb – Crumb

D - Dorsal

DE-Cad – *Drosophila* Epithelial Cadherin

Ds – Desmosomes

Dia – Diaphanous

DN – Dominant Negative

Drak – Death associated protein kinase

Dzy - Dizzy

E-Cad – Epithelial Cadherin

ECM – extracellular matrix

Ed – Echinoid

EM – Electron Microscopy

EMT – Epithelial to Mesenchyme Transition

ER – Endoplasmic Reticulum

F-actin – Filamentous actin

GAP – GTPase Activating Protein

GDP – Guanosine Diphosphate

GEF – Guanine Nucleotide Exchange Factor

GFP - Green Fluorescent Protein

GoF – Gain of Function

GTP - Guanosine Triphosphate

HEK293 – Human Embryonic Kidney 293

IR – Ionising Radiation

MCF7 – Michigan Cancer Foundation 7

MDCK – Madine-Darnby Canine Kidney

MET – Mesenchyme to Epithelial Transition

MF – Morphogenetic Furrow

MLCK – Myosin Light Chain Kinase

MRLC – Myosin Regulatory Light Chain

MT – Microtubule

Myo II – Myosin II

M/Z – Maternal/Zygotic

N17 – Dominant Negative

P - Posterior

PAK – Polo Associated Kinase

Par – Partitioning defective protein

PATJ – Protein Associated with Tight Junction

PM – Plasma Membrane

Pnt – Pointed

PR – Photoreceptor

RA – Ras Association

Rap1 - Ras Associated Protein 1

ROCK – Rho kinase

Scrib – Scribble

SJ – Septate Junction

Spot Adherens Junctions – sAJs

Std - Stardust

Sqh – Spaghetti Squash

TF – Transcription Factor

V – Ventral

V12 – Constitutively active

ZA - Zonula Adherens

Chapter 1. Introduction

One of the most prominent questions in biology concerns how cells form and interact with each other to make multicellular organisms. Epithelial cells are a highly abundant and conserved cell type, which give rise to a variety of organs. The evolutionarily conserved appearance of epithelial cells reflects the requirement of tissues to be able to separate the inside of the cell from the external environment (Cereijido et al. 2004). Epithelial cells are polarised along the apical (top) and basal (bottom) axis. Establishment of epithelial apical-basal polarity is a prerequisite for the formation of cell-cell contacts, which allow tissue morphogenesis and directional transport of ions and solutes across the epithelium. Several polarity regulators function together to set up the apical domain facing the external environment or a lumen and the basolateral domain in contact with the neighbouring cells or basal substratum (**Figure 1.1)**.

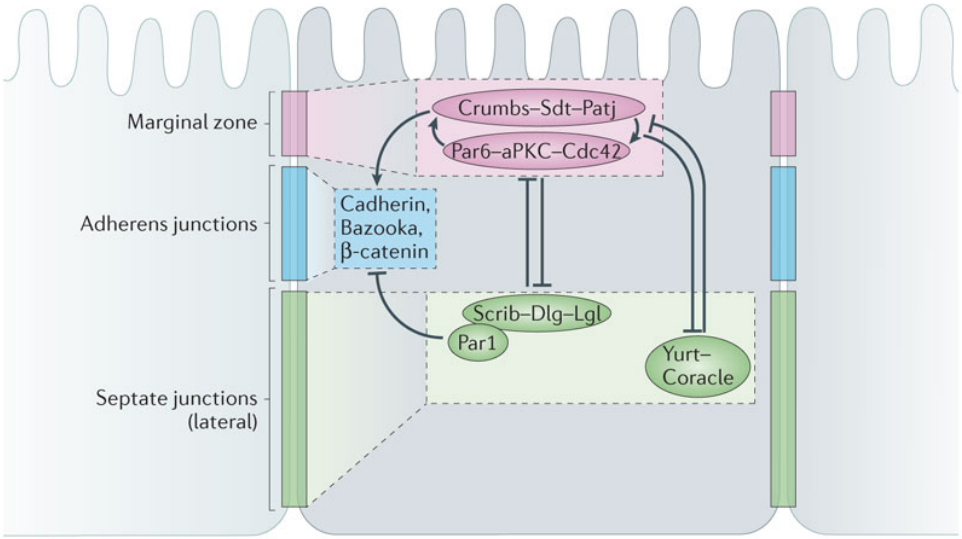

Figure 1.1: Epithelial apical-basal polarity in *Drosophila*. Diagram representing key components of the apical-basal polarity network, which establish the distinct compartments that constitute epithelial cells. The apical-most region is known as the *Marginal Zone*, which contains the apical complexes Crb-Sdt-PatJ and the Cdc42-Par6-aPKC module. Cell-cell contacts known as the *Zonula Adherens (ZA)* are formed in a region below the *Marginal Zone*. The *ZA* forms a belt of *Adherens Junction* material, including E-Cadherin and Catenins around the circumference of the epithelial cell, allowing cells to form an epithelial sheet. Septate junctions are found basal to the *ZA* and contain the Scrib-Dlg-Lgl complex, the Yurt-Cora complex and Par1. Image from (Thompson et al. 2013).

In addition, cell-cell contacts ensure the close adhesion between cells and provide the barrier function characteristic of epithelial cells (Tepass et al. 2001). In epithelial cells, these cell-cell contacts are known as *Adherens Junctions (AJs),* which were first identified as electron dense structures located at the apical end of the lateral membrane at the interface between cells (Farquhar and Palade 1963; Harris and Tepass 2010). *Zonula Adherens (ZA)* are a prominent example of *AJs* that occur in most epithelial cell types (**Figure 1.1**). The *ZA* forms a belt of *AJ* material that links the cells in a continuous sheet and separates the apical and basal compartments of polarised epithelial cells (Harris and Tepass 2010).

In metazoans, the organisation of the *AJ* is largely conserved (Farquhar and Palade 1963; Harris and Tepass 2010), highlighting its central role in cell biology. However, there are a few differences between the architecture of other cell-cell junctions (**Figure 1.2**). In vertebrate epithelial cells, a specialised plasma membrane (PM) microdomain known as the Tight Junction (TJ) forms apical to the *ZA*. However, in *Drosophila,* epithelial cells do not contain TJs, instead the *Septate Junction* (*SJ)* acts as a paracellular diffusion barrier basal to the *ZA* (Tepass and Hartenstein 1994b; Fleming et al. 2000; Genova and Fehon 2003). In addition to lacking TJs, *Drosophila* epithelial cells do not contain desmosomes or hemidesmosomes (Tepass and Hartenstein 1994b).

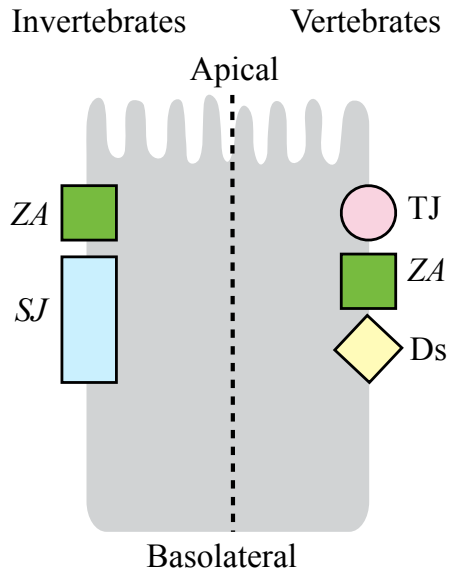

Figure 1.2: Cell surface polarity and cell-cell junctions in vertebrate and invertebrate epithelial cells. The apical and basolateral domains are separated by the formation of cell-cell junctions. In vertebrates, epithelial cell-cell junctions consist of Tight Junctions (TJs; **pink**), the *Zonula Adherens* (*ZA;* **green**), and Desmosomes (Ds; **yellow**). In invertebrate epithelia, TJs do not exist and instead the *Septate Junctions* (*SJs*; **blue**) act as a paracellular diffusion barrier basal to the *ZA*.

A significant part of our knowledge regarding apical-basal polarity comes from studies conducted on the fruit fly, *Drosophila melanogaster*. Below, I will outline the key model systems of the fly that have been used to study epithelial apical-basal polarity and their respective advantages.

1.1 The *Drosophila* embryo

The *Drosophila* embryo has been useful for the identification of key players involved in polarity establishment and maintenance. Unlike in vertebrate model organisms, *Drosophila* is easily subjected to genetic manipulation. Cell polarity and *AJ* morphogenesis in the *Drosophila* embryo has been studied in two contexts: the specification of polarity in the syncytial blastoderm and *ZA* specification during gastrulation.

1.1.1 Cellularisation and spot *Adherens Junction* assembly

Following fertilisation of the egg, the early *Drosophila* embryo undergoes rapid nuclear cell divisions without cytokinesis, resulting in the formation of a syncytial blastoderm. At this stage, the embryo contains around 6000 nuclei, which share the same cytoplasm. The subsequent subdivision of the cytoplasm occurs by invagination of the embryonic PM to surround and compartmentalise each nuclei (**Figure 1.3**). This process of cellularisation requires the establishment of a polarised epithelial blastoderm, linked together by apical *AJs* (Harris 2012).

During cellularisation, cell contacts start with the positioning of spot *AJs,* which consist of clusters of DE-Cadherin/Catenin (DE-Cad/Cat), and require the scaffold protein Bazooka (Baz), the *Drosophila* homolog of Par3. Baz engages with DE-Cad/Cat molecules at a ratio of 1:7 (McGill et al. 2009), suggesting that dynamic and transient interactions between Baz and spot *AJ* components regulate formation of the *AJ*. Spot *AJs* assemble along the lateral membrane and eventually coalesce to form the *ZA*. Baz forms a landmark for spot *AJ* assembly at the same apical-basal position as centrosomes in the *Drosophila* embryo (Harris and Peifer 2004; Harris and Peifer 2005). In the fly embryo, Baz localises to apical-lateral spot *AJs* independently of *AJ* proteins and has been shown to recruit and aggregate apically pre-assembled clusters of DE-Cad/Cat (Harris and Peifer 2004; McGill et al. 2009), thereby contributing to the formation of the *ZA*. In gastrulating embryos, loss of *baz* leads to the mislocalisation of the spot *AJs*, which subsequently leads to the disruption of epithelial tissues (McGill et al. 2009).

In conclusion, confinement of Baz to the apical-lateral border of the cell, allows Baz to interact with *AJ* material. However, Baz is not required for the accumulation of *AJ* material, which form spot *AJs* along the lateral membrane, independently of Baz

(Harris and Peifer 2004; McGill et al. 2009). This suggests that pathway(s) must exist that support(s) the assembly of *AJ* independently of Baz.

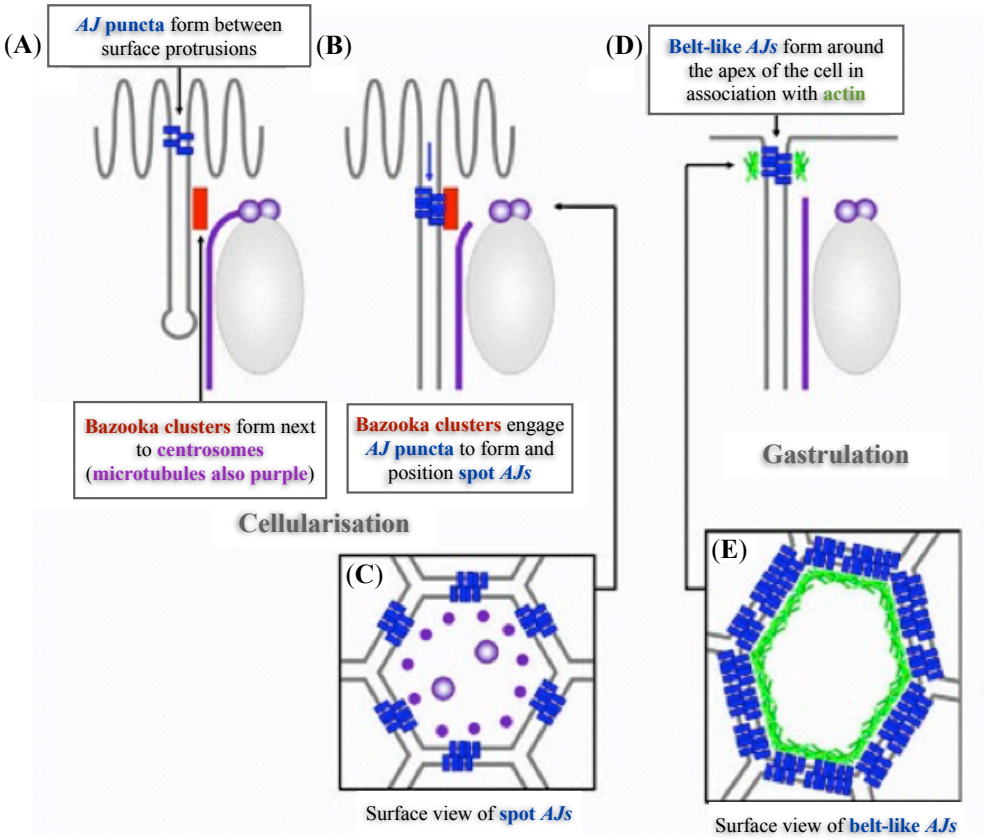

Figure 1.3: Establishment of apical-basal polarity during cellularisation of the fly syncytial blastoderm. A schematic diagram showing the process of cellularisation (**A**), which is the simultaneous compartmentalisation of approximately 6000 nuclei, mediated by plasma membrane (**grey**) invagination from the embryo surface. The process of cellularisation requires the formation of apical *Adherens Junctions (AJs)* known as spot *AJs*. Spot *AJ* formation is initiated by clusters of Bazooka (Baz; **red**), which are positioned next to the centrosome (**purple circles**), from which microtubules (MTs) emanate (**purple line**). At this position, Baz functions to recruit clusters of DE-Cad/Cat (**blue**; **B**), which subsequently form spot *AJs*. A surface view of the nascent epithelia, at the level of the centrosomes is shown in (**C**). After cellularisation, during gastrulation of the fly embryo, the spot *AJs* lose their association with centrosomal MTs, to form connections with the F-actin cytoskeleton (**green**). This allows spot *AJs* to form belt-like *AJs* known as the *ZA* (**D**). A surface view of a gastrulating epithelial cell, at the level of the *ZA* is shown in (**E**). Figure adapted from (Harris 2012).

1.1.2 Apical positioning of Bazooka

In the *Drosophila* embryo, several mechanisms are known to position Baz apically including an apical-lateral F-actin-based scaffold and basal-to-apical dynein-based transport (Harris and Peifer 2005). Moreover, Par1-mediated phosphorylation

excludes Baz from the basal domain (Krahn et al. 2009; Benton and St Johnston 2003), thereby promoting apical accumulation of Baz. Par1 is a serine-threonine kinase that was first identified in *C. elegans,* where it is required for the one-cell zygote to produce asymmetries that allow the formation of distinct daughter cells (Kemphues et al. 1988). Par1 accumulates on the lateral PM of *Drosophila* follicular epithelial cells (Doerflinger et al. 2003; Vaccari et al. 2005), where it regulates Baz by phosphorylating it and preventing the Par-complex (Baz-Par6-aPKC) from localising to the lateral domain (Benton and St Johnston 2003). Phosphorylation of Baz by Par1 permits binding of the conserved regulatory 14-3-3 protein to Baz and prevents binding of Baz to the apical determinant aPKC (Benton and St Johnston, 2003; **Figure 1.1**). Phosphorylation of Baz by Par1 is an important mechanism during polarised cortical partitioning in *Drosophila* epithelial cells. However, during polarity remodelling in the embryo, FE and developing pupal photoreceptor, Par1 is largely dispensable (Benton and St Johnston 2003; McKinley and Harris 2012; Nam et al. 2007), indicating that other mechanisms are at play to prevent Par-complex accumulation at the lateral PM.

1.1.3 Role of Crumbs in the formation of the *Zonula Adherens*

Crb is a transmembrane protein and one of the first regulators of epithelial polarity to be identified in *Drosophila* embryonic epithelial cells (Tepass et al. 1990). *Drosophila* homozygous null mutants of *crb* cause an almost complete loss of cuticle with a few remaining "crumb-like" particles (Tepass et al. 1990). *crb* homozygous null mutants lose apical-membrane identity (Wodarz et al. 1993) and *crb* overexpression results in the expansion of the apical membrane at the expense of the basal-lateral membrane (Wodarz et al. 1995). Crb is localised apically to the *ZA* at the *Marginal Zone* (*MZ)* and apical membrane in most epithelia, therefore establishing Crb as an apical determinant (Tepass, 1996). However, in the embryo,

Crb is not required for the establishment of spot *AJs* but rather for the formation of the *ZA* during gastrulation (Thompson et al. 2013). During this process, Crb functions to compete with Baz for binding with the apical determinant, aPKC (Morais-de-Sá et al. 2010). aPKC-dependent phosphorylation of Baz, leads to its dissociation from Baz, allowing aPKC to form a complex with Crb (Morais-de-Sá et al. 2010; Walther and Pichaud 2010).

Loss of *stardust* (using zygotic *sdt* mutants) results in similar epithelial defects caused by the loss of *crb* in fly embryos and photoreceptors (Tepass and Knust 1993; Hong et al. 2003). Within fly embryos, double mutant combinations of *sdt* and *crb* suggested that these genes are part of one pathway (Tepass and Knust 1993). Baz recruits Sdt to the PM and aPKC-dependent phosphorylation of Baz weakens the interaction between Baz and Sdt. This allows Sdt to disassociate from Baz and bind and correctly position Crb to regulate apical-basal polarity (Krahn et al. 2010). In conclusion, during polarity remodelling, Crb promotes *ZA* assembly by recruiting Par6-aPKC at the apical pole of the cell.

1.2 The remodelling *Drosophila* photoreceptor

The *Drosophila* photoreceptor is a popular model system for studying apical-basal polarity remodelling during organogenesis (Izaddoost et al. 2002; Pellikka et al. 2002; Hong et al. 2003; Walther and Pichaud 2010; Walther et al. 2016). The *Drosophila* adult compound eye is composed of a hexagonal array of approximately 800 ommatidia, that are regularly spaced and homogenous in size. Such a repetitive structure makes the *Drosophila* eye highly amenable to genetic analysis, as even subtle defects in retinal morphogenesis are amplified several fold and therefore easily detected (Dickson and Hafen 1994). Unlike in the embryo, mosaic analysis can be

easily carried out in *Drosophila* photoreceptors, allowing comparison between *wild-type* and mutant cells within the same tissue. In addition, the *Drosophila* photoreceptor forms long membrane domains that are highly polarised, which can be precisely measured using Electron Microscopy (EM).

Taken together, the *Drosophila* photoreceptor is a very powerful model to study apical membrane morphogenesis and polarity remodelling using classical genetic approaches. Cell polarity and *AJ* morphogenesis in the *Drosophila* photoreceptor has been studied in two contexts: *AJ* remodelling during cell intercalation in third instar imaginal discs and following rotation of the apical-basal axis in the pupal photoreceptor.

1.2.1 Polarity remodelling in the developing eye

The developing fly retina is a sensory neuroepithelium, which undergoes the differentiation of many different cell types. This is accompanied by a series of cell shape changes that are initiated through apical constriction and discrete events of *AJ* remodelling (Ready et al. 1976). Patterning of this neuroepithelium occurs through the transient constriction of cells within the Morphogenetic Furrow (MF), that consists of a morphogenetic wave travelling in the Anterior/Posterior (A/P) direction (**Figure 1.4A-B)**. The MF generates an array of regularly spaced clusters of photoreceptors known as ommatidia, which requires remodelling of the cell's *AJ* (Wolff and Ready 1991). The multicellular patterning that occurs during ommatidia morphogenesis has been carefully analysed and documented by several labs (Ready et al. 1976; Wolff and Ready 1991; Corrigall et al. 2007; Escudero et al. 2007; Robertson et al. 2012). In the wake of the MF, multicellular patterning events lead to the formation of 'lines', 'arcs', 'pre-clusters' and 'rosettes', resulting in a patterned array of cells across the eye (**Figure 1.4**). The formation of these structures within

the fly eye is regulated by Rho kinase and p-Myosin II/p-Myo II (Escudero et al. 2007; Robertson et al. 2012; Pichaud 2014). However, more work is required to precisely underpin the effectors that govern *AJ* remodelling during patterning of the eye. Taken together, the developing fly retina provides a useful model system to investigate *AJ* remodelling during organogenesis.

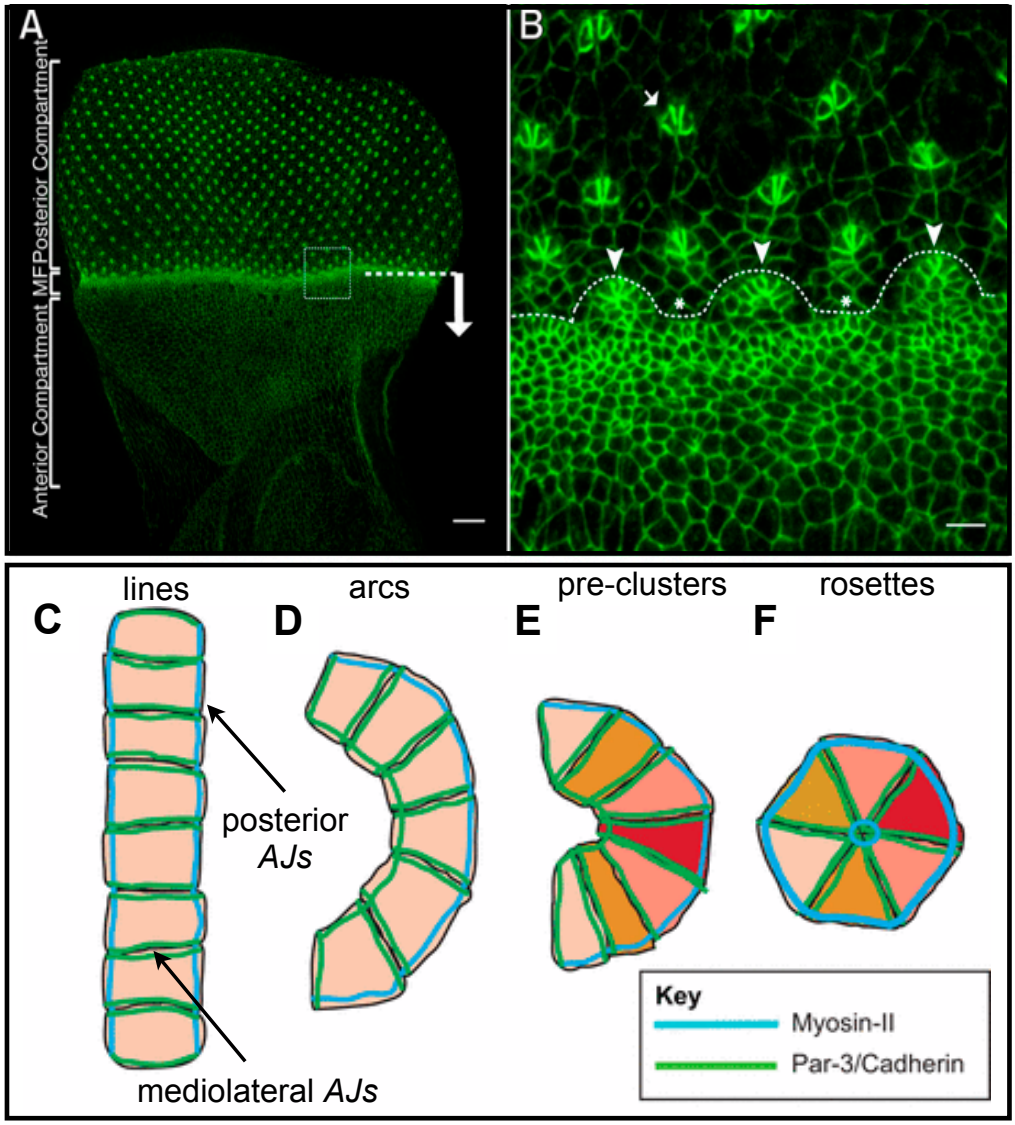

Figure 1.4: Ommatidial patterning in the developing *Drosophila* eye disc. Wild-type third instar eye imaginal discs marked with DECad::GFP (**green**; **A**). The anterior and posterior compartments are indicated along with the Morphogenetic Furrow (MF) marked by a dashed white line. The scale bar refers to 20 µm. The insert shown in (**A**) is enlarged to better illustrate the patterning events that characterise early stages of retinal morphogenesis (**B**). Lines (**white asterisks**) and arcs (**white arrowheads**) emanate from the MF and these multicellular structures subsequently form 5-cell rosettes (**white arrow**). The scale bar refers to 4 µm. A schematic representation of a line (**C**), arc (**D**), pre-cluster (**E**) and rosette (**F**) highlights the planar polarised distribution of Rho kinase/ROCK and p-Myo II (**blue**) and Baz/DE-Cad (**green**). Image adapted from (Robertson et al. 2012; Harding et al. 2014).

Several cell types that derive from epithelial cells adopt a more complex and specialised morphology. One such example is the *Drosophila* photoreceptor, which differentiates from the epithelial cells of the eye imaginal disc. The architecture of the eye is established during mid-pupal development, beginning with a 90° rotation of the apical-basal axis of the photoreceptor. The apical membrane of the cell then undergoes a dramatic expansion forming an array of microvilli, the photosensitive rhabdomere and a supporting stalk membrane, which connects the rhabdomere to the *ZA* (**Figure 1.5**). This expansion is marked by an extension of the cell along the proximal-distal axis of the retina (Longley and Ready 1995). Such morphological changes require sustained remodelling of the *ZA* and maintenance of separate apical and basolateral domains.

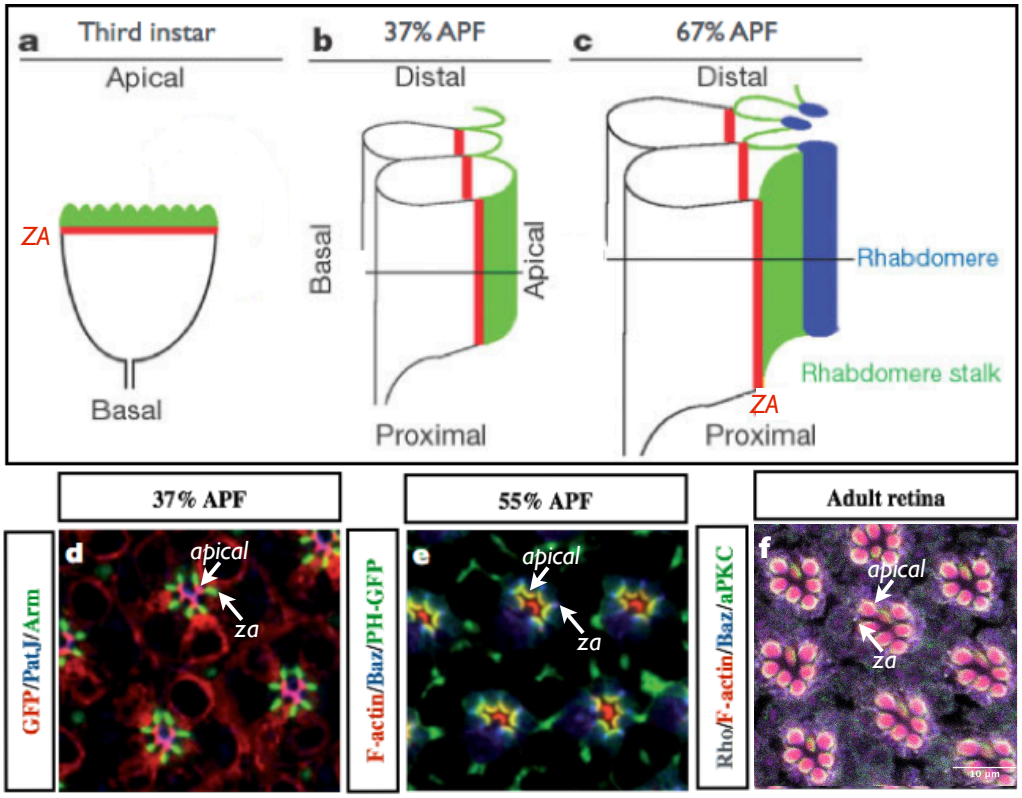

Figure 1.5: *Drosophila* photoreceptor development. The *Drosophila* photoreceptor differentiates from epithelial cells of the third instar eye imaginal disc (**a**), where the apical membranes face the retinal surface. During mid-pupal development (37% APF; **b**), photoreceptor cells rotate along the apical-basal axis of the cell. Rotation of photoreceptors reorganises the apical membranes to face each other. The *ZA* ensures that the distal apical membrane is anchored to the retinal surface, whereas the proximal apical membrane is attached to the retinal floor. Following rotation, the apical membrane undergoes a dramatic expansion (**c**) forming an array of microvilli, the photosensitive rhabdomere (**blue**) and a supporting stalk membrane (**green**), which connects the rhabdomere to the *ZA* (**red**). This expansion is marked by an extension of the cell along the proximal-distal axis as indicated in the schematic (**c**). Immunohistochemistry for fly pupal retina at 37% APF is shown in (**d**) stained for ubiquitous GFP, the apical marker PatJ and *ZA* marker Arm. Fly pupal retina at 55% APF is shown in (**e**) stained for F-actin, the *ZA* marker Baz and PH-GFP to stain phosphoinositol triphosphate PInst(3,4,5)P3[17]. Fly adult retina is shown in (**f**) stained for the Rhodopsin-1/4C5 antibody, F-actin, the *ZA* marker Baz and the apical marker aPKC. The *ZA* and the apical membrane have been indicated in (**d-f**). Panels **a-c** were adapted from (Izaddoost et al. 2002) and panels **d-e** were adapted from (Walther and Pichaud 2006).

1.3 Apical membrane morphogenesis

In vertebrate and invertebrate epithelial cells, apical membrane morphogenesis consists of the separation of the apical and lateral membrane domains. This process is regulated by conserved polarity factors that can be classified into two main groups: the apical and the basal polarity proteins. The main apical polarity factors have traditionally been grouped into two main protein complexes: The Par (Par3-Par6-aPKC) and Crb (Crb-Sdt-PatJ) complex (**Figure 1.1**). In *Drosophila,* apical

membrane morphogenesis requires the confinement of aPKC, Crb and Sdt to the apical pole of the cell (Krahn et al. 2010). This is accompanied by the exclusion of Baz from the apical membrane to the boundary between the apical and lateral membrane, where Baz promotes *ZA* assembly. In the developing fly photoreceptor, Cdc42 binding to Par6 enables the recruitment of Par6-aPKC at the apical membrane (Walther and Pichaud 2010). In this context, Crb enables the apical exclusion of aPKC-phosphorylated Baz (Walther and Pichaud 2010) by capturing aPKC and Par6 at the apical pole of the cell. As mentioned earlier, apical exclusion of Baz is crucial for setting up the boundary between the apical membrane and the *ZA* by recruiting *AJ* material at the border between the apical and lateral PM.

1.4 *Zonula Adherens*

The *ZA* includes two principal adhesion molecules: E-Cad and Nectin (Niessen and Gottardi 2008). E-Cad belongs to the classical Cad family of adhesion molecules responsible for Ca^{2+}-dependent cell-cell adhesion (Nelson et al. 2013). All members of this family are single pass transmembrane proteins, which engage with identical E-Cad molecules on the surface of adjacent cells (Leckband and Sivasankar 2000). *Drosophila* E-Cad (DE-Cad) was identified as a homolog of vertebrate classic E-Cad (Oda et al. 1994). The cytoplasmic domain of DE-Cad shows significant identity to that of vertebrate E-Cad. However, the extracellular domain of DE-Cad exhibits less similarity to vertebrate E-Cad due to a large insertion near the extracellular domain and an extra E-Cad domain repeat in vertebrate E-Cad. Despite these dissimilarities, DE-Cad is functionally similar to vertebrate E-Cad, for example, through its association with similar binding partners (Oda et al. 1994).

1.4.1 β-Catenin

Several proteins bind the conserved cytoplasmic domain of E-Cad to promote *AJ* morphogenesis. E-Cad interacts with β-Cat (*Armadillo/Arm* in *Drosophila*) shortly after E-Cad synthesis (Chen et al. 1999). This association is thought to begin in the endoplasmic reticulum (ER) and correlates with the efficient and targeted transport of E-Cad to the PM through the biosynthetic pathway in polarised MDCK cells (Chen et al. 1999; Farr et al. 2015). Once at the PM, β-Cat binds α-Cat and recruits it to the *AJ* (Nagafuchi and Takeichi 1988; Ozawa et al. 1989; Ozawa et al. 1990; Oyama et al. 1994). The requirement of β-Cat/Arm for *AJ* formation has been shown in fly epithelia (Cox et al. 1996; Müller and Wieschaus 1996; Orsulic and Peifer 1996), where *AJs* fail to assemble in the absence of *arm*, leading to severe cell adhesion defects.

1.4.2 p120-Catenin

The cytoplasmic domain of E-Cad also interacts with p120-Cat (Reynolds et al. 1994; Shibamoto et al. 1995). In vertebrates, p120-Cat interaction with E-Cad counteracts E-Cad endocytosis and degradation, therefore enhancing the accumulation of E-Cad at the PM (Ireton et al. 2002; Davis et al. 2003). Moreover, p120-Cat links E-Cad to MTs, which promotes the transport of E-Cad to the PM (Chen et al. 2003; Meng et al. 2008). These studies highlight the role of p120-Cat as a modulator of E-Cad function in vertebrates. In contrast to other components of the E-Cad/Cat complex, p120-Cat is not essential for fly development and is partially redundant with other regulators of cell-adhesion (Myster et al. 2003; Pacquelet et al. 2003). Taken together, these studies suggest that in flies, as long as α-Cat can bind to DE-Cad, DE-Cad-based morphogenesis can proceed without additional regulatory inputs from p120-Cat.

1.4.3 α-Catenin

The cytoplasmic domain of E-Cad also interacts with α-Cat. α-Cat can bind F-actin, thereby linking *AJs* to the actin cytoskeleton, which is essential for cell adhesion (Rimm et al. 1995; Pappas and Rimm 2006). This explains the close association of E-Cad with the F-actin cytoskeleton. Moreover, α-Cat binds preferentially to F-actin as a dimer, whereas monomeric α-Cat binds more strongly with the E-Cad/β-Cat module. However, the dimerisation domain of α-Cat overlaps with the binding site for β-Cat (Pokutta and Weis 2000). Therefore, a simple model whereby a quaternary complex composed of E-Cad, β-Cat, α-Cat and F-actin could not be found experimentally (Drees et al. 2005; Yamada et al. 2005; Desai et al. 2013). This implies that α-Cat cannot bind to E-Cad/β-Cat complex and F-actin at the same time. Therefore, α-Cat, might be a key regulator of F-actin dynamics rather than a stable F-actin linker (**Figure 1.6**). However, more recent work in various fly tissues has shown that, α-Cat cell adhesion is not dependent on dimerisation (Desai et al. 2013), therefore arguing against the allosteric model proposed by the Nelson lab. Nevertheless, interactions between the *AJ* and the F-actin cytoskeleton might instead be mediated through F-actin-binding proteins, including Afadin. Moreover, these interactions might be transient and components of the *ZA* may exist in a constant equilibrium, which allow these interactions to change depending on the developmental cues and the concentrations of the proteins that make up the *AJ*.

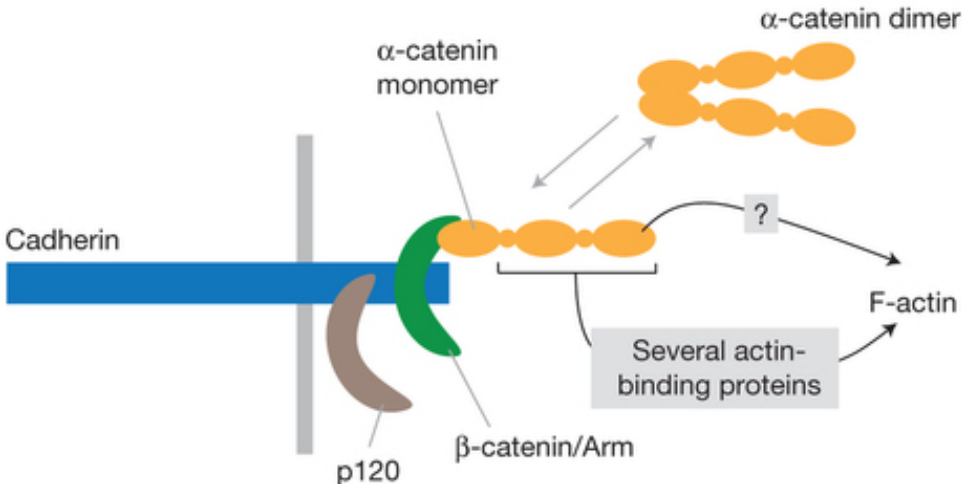

Figure 1.6: A model of *Adherens junction* formation. A schematic representation of α-Cat dimers (**orange**) that form a cytoplasmic pool, which is inactive in adhesion but instead, forms a dynamic equilibrium with monomeric α-Cat. The monomeric fraction of α-Cat is recruited to the *Adherens Junction (AJ)* through interaction with β-Cat/Arm (**green**), leading to the stabilisation of α-Cat. Monomeric α-Cat can in turn interact with the F-actin cytoskeleton through several actin-binding proteins. Image adapted from (Desai et al. 2013).

1.4.4 Nectins and Afadins

Nectins are a class of transmembrane Ca^{2+}-independent adhesion molecules that are localised at the *AJ* through binding of the cytoplasmic adaptor molecule, Afadin (Takahashi et al. 1999). Similar to α-Cat, in vertebrates, Afadin can bind to F-actin and several actin-associated proteins (Tachibana et al. 2000; Pokutta et al. 2002; Wei et al. 2005). However, there are four mouse *nectins*, which complicates loss-of-function analysis, whereas, *Drosophila* has one *afadin* homolog known as *canoe (cno)*. Cno is able to bind to Echinoid (Ed), the fly homolog of Nectin and recruit it to the *AJ* (Wei et al. 2005). Similar to what has been shown in mice (Kurita et al. 2013; Tanaka-Okamoto et al. 2014), in flies, Cno regulates polarity and cell adhesion by linking *AJs* to the F-actin cytoskeleton (Takahashi et al. 1998; Boettner et al. 2003; Sawyer et al. 2009; Sawyer et al. 2011). Accordingly, *Drosophila* zygotic *cno* mutants display defects in processes that rely on cell shape changes and *AJ* remodelling in the fly embryo, such as dorsal closure (Takahashi et al. 1998; Boettner et al. 2003), ventral furrow formation (Sawyer et al. 2009) and germ band

extension (Sawyer et al. 2011). It is important to note that Cno is not essential for *AJ* assembly in the fly embryo, but leads to the uncoupling of the F-actin cytoskeleton from the *AJ,* thereby, leading to defects in cell shape (Sawyer et al. 2009). These studies highlight a key role for Cno in linking the *AJ* to the F-actin cytoskeleton, thereby allowing epithelial cells to respond to changes in cell shape.

1.4.5 Rho GTPases

Small GTPases act as molecular switches that cycle between an active (GTP-bound) and an inactive (GDP-bound) state. The activity of GTPases is regulated through its guanine nucleotide exchange factors (GEFs), which activate the switch by catalysing exchange of GDP for GTP. Conversely, GTPase activating proteins (GAPs) stimulate the intrinsic activity of the GTPase to inactivate the switch. It is through the active GTP-bound state that Rho GTPases can interact with their effector proteins and perform their regulatory functions (Jaffe and Hall 2005). The function of Rho GTPases can be regulated in a spatial-temporal manner, by localising GEFs and GAPs to specific regions of the cell (Etienne-Manneville and Hall 2002). Rho GTPases control a wide variety of cellular processes, including apical-basal polarity and *ZA* remodelling (Etienne-Manneville and Hall 2002). Moreover, E-Cad and Nectin can signal through Rho GTPases, including Rho, Rac and Cdc42, to support the formation and maintenance of *AJs* (Tepass and Harris 2007). Rho GTPases have also been shown to be involved in many actin-dependent processes including cell migration (Nobes and Hall 1999; Braga et al. 2000; Plutoni et al. 2016), adhesion (Braga et al. 1997; Hordijk et al. 1997; Malliri et al. 2004), polarity (Schwamborn and Püschel 2004; Mack and Georgiou 2014) and morphogenesis (Luo et al. 1994; Vogler et al. 2014).

Rho GTPases such as Cdc42 are also required for normal rates of DE-Cad endocytosis in the fly notum, neuroectoderm and wing imaginal discs (Georgiou et al. 2008; Harris and Tepass 2008; Leibfried et al. 2008). *Cdc42* dominant negative *($Cdc42^{DN}$)* fly embryos lose *AJs* during neuroblast ingression (Harris and Tepass 2008), a process whereby cell-cell contacts between neuroblasts are broken down causing delamination (ingression) from the epithelium. Following delamination, remaining cells form new *AJs* to maintain integrity of the epithelium. Cdc42 and the Par complex cooperate in regulating the structure of the fly neuroectoderm by maintaining levels of Crb at the cell surface, which is required for the stabilisation of *AJs* (Harris and Tepass 2008). $Cdc42^{DN}$ neuroblasts display enhanced rates of endocytosis with abnormally large endosomes containing DE-Cad, Par complex proteins and Crb (Harris and Tepass 2008). Taken together, in the fly embryo Cdc42 functions as a negative regulator of the frequency of apical endocytosis and as a positive regulator of the progression of apical cargo from the early to late endosome. However, in the fly notum (Georgiou et al. 2008) and wing disc (Leibfried et al. 2008) Cdc42/Par6/aPKC regulate *AJ* stability through actin-dependent endocytosis, thereby ensuring rapid turnover of *AJs*. These studies highlight a role for small GTPases such as Cdc42 in regulating the accumulation and stability of *AJ* material at the *ZA*. However, it is important to note that the diversity in the requirement of apical determinants such as Cdc42 in the regulation of vesicle trafficking is likely to be cell-type and context dependent. This unfortunately, complicates comparisons between different model systems and highlights the importance of studying mechanisms that regulate *AJ* stability in different tissues and developmental contexts.

1.5 *Zonula Adherens* remodelling

During organogenesis, the epithelial *ZA* has to be remodelled and maintained as tissues undergo changes in cell shape. Epithelial polarity remodelling depends on

Baz in the fly photoreceptor (Walther and Pichaud 2010), follicular epithelium and blastoderm (Morais-de-Sá et al. 2010). During polarity remodelling, Baz is localised at the *ZA*, whereas, Crb, Sdt, PatJ and aPKC-Par6 are localised apically. At the *ZA*, Baz is thought to promote *ZA* assembly, possibly by recruiting Arm and Ed (Wei et al. 2005; Morais-de-Sá et al. 2010; Walther and Pichaud 2010). In the fly retina, *baz* mutant photoreceptors show a strong reduction in the expression of aPKC, Crb and Par6 (Walther et al. 2016). Moreover, *baz* mutant photoreceptors fail to specify a clear *ZA* and *AJ* material is scattered along the apical-basal axis of the cell. These findings demonstrate that during *ZA* remodelling, Baz is required to support the recruitment of Par6-aPKC and Crb to the apical pole of the cell. Since in the absence of Baz, *AJ* material still accumulates at the cortex, other mechanisms must exist to regulate *AJ* morphogenesis.

During *ZA* remodelling and maturation*, AJ* morphogenesis is regulated by the Cdc42 effector p21-activated serine/threonine kinase, Pak4 (*Drosophila* Mushroom bodies tiny, Mbt) in the mouse nervous system (Tian et al. 2011), human bronchial epithelial cells (Wallace et al. 2010) and the fly photoreceptor (Walther et al. 2016). In the fly photoreceptor, Mbt is a core component of the *AJ* as its localisation remains at the *ZA* of cells lacking all apical determinants and is only lost when *AJs* are removed (Walther et al. 2016). In the absence of *mbt*, some *AJ* material can still be detected at the cortex. However, no *AJ* material is detected in *baz*/*mbt* double mutants, suggesting that *mbt* supports *AJ* morphogenesis independently of *baz* (Walther et al. 2016).

Mbt influences the stability of DE-Cad/Cat complex in non-polarised S2 cells by phosphorylating β-cat/Arm, (Menzel et al. 2008). In the remodelling *Drosophila* photoreceptor, Mbt stabilises DE-Cad at the *ZA* by promoting the cortical accumulation of β-Cat/Arm and Baz through phosphorylation of β-Cat/Arm at serine

561 and 688 (Walther et al. 2016). Moreover, in *mbt* null photoreceptors, Baz accumulates laterally leading to ectopic aPKC and Arm at the lateral membrane. Therefore, Mbt promotes Baz retention at the *ZA* of remodelling photoreceptors, where it functions redundantly to Par1 to prevent lateral accumulation of Baz (Walther et al. 2016). Baz is required for the apical accumulation of aPKC-Par6 and for the accumulation of *AJ* material at the *ZA*, which points to an important cross-talk between *ZA* and apical proteins through Baz (**Figure 1.7**).

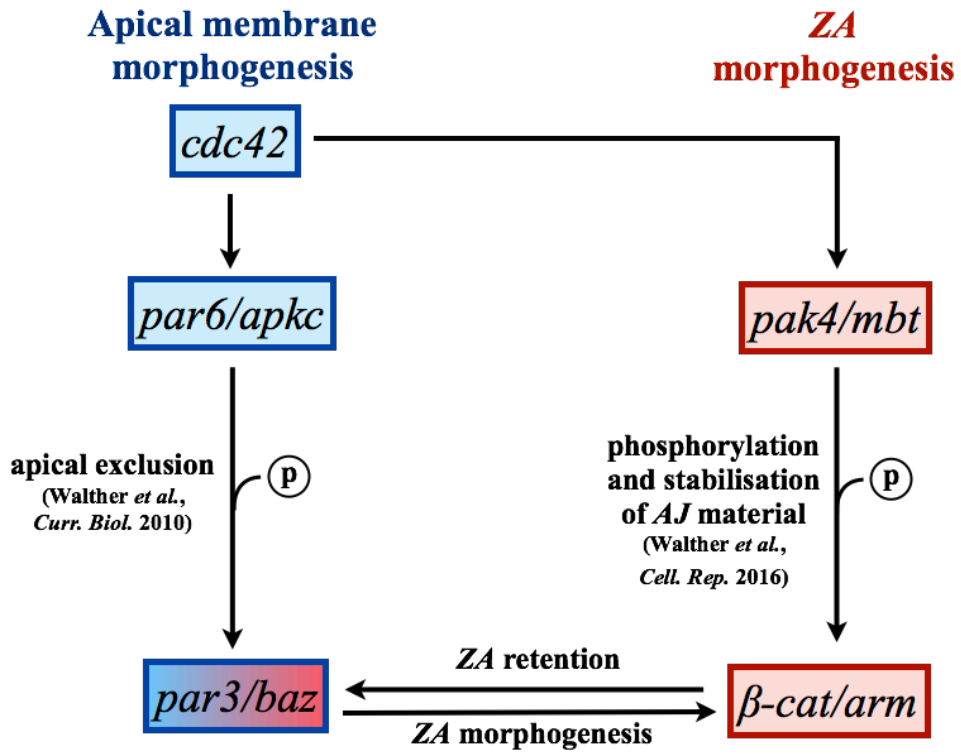

Figure 1.7: Cross-talk between apical membrane morphogenesis and *ZA* morphogenesis. A schematic diagram outlining the key stages that regulate polarity remodelling in the pupal fly photoreceptor: apical membrane differentiation (**blue**) and *ZA* morphogenesis (**red**). In vertebrate and invertebrate cells Pak4/Mbt functions downstream of the small GTPase, Cdc42, a known regulator of aPKC-Par6 (Schneeberger and Raabe 2003; Wallace et al. 2010; Walther et al. 2016). aPKC phosphorylates and excludes Baz from the apical membrane to the border between the apical-lateral membrane where the *ZA* is formed (Walther and Pichaud 2010). Mbt is positioned at the *ZA* where it accumulates *AJ* material and Baz. Importantly, the *ZA* is not just a consequence of apical-basal polarity but can influence apical-basal polarity through retention of Baz at the remodelling *ZA*.

Since in *mbt* null mutant photoreceptors, *AJ* material is still detected at the cell cortex, other pathways must function to regulate accumulation of *AJ* material at the remodelling *ZA*. As no *AJ* material is detected in double *baz, mbt* mutant cells, such pathways appear to be linked to *baz* function. Accordingly, investigating the nature of these pathways and mechanism is a main focus of this thesis.

1.6 Rap1 GTPase

A potential regulator of *AJ* morphogenesis and *ZA* remodelling is the small GTPase Rap1. *rap1* belongs to *ras* superfamily of genes and can be regulated by several GEFs, which presumably allow Rap1 to be activated in particular locations of the cell or in a tissue-dependent fashion (**Figure 1.8)**. In *Drosophila,* the known Rap1 GEFs include: Epac (Dupuy et al. 2005), C3G (Ishimaru et al. 1999) and PDZGEF/Dizzy (Lee et al. 2002). In flies, one GAP protein, Rapgap1 has been identified to date (Chen et al. 1997).

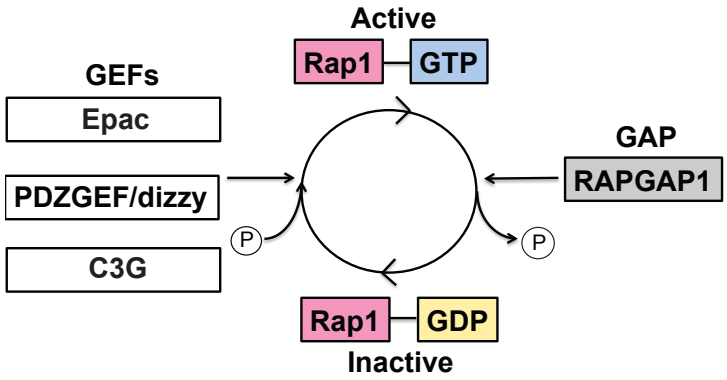

Figure 1.8: Rap1 GTPase regulation by its GEFs and GAPs in *Drosophila.* Rap1 is cycled between its active (GTP-bound) and inactive (GDP-bound) state through its GEFs and GAPs. In *Drosophila,* three known Rap1 GEFs: Epac (Dupuy et al. 2005), PDZGEF/Dizzy (Lee et al. 2002). and C3G (Ishimaru et al. 1999), whereas one GAP protein, Rapgap1 has been identified to date (Chen et al. 1997).

rap genes have been characterised in several species including *Drosophila* (Neuman-Silberberg et al. 1984; Hariharan et al. 1991), *Dictyostelium* (Robbins et al. 1991) and mammals (Pizon et al. 1988; Kitayama et al. 1989). Human and *Drosophila rap* genes exhibit 88% sequence identity at the amino acid level and human *rap1a* can partially substitute for *Drosophila* Rap1 function (Asha et al. 1999), highlighting a conserved role for Rap1 in humans and flies. Rap1 has been associated with a plethora of cellular functions, some of which I will discuss below.

1.6.1 Rap1 as a regulator of *Drosophila* morphogenesis

Early studies in *Drosophila* implicated a broad role for Rap1 during morphogenesis. The removal of *rap1* during embryogenesis, oogenesis and imaginal disc development led to defects in ventral furrow formation, dorsal closure, follicle and photoreceptor cell development (Asha et al. 1999). However, the molecular basis for the function of *rap1* as a regulator of these various morphogenetic processes remains unclear.

1.6.2 Rap1 as a regulator of cell-cell adhesion

Rap1 has long been associated with integrin-mediated cell-extracellular matrix (ECM) adhesion (Bos et al. 2003; Huelsmann et al. 2006; Severson et al. 2009). However, more recent work in *Drosophila* wing discs has implicated a role for Rap1 in regulating DE-Cad-based cell-cell adhesion (Knox and Brown 2002). Wing discs mutant for *rap1* display defects in cell shape with a more rounded rather than normal hexagonal appearance (Knox and Brown 2002). The area of the apical but not the basal surface of cells was reduced in *rap1* mutants relative to *wild-type*, suggesting that Rap1 plays a role in regulating the apical but not the basolateral domain. Moreover, in *rap1* mutant cells the distribution of *AJ* material was localised predominantly to one side of the cell, rather than evenly distributed around the

circumference as seen in *wild-type* wing epithelial cells. This indicates that Rap1 is required for the correct distribution of *AJ* material in epithelial cells, which is fundamental in the formation of cell-cell contacts.

Moreover, Rap1 localisation is consistently enriched at the *AJ* between newly formed sister cells after cell division, which coincides with the localisation of α-Cat, β-Cat and Cno. These observation led the authors to propose a model whereby Rap1 functions in reorganising the *AJ* through remodelling of the F-actin cytoskeleton, to ensure the maintenance of *AJ* material around the circumference of the cell during or after cytokinesis (Knox and Brown 2002). However, whether this mechanism also exists in post-mitotic cells is not clear and in particular during *ZA* remodelling.

Rap1 has also been shown to be involved in cell-cell adhesion in mammalian cell culture (Hogan et al. 2004). In human breast cancer (MCF7) and HEK293 cells, formation of E-Cad trans-dimers induces binding of the Rap1GEF C3G, to the cytoplasmic tail of E-Cad. Consequently, this enhances Rap1 activity, which is required for the accumulation of E-Cad at the nascent cell-cell contacts thus, helping to establish mature E-Cad-based cell-cell contacts. However, C3G and β-Cat compete for binding with E-Cad as they both interact with overlapping regions on E-Cad (Hogan et al. 2004). Indeed, overexpression of β-Cat reduces the amount of C3G bound to E-Cad. However, in MCF7 cells containing mature, established cell-cell contacts, C3G does not interact with E-Cad (Hogan et al. 2004), suggesting that C3G is involved in the early stages of cell-cell contact formation and not in the maintenance of mature contacts. This suggests that Rap1 is required for the accumulation of E-Cad, which is essential in the maturation of *AJs*.

Accordingly, the expression of RapGAP inhibits Rap1 activity and prevents the recruitment of E-Cad in MCF7 cells (Hogan et al. 2004). This suggests that Rap1

activity is involved in recruiting and accumulating E-Cad at nascent cell-cell contact sites. However, upon examination at later stages following calcium switch, E-Cad starts to accumulate at cell-cell contacts in the absence of Rap1 (Hogan et al. 2004). Therefore, Rap1-independent mechanisms must also function in the accumulation of E-Cad in MCF7 cells.

1.6.3 Rap1 binds the actin-interacting protein Canoe

Binding of Rap1 to the F-actin cytoskeleton can be mediated through actin binding proteins such as Afadin. Yeast two-hybrid assays have revealed an interaction between active Rap1A and Afadin-6 through its N-terminal Ras Binding Domains (Linnemann et al. 1999; Boettner et al. 2000). Further analysis revealed colocalisation of these proteins at the PM of MCF7 cells (Boettner et al. 2000), suggesting that Afadin-6 is a possible effector of Rap1 and there is potential interplay between these proteins. The interaction between Afadin-6/Cno and Rap1 was later confirmed using the *Drosophila* embryonic cDNA library and colocalisation between these two proteins was shown in the *Drosophila* embryonic epithelia (Boettner et al. 2003), suggesting a conserved interaction between Rap1 and Afadin-6/Cno in vertebrates and invertebrates.

1.6.4 *rap1* is essential for *AJ* morphogenesis

In the fly blastoderm, Baz was initially identified as the upstream cue required for the apical positioning of *AJs* (Harris and Peifer 2004; Harris and Peifer 2005). However, later work identified a role for Rap1/Cno in apical positioning of *AJs* and Baz during the establishment of apical-basal polarity (Choi et al. 2013). Indeed, it was shown that *maternal/zygotic* (*m/z*) mutant *rap1* embryos display fragmented cuticle formation during *Drosophila* embryogenesis (Choi et al. 2013). This fragmented cuticle phenotype is a consequence of the mispositioning of apical spot *AJs* (Choi et

al. 2013). Accumulation of Baz and apical spot *AJs* material was considerably reduced in *m/z rap1* mutant embryos, with Baz and *AJ* material localising all along the lateral membrane (Choi et al. 2013), suggesting that *rap1* is required for the initial positioning of Baz and apical spot *AJs*. Similarly, null mutant fly embryos for *cno* (cno^{R2}) also led to mislocalisation of Baz and apical spot *AJs* (Choi et al. 2013). In addition, *rap1* is required for the localisation of Cno in the cellularising fly embryo (Sawyer et al. 2009; Choi et al. 2013). Taken together, these studies suggest that *rap1* functions upstream of *cno* in the apical positioning of Baz and spot *AJs* in the fly embryo during cellularisation. However, *baz* and *aPKC* are also required in part for the positioning of Cno (Choi et al. 2013), suggesting that a complex genetic network regulates the establishment of apical-basal polarity. More work is required to gain mechanistic insight into how Rap1 regulates accumulation of *AJ* material and Baz during polarisation of epithelial cells.

Further insight into the relationship between Rap1/Cno and the *AJ* can be found when examining dorsal closure of the *Drosophila* embryo. Indeed, both Rap1 and Cno are localised at the *AJ*, where Cno acts as a Rap1 effector (Boettner et al. 2003). As mentioned earlier, Cno binds Rap1 through its Ras Association (RA) domains and loss of these domains ($cno^{\Delta N}$) leads to defects in dorsal closure that are more mild than those seen in *cno* null mutant embryos (Boettner et al. 2003). Moreover, ectopic expression of Cno can substantially rescue dorsal closure defects observed when dominant negative *rap1* ($rap1^{N17}$) is expressed in the fly embryo. However, no rescue is observed using the $cno^{\Delta N}$ allele. These experiments show that binding of Cno to Rap1 is required for the function of Rap1 as a regulator of dorsal closure. However, *cno* can regulate *AJ* remodelling independently of *rap1* using as yet unknown mechanisms. It has been proposed that binding of Rap1 to Cno couples the *AJ* to the F-actin cytoskeleton. However, how the Rap1/Cno module regulates *AJ* remodelling during epithelial morphogenesis remains unclear.

rap1 has been shown to be upstream of *Cdc42* and the *Par* complex during the determination of neuronal polarity in cultured rat hippocampal neurons (Schwamborn and Püschel 2004). During neuronal polarisation in the rat, Rap1B localises at the tip of a single neurite and directs the recruitment of Cdc42, which in turn specifies the axon (Schwamborn and Püschel 2004). Similarly, in yeast the Rap1 homolog *rsr1* functions upstream of *Cdc42* to determine the localisation of the bud site, which is a polarised process (Marston et al. 2001). Deletion or constitutive activation of *rsr1*, leads to randomisation of the bud site location (Bender and Pringle 1989; Ruggieri et al. 1992). Therefore, work in yeast and mammalian neurons highlight a conserved role for the function of Rap1 and Cdc42 in the regulation of polarity. Whether Rap1 functions together with Cdc42 to regulate epithelial polarity remodelling has not been tested.

1.6.5 PDZGEF/Dizzy regulates *Drosophila* morphogenesis

The Rap1GEF, PDZGEF/Dizzy was identified in a gain of function, misexpression screen used to identify genes involved in migration of embryonic macrophages in *Drosophila* (Huelsmann et al. 2006). PDZGEF/Dizzy binds Rap1 through its RA domain and regulates cell shape and migration of macrophages through modulation of integrin-mediated adhesion and stabilisation of cellular protrusions in the *Drosophila* embryo (Huelsmann et al. 2006). Similarly, PDZGEF/Dizzy regulates cell shape and epithelial migration during dorsal closure in gastrulating *Drosophila* embryos (Boettner and Van Aelst 2007). Whether PDZGEF/Dizzy is also involved in Rap1-dependent accumulation of DE-Cad within other instances of polarity remodelling, including *ZA* morphogenesis needs to be tested.

1.7 Transcriptional regulation of polarity

Several polarity genes were first identified as tumour suppressors in *Drosophila* and this function has been extended to mammalian genes (Bilder 2004; Bergstralh and St Johnston 2012). Moreover, misexpression of polarity genes can lead to apoptosis (Roegiers et al. 2001; Warner et al. 2010), alter cell fate (Ruohola et al. 1991; Wolff and Rubin 1998) and lead to migration defects (Pinheiro and Montell 2004; Qin et al. 2005). To allow these processes to function optimally, the levels at which these polarity genes are expressed needs to be regulated. Currently, very little is known regarding the mechanisms that regulate polarity gene expression. Transcription factors (TFs) might regulate expression of polarity proteins, which subsequently assemble into the distinct compartments that constitute the epithelial cell. Whether transcriptional regulation occurs during polarity remodelling is not clear. However, examples of transcriptional regulation of polarity genes can be found during epithelial to mesenchymal transition (EMT).

In the fly embryo, during EMT, cells lose their columnar shape and become more rounded and migratory, thus losing their characteristic epithelial feature. Apical and *AJ* proteins are subsequently lost from the surface and overall accumulation of these proteins is reduced (Smallhorn et al. 2004; Campbell et al. 2009; Huang et al. 2012; Lamouille et al. 2014). The transition from a polar to non-polar cell is coincident with the loss of the apical determinants Crb and Sdt and low levels of DE-Cad, Baz and aPKC, which accumulate in punctate structures instead of at the membrane. Presumably, these punctate structures are spot *AJs* that allow dynamic adhesions during collective migration (Campbell et al. 2009). During *Drosophila* gut specification, the GATA factor Serpent (Srp) regulates EMT to specify cell state (Reuter 1994). During gut development, Srp levels dramatically decrease as endodermal cells migrate to the correct location. Here cells undergo mesenchyme to

epithelial transition (MET), a reverse process in which the cell gains epithelial features, finally forming the midgut epithelium (Tepass and Hartenstein 1994a). Prolonged Srp expression prevents the midgut cells from re-establishing epithelial characteristics (Campbell et al. 2011). These results suggest that Srp expression has to be turned off for cells to cease migratory behaviour and gain epithelial characteristics. Further analysis revealed that Srp directly represses the expression of *crb* by binding to GATA sites within the *crb-cis* regulatory module. This results in the relocalisation of DE-Cad and F-actin away from the *AJ* and instead around the cell cortex in *Drosophila* embryos undergoing EMT (Campbell et al. 2011). Likewise, the human homolog of Srp, hGATA-6 indirectly affects levels of E-Cad accumulation at the *AJ* by repressing expression of the *crb2* gene in MDCK cells (Campbell et al. 2011). Work in the *Drosophila* gut and MDCK cells highlight a conserved role for Srp in the transcriptional regulation of E-Cad accumulation and polarity during epithelial morphogenesis. Similar studies need to be undertaken to elucidate further transcriptional mechanisms required for polarisation of epithelial cells.

1.8 Specific aims

The specific aims of my PhD thesis include the identification of potential transcriptional regulators of *ZA* morphogenesis, using the developing retina as a model system. To this end, I have carried out a transcriptional profiling approach throughout the development of the fly retina. Moreover, using a candidate-based approach, I have characterised the role and molecular basis for the function of *rap1/dizzy* in regulating *ZA* remodelling in the pupal fly photoreceptor. The main hypothesis I have tested is that *rap1* regulates *ZA* morphogenesis by influencing the accumulation of *Adherens junction* material at the plasma membrane. Finally, to identify novel regulators of apical membrane morphogenesis and *ZA* remodelling, I have conducted a large-scale genetic modifier screen in the adult fly eye.

Chapter 2. Materials & Methods

2.1 Fly food and stocks

Stocks of *Drosophila* melanogaster were maintained in vials containing fly food at either 18°C or 22°C. Fly food composition is as follows: 39 l dH20, 675 g yeast, 390 g soy flour, 2.85 kg yellow cornmeal, 224 g agar, 3 l light corn syrup and 188 ml propionic acid. Crosses were carried out at 25°C unless otherwise stated.

2.2 Genetic techniques

2.2.1 Gal4-UAS system

Overexpression experiments were carried out using the Gal4/UAS system, which was derived from yeast and has been adapted for genetic manipulation in *Drosophila* (Brand and Perrimon 1993). Gal4 is a DNA-binding protein that specifically recognises target UAS motifs and activates gene transcription from this site. Temporal and spatial control of gene expression can be achieved by the expression of Gal4 under the control of an inducible promoter or that of another gene. In this thesis, the synthetic promoter element Glass Multimer Reporter (GMR)-Gal4 (Freeman 1996) is commonly used to drive the expression of genes in the imaginal discs posterior to the MF. In addition to GMR-Gal4, npgal4^{2631}-Gal4 (National Institute of Genetics, Japan) is commonly used in this thesis to express genes in most cells within the third instar fly eye disc, both anterior and posterior to the furrow as well as in the wing disc (O'Keefe et al. 2009).

2.2.2 Mosaic analysis

Mitotic clones were generated by the Flp-FRT mediated mitotic recombination (Xu and Rubin 1993). This system allows mosaic patches of mutant tissue to be generated

amongst *wild-type* tissue (Xu and Rubin 1993). In this way, a direct comparison can be made between mutant and *wild-type* cells. This technique relies on recombination induced by the expression of a Flip recombinase (Flp) that results in recombination events at specified FRT sites. *Wild-type* cells commonly express a reporter such as GFP driven under the control of a ubiquitous promoter. Mutant clones are identified by the lack of this reporter, which is lost as a consequence of the recombination event. By using an appropriate promoter, expression of the Flp recombinase can be driven in a temporal and/or tissue specific manner, thereby allowing the recombination event to be more controlled. In this thesis, the eye specific promoter *eyeless* (Newsome et al. 2000) is commonly used to allow the generation of mosaic patches of mutant and *wild-type* tissue in the fly eye.

2.3 Genotypes

Canton S and *yw* flies were used for control experiments.

Microarray candidate-based screen

Gmrgal4/CyoGFP;UAS-dicer/TM6B, Tb (Chiara Mencarelli)

;;UAShlhmdelta (Bloomington Stock Centre 26677).

;;UASovo (Bloomington Stock Centre 38427 and 38429)

;UASovo; (Bloomington Stock Centre 38428 and 38430).

;UASbroad; (Bloomington Stock Centre 51190)

UASbroad;; (Bloomington Stock Centre 51191 and 51193).

;UAShlhm7; (Bloomington Stock Centre 26681).

;UAShlhm5; (Bloomington Stock Centre 26680).

UASsidestep;; (Bloomington Stock Centre 9679).

;;UASCG7372 (Bloomington Stock Centre 29679).

;UASsensless; (Bloomington Stock Centre 42209).

;;UASeip93F (Bloomington Stock Centre 30179).

;UASlola; (Bloomington Stock Centre 17254).

;;UASjumu (Bloomington Stock Centre 26897).

UASCG33178;; (Bloomington Stock Centre 32585).

;UASgcm; UASgcm (Bloomington Stock Centre 5446).

;;UAShlhmbeta (Bloomington Stock Centre 26675).

;;UAShr46^{IR} (Bloomington Stock Centre 27253 and 27254).

;;UASCG8301^{IR} (Bloomington Stock Centre 41643)

;*UASCG8301^{IR};* (Bloomington Stock Centre 62206).

;UASdrumstick^{IR}; (Bloomington Stock Centre 42548).

;;UASescargot^{IR} (Bloomington Stock Centre 28514, 34063 and 57148)

;UASescargot^{IR}; (Bloomington Stock Centre 42846)

;;UASvrille^{IR} (Bloomington Stock Centre 25989)

;UASvrille^{IR}; (Bloomington Stock Centre 40862).

;;UASslbo^{IR} (Bloomington Stock Centre 27043 and 53309).

;;UASeip78C^{IR} (Bloomington Stock Centre 26718).

;;UASpdp1^{IR} (Bloomington Stock Centre 26212)

;UASpdp1^{IR}; (Bloomington Stock Centre 40863)

;;UASCG10348^{IR} (Bloomington Stock Centre 27076 and 44091).

;;UASeip74EF^{IR} (Bloomington Stock Centre 29353).

;;UASken^{IR} (Bloomington Stock Centre 34739).

;;UASCG4404^{IR} (Bloomington Stock Centre 31923 and 50527).

Fly lines used in Chapter 4:

ubiECadGFP (Oda and Tsukita 2001).

npgal4^{2631}-Gal4/CyOGFP (O'Keefe et al. 2009).

UAS rap1^{V12}/CyOactinGFP (Boettner et al. 2000).

FRT80Brap1^{CD5}/TM6B, Tb (Boettner et al. 2003).

FRT80BubiGFP (Xu and Rubin 1993).

rap1::GFP/CyO; TM2/TM6 (Knox and Brown 2002).

dPDZGEF::EGFP/TM6B (Boettner and Van Aelst 2007).

dizzy^{A12}, FRT40/CyOGFP (Huelsmann et al. 2006).

eyFLP; FRT40ubiGFP (Xu and Rubin 1993).

GMRGal4/GMRGal4 (Freeman 1996).

Baz^{xi}, sdt^{XP96}, FRT9.2/FM7GFP;Tft/CyO (Müller and Wieschaus 1996).

uasbazGFP/CyO; GMRgal4/TM2 (Benton and St Johnston 2003).

mbt^{P1}/ mbt^{P1};; (Schneeberger and Raabe 2003).

;;FRTcno^{R2}/TM6fmiGFP, Sb, Ser (Sawyer et al. 2009).

FRT9.2ubiGFP (Bloomington Stock Centre 5154).

UASrapgap1 (Bloomington Stock Centre 22196).

Candidate-based screen

;;UASalpha-cat^{IR} (Bloomington Stock Centre 33430).

;UASap2alpha^{IR}/CyO; (Bloomington Stock Centre 12319)

;UASap2alpha^{IR}/Sm6a; (Bloomington Stock Centre 42155)

;;UASap2alpha^{IR} (Bloomington Stock Centre 27322).

;;UASbaz^{IR} (Bloomington Stock Centre 35002)

;UASbaz^{IR}; (Bloomington Stock Centre 35122, 35123 and 39072)

;UAScanoe^{IR}; (Bloomington Stock Centre 38194)

;;UAScanoe^{IR} (Bloomington Stock Centre 33367).

;UASdia^{5}/CyO; (Bloomington Stock Centre 9138).

;;UASdia^{IR} (Bloomington Stock Centre 28541).

;UASdia^{k07135}/CyO; (Kyoto Stock Centre 102532).

;;UAS-ECad^{IR} (Bloomington Stock Centre 27802).

;UAS-ECad^{KK} (VDRC Stock Centre 103962).

;;UAS-sqh^{EE} (Bloomington Stock Centre 64411).

;;UASrab4^{IR} (Bloomington Stock Centre 33757).

;;UASrab5^{IR} (Bloomington Stock Centre 30518 and 34832).

;UASrab5^{IR}*;* (Bloomington Stock Centre 51847).

;;UASrab7^{IR} (Bloomington Stock Centre 27051).

;;UASrab8^{IR} (Bloomington Stock Centre 34373).

;;UASrab11^{IR} (Bloomington Stock Centre 27730).

;UASralA^{IR}*;* (VDRC Stock Centre 105296).

;;UASrock^{IR} (Bloomington Stock Centre 28797, 34324, 35305).

;UASstar$^{48\text{-}5}$*;* (Gaengel and Mlodzik 2003).

Large-scale genetic modifier screen

KK and GD RNAi library ordered from VDRC.

2.4 Immunofluorescence Protocol

Third instar larval eye and wing discs were dissected 6-7 days after egg laying (AEL). Imaginal discs were dissected in 1X phosphate buffered saline (PBS) and fixed in 4% formaldehyde for 15 minutes at room temperature. Primary and secondary antibodies were incubated in PBS, 0.3% Triton-X overnight and for 3 hours respectively. Samples were mounted in Vectashield mounting medium (Vector Laboratories) and imaged using a Leica SP5 confocal microscope, using the 63X NA 0.6-1.4-oil immersion objective. Fiji (Schindelin et al. 2012) was used to process images.

Pupal retina and nota were collected and staged as white pupae (0% after puparium formation (APF)) and placed in a humidity chamber dish at 25°C, unless otherwise

stated. Pupal retina was described as in (Walther and Pichaud 2006). Pupal nota were dissected at 24 hours APF as described in (Jauffred and Bellaiche 2012). The staining protocol is the same as described above.

2.5 Antibodies

List of primary (**Table 1**) and secondary (**Table 2**) antibodies used in this thesis have been listed in the Appendix.

2.6 Imaging

2.6.1 Transmission Electron Microscopy

A day before harvesting the flies for TEM, flies were placed on fresh food overnight. Fly retinas were dissected in 1X PBS and transferred to an eppendorf tube containing the fixative: 2% paraformaldehyde (sigma), 2% gluteraldehyde (Ted Palla), 0.1M sodium cacodylate and 0.1% tannic acid. The retinas were left to rotate at 4°C overnight. The following day the samples were washed 5 times with 0.1M cacodylate buffer and then stained with 2% osmium tetroxide at 4°C on the rotator. The samples were subsequently washed 5 times with distilled water and then the samples were left in uranyl acetate overnight at 4°C. The uranyl acetate was removed by washing 3 times with distilled water. This was followed by serial dehydrations in ethanol (50%, 70% and 90%) for 5 minutes each followed by 3 washes in 100% EM grade ethanol for 5 minutes each. Ethanol was removed by washing in propylene oxide twice for 15 minutes. This was followed by washes with 1:1 mix of propylene oxide:EPON resin (9.6g TAAB 812 Resin, 3.8g dodecenyl succunic anhydride, 6.6g methyl nadic anhydride, 0.4g 2,4,6-tri(dimethylaminomethyl) phenol) left for 5 hours on the rotator. This was then replaced with 100% EPON and rotated overnight at room

temperature. The retina was then orientated in beam molds (EMS) and cured overnight in the 90°C oven. Finally, the retina is ready for sectioning and lead citrate staining. Imaging was carried out using the Technai G2 Spirit Electron Microscope and analysed using iTEM and Fiji (Schindelin et al. 2012).

2.6.2 Scanning Electron Microscopy

A day before harvesting the flies for SEM, flies were placed on fresh food overnight. Whole flies were fixed in an eppendorf tube containing 2% paraformaldehyde, 2% gluteraldehyde, 0.1M sodium cacodylate and 1 drop (~40uL) of Triton-X-100 for 2 hours at room temperature. The fixed flies were then serial diluted in ethanol as described below:

- Rotate in fresh 25% ethanol overnight at room temperature.
- Rotate in fresh 50% ethanol for 6-8 hours at room temperature.
- Rotate in fresh 75% ethanol overnight at room temperature.
- Rotate in fresh 90% ethanol for 6-8 hours at room temperature.
- Rotate in 100% ethanol overnight at room temperature.

The flies were subsequently critical point dried using the Automated Critical Point Dryer Leica EM CPD300. The dried flies were mounted on aluminium stubs using sticky carbon spots before gold coating. Imaging was carried out on a Field Emission Gun (FEG) Scanning Electron Microscope.

2.6.3 FRAP experiments

Whole mount *ubi-DE-Cad::GFP* pupae were mounted at 40% APF by carefully removing the pupal cuticle and carefully exposing the retina. Live imaging was performed on a Leica SP5 confocal with a 63x 1.4 numerical aperture (NA) oil

immersion objective and the following settings: pixel resolution 512 x 512; speed 400 Hz; 20% 488-nm laser power at 20% argon laser intensity; and 5x zoom. The basal tip of the *ZA* was marked with a five-pixel-diameter circle region of interest (ROI) and photo-bleached with a single pulse using 80% 488-nm laser power at 20% argon laser intensity. *ZA* recovery was recorded every 10 seconds with the previously mentioned settings for 100 frames as summarised in **Table 3** (see **Appendix**).

Time series from FRAP experiments were corrected for drift in Fiji (Schindelin et al. 2012) using the StackReg plugin, and for each experiment, three different z-axis profiles were plotted: (1) from the photo-bleached area; (2) from an equivalent area of a neighboring non-photo-bleached *AJ*; and (3) from an equivalent area of background. The obtained data were normalised using easyFRAP (Rapsomaniki et al. 2012). Data was fitted to a two-phase association curve in GraphPad Prism. Mobile fractions (y value at infinite times) were determined with Prism based on the fitting curves obtained. The p values were calculated with an unpaired two-tailed Student's t test with Welch's correction. For all data, graphical representation and statistical analysis were performed in GraphPad Prism version 6.0 for Mac (GraphPad Software; http://www.graphpad.com). Error bars represent the SEM of each dataset.

2.7 Quantification of images

2.7.1 Ommatidial cluster perimeter

Confocal images of third instar fly eye imaginal discs stained for Arm were used to measure the perimeter of ommatidial clusters using the oval tool in Fiji (Schindelin et al. 2012). Samples were tested for statistical significance using an unpaired two-tailed Student's t-test.

2.7.2 Arm fluorescence intensity

Arm fluorescence intensity measurements were determined by analysing confocal images of third instar fly eye imaginal disc clones. Mean intensity was measured using the box tool in Fiji (Schindelin et al. 2012). Data was normalised by dividing the intensity measurements with the brightest *wild-type* intensity measurement, thereby resulting in a ratio with arbitrary units. Samples were tested for statistical significance using an unpaired two-tailed Student's t-test.

2.7.3 aPKC fluorescence intensity

aPKC fluorescence intensity measurements were determined by analysing confocal images of pupal photoreceptor $dizzy^{\Delta 12}$ clones. Mean intensity was measured using the box tool in Fiji (Schindelin et al. 2012). Data was normalised by dividing the intensity measurements with the brightest $dizzy^{\Delta 12}$ intensity measurement, thereby resulting in a ratio with arbitrary units. Samples were tested for statistical significance using an unpaired two-tailed Student's t-test.

2.7.4 Baz fluorescence intensity

Baz fluorescence intensity measurements were determined by analysing confocal images of $npgal4>rap1^{IR}$ pupal photoreceptors. Mean intensity was measured using the box tool in Fiji (Schindelin et al. 2012). Data was normalised by dividing the Baz intensity measurements with the brightest *wild-type* Baz intensity measurement, thereby resulting in a ratio with arbitrary units. Samples were tested for statistical significance using an unpaired two-tailed Student's t-test.

2.7.5 *rap1* and *dizzy::GFP* fluorescence intensity

Endogenous levels of Rap1 (Knox and Brown 2002) and Dizzy (Boettner and Van Aelst 2007) were measured using rescue transgenes. Intensity measurements were determined by analysing confocal images. Mean intensity was measured using the box tool in Fiji (Schindelin et al. 2012). Data was normalised by dividing the intensity measurements taken at the *ZA* and apical domain with the brightest *wild-type* Dizzy or Rap1::GFP intensity at the *ZA,* thereby resulting in a ratio with arbitrary units. Samples were tested for statistical significance using an unpaired two-tailed Student's t-test.

2.7.6 *ZA* length measurements

Junction length were measured by analysing confocal images of pupal retina at 40% APF. Mean length was measured using the box tool in Fiji (Schindelin et al. 2012). Data was normalised by dividing the *ZA* length measurements with the longest *wild-type ZA* length measurement, thereby resulting in a ratio with arbitrary units. Samples were tested for statistical significance using an unpaired two-tailed Student's t-test. For experiments consisting of more than one experimental condition, statistical significance was determined with one-way ANOVA.

2.7.7 Apical surface area

Apical surface was determined by analysing confocal images of pupal retina at 40% APF. Mean area was measured for aPKC only, using the freehand tool in Fiji (Schindelin et al. 2012) after merging images of aPKC and Arm. Data was normalised by dividing the apical area measurements with the largest apical area calculated for *wild-type*, thereby resulting in a ratio with arbitrary units. Samples were tested for statistical significance using an unpaired two-tailed Student's t-test.

2.7.8 EM measurements

Defects in apical membrane and *ZA* morphogenesis were determined by analysing images taken from female flies only. Rhabdomere ratio, stalk membrane and *ZA* length were measured using the line tool in iTEM imaging software (ResAlta Research Technologies). Samples were tested for statistical significance using an unpaired two-tailed Student's t-test.

2.8 Microarray

2.8.1 Time course and isolation of retina

For each microarray hybridisation, 30 staged *wild-type (yw)* pupae were dissected in 1x PBS supplemented with RNAse inhibitor (Sigma Aldrich) at 25, 30, 35, 40 and 45 APF. The lamina was subsequently removed using needles to avoid contamination from glial cells. Each microarray hybridisation assay was carried out in triplicate.

2.8.2 RNA extraction

RNA extractions and hybridisations were carried out in triplicate. Retina free of brain tissue was placed in 1 mL of TRIzol reagent (Invitrogen) and the solution was applied on a QIAshredder column (Qiagen). 400 μL of chloroform was added and the solution was applied to a gDNA column (Qiagen). Total RNA was purified using the Nanodrop 2000 spectophotometer (Thermo Scientific) and qualitative analysis was carried out using an Agilent 21000 Bioanalyser (Agilent Technologies).

2.8.3 Microarray analysis

Probes were generated and hybridised according to standard Affimetrix procedure onto GeneChip *Drosophila* Genome 2.0 arrays. Transcripts were considered to be

differentially expressed when their levels showed a minimum of a 2-fold difference with a P-value cut off point of 0.05.

Chapter 3. Transcriptional profile of the developing pupal retina

Many of the studies regarding transcriptional control of polarity have focused on the TF cascade accompanying the loss of polarity during EMT. In epithelial cells, the transcription cascade that initiates polarity establishment and polarity remodelling is surprisingly understudied. The gene networks that control epithelial apical-basal polarity, will help our understanding of how cells attain their identity and undergo changes in cell shape. To this end, we used the *Drosophila* photoreceptor as a model system. Photoreceptor maturation involves the specialisation of membrane domains, which requires extensive polarity remodelling. *Drosophila* photoreceptors begin to undergo polarity remodelling at approximately 37.5% APF. This step of polarity remodelling begins with a 90° rotation of the cell's apical-basal axis (Ready 1989). This is required to align the future light gathering organelle, called the rhabdomere, with respect to the lens to brain (proximal-distal) axis of the eye. This rotation marks the beginning of a phase of sustained polarised membrane growth and maturation in this epithelial cell (Ready 1989). The onset of polarity remodelling in the fly pupal photoreceptor is characterised by the repositioning of the cell's *ZA* (**Figure 3.1**), which is accompanied by the elaboration of a specialised sub-apical membrane domain called the stalk membrane (Ready 1989). This membrane domain supports the rhabdomere and projects it toward the lumen of the ommatidium.

In order to uncover the genes that are involved in the transcriptional control of polarity remodelling and photoreceptor *ZA* morphogenesis, we carried out transcriptional profiling of retinas at the onset of polarity remodelling.

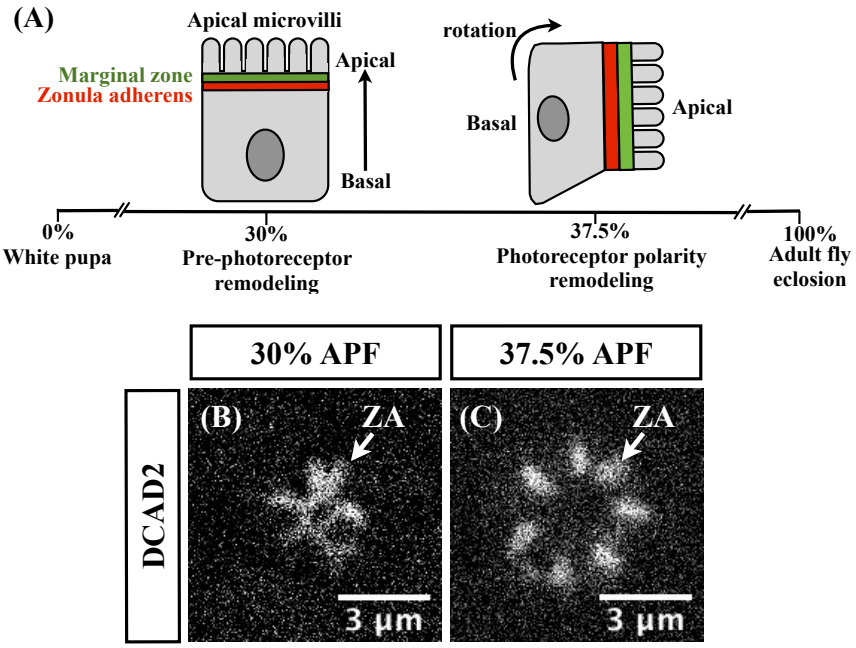

Figure 3.1: The onset of polarity remodelling in the fly pupal photoreceptor begins with a 90° rotation of the cell's *ZA*. Schematic representation of a *Drosophila* pupal photoreceptor cell, before (30% APF) and after the onset of polarity remodelling (37.5% APF). Polarity remodelling leads to the rotation of the epithelial cell and repositions the apical and basal membrane (**A**). Immunohistochemistry experiments to stain photoreceptor cells with a DE-Cad antibody (DCAD2) before (**B**) and after (**C**) the onset of polarity remodelling, highlights the change in the position of the *ZA*.

In order to carry out the transcriptional profiling over time, we set up a series of microarray experiments on the fly pupal retina at different stages of development (25, 30, 35, 40 and 45% APF). With this approach, we were able to determine which genes undergo up or down-regulation of transcription throughout these developmental time points. The chosen time points served to determine the genes that are regulated before (24-30% APF), during (35-40% APF) and after (45% APF) the onset of polarity remodelling. **Figure 3.2** outlines the protocol used to prepare RNA samples from *Drosophila* retinas for microarray analysis. *Drosophila* white pupae (0% APF) were staged and subsequently dissected at 25, 30, 35, 40 and 45% APF. To avoid contamination with glial cells from the lamina, the retina was separated from the lamina manually. The isolated retinas were then processed to extract RNA and analysed by microarray. Each time point was repeated in triplicate to ensure reliability of data.

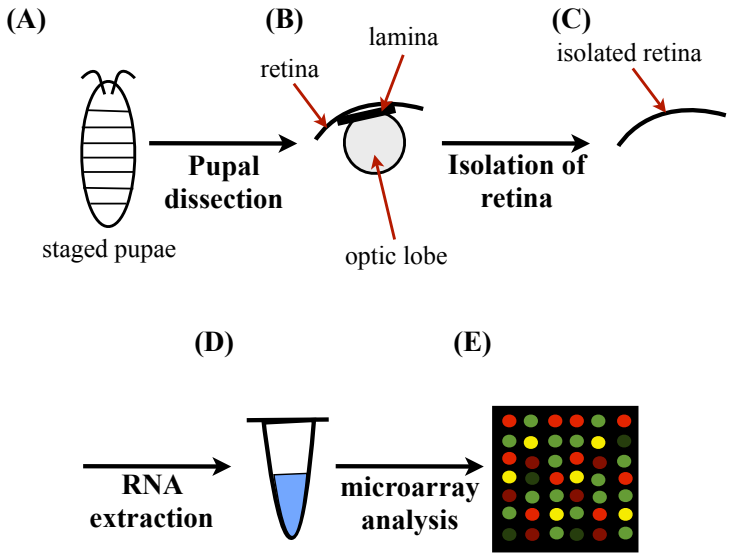

Figure 3.2: Preparation of *Drosophila* pupal retina for microarray analysis. A schematic representation of the key stages involved in the preparation of the fly pupal retina for microarray analysis. Initially, pupae are staged to the desired age (**A**) and dissected to isolate pupal retina (**B**). This is followed by the separation of the optic lobe and lamina to prevent contamination of the retina with other tissue (**C**). The isolated retinas are then processed to extract RNA (**D**), which is then used for microarray analysis (**E**). All time points were analysed in triplicate.

3.1 Statistical analysis of microarray data

The data obtained from the microarrays, were analysed by Delphine Potier in S. Aert's lab (Leuven, Belgium) using **H**ierachical **CL**ustering (**HCL**; Eisen et al. 1998), to confirm the quality and reliability of the replicates. This analysis is shown as a hierarchical tree, with similar genes and experiments clustered by a series of branches (**Figure 3.3A**). This analysis highlighted the clustering of replicates, with the 25 and 30% time points showing a very similar clustering pattern. This indicates, that within 25 and 30% of pupal retinal development, fewer changes in gene expression occur relative to the other time points. Similarly, Delphine used **P**rincipal **C**omponent **A**nalysis (**PCA**; Jolliffe, 2002), a statistical procedure used to find patterns in data sets, which can be displayed in a way that highlights the similarities and differences between data sets. This analysis confirmed clustering of all three replicates that were analysed for each time point, suggesting that the replicates are indeed very similar to each other and are therefore reliable (**Figure 3.3B**). Secondly,

the 25 and 30% time points show very similar clustering, which is in agreement with what was observed with HCL.

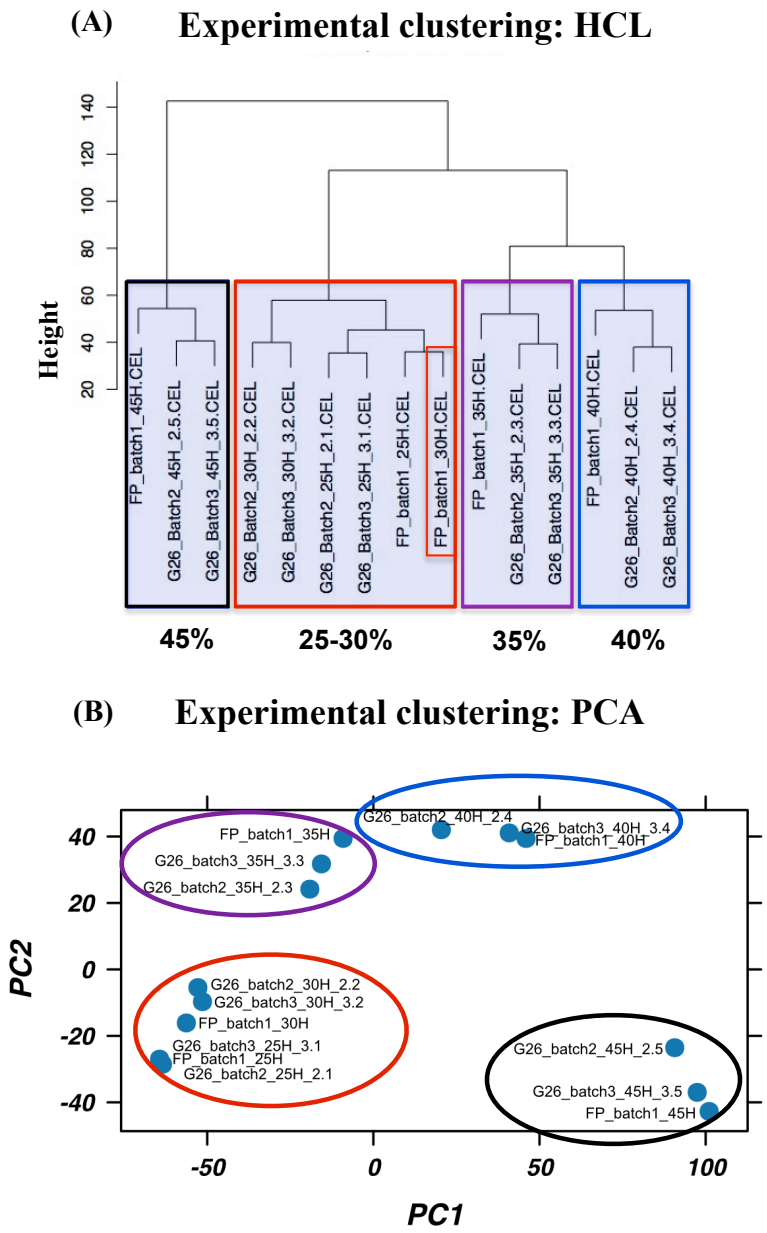

Figure 3.3: Statistical analysis of microarray data confirms clustering and reliability of replicates. Microarray data was analysed by **H**ierachical **Cl**ustering, **HCL**; (Eisen et al. 1998) to confirm the quality and reliability of the replicates. This analysis is shown as a hierarchical tree (**A**), with similar genes and experiments clustered by a series of branches. Similarly, **P**rincipal **C**omponent **A**nalysis, **PCA** (Jolliffe 2002) was used to find patterns in the microarray data, which has been displayed as a graph (**B**) to highlight the similarities between the time points. Both HCL and PCA confirmed clustering of the 25 and 35% time points, suggesting that the replicates are very similar to each other and therefore fewer changes in gene expression occur relative to the other developmental time points. For further clarity, I have colour coded the different time-points as follows: 25-30% APF (**red**), 35% APF (**purple**), 40% APF (**blue**) and 45% APF (**black**).

3.2 Gene ontology tools to organise microarray data

Following on from the quality control checks, we used the web-based gene ontology tool **G**ene **O**ntology en**RI**chment ana**L**ysis and visua**L**is**A**tion tool, **GORILLA** (Eden et al. 2009) to separate the microarray data into the following gene categories:

- Transmembrane proteins
- Cytoskeleton-related
- Trafficking
- Kinases
- Phosphatases
- Motor proteins
- Transcription factors

The top 25% most highly expressed and variable genes (i.e. the genes that displayed the largest variations in gene transcription and therefore seem to transcriptionally regulated) were sorted by passing the microarray data through expression and variability filters. Heat maps were generated and are presented in the **Appendix (Table 4-10)**. In this way, we were able to determine which genes are most highly expressed in the developing retina at around 35% APF and therefore correlate with the onset of polarity remodelling. Similarly, I could determine which genes are expressed at low levels at around 35% APF, and therefore negatively correlate with the onset of polarity remodelling in the fly pupal retina. As very little is known regarding the transcriptional control that coordinates polarity remodelling and *ZA* morphogenesis during organogenesis, I decided to focus my attention on the TFs that were identified in the microarray screen.

3.3 Transcription factor secondary screen

3.3.1 Loss-of-function analysis

To further probe the TFs that were identified in the microarray screen, we reasoned that a secondary screen would help confirm whether these TFs indeed play a role in polarity remodelling/*ZA* morphogenesis. To this end, I focused on the top 50 most variable genes encoding TFs, which are the genes that displayed the largest variations in gene transcription and therefore seem to be regulated transcriptionally (see **Appendix: Table 10**). The genes that are highly expressed when polarity remodelling is initiated (at 35% AFP), were screened by loss-of-function analysis to test whether expression is required for photoreceptor polarity remodelling. To this end, available *Drosophila* RNAi lines, generated by the Transgenic RNAi project (TRiP) were tested for polarity defects by immunofluorescence. Pupae were maintained at 18°C for 24 hours to reduce *GMR-Gal4* driver expression and suppress any early defects in retinal development. Subsequently, pupae were shifted to 25°C to increase *GMR-Gal4* levels and therefore the expression of the desired RNAi.

From the genes tested, 18 of the top 50 genes displayed an increase in gene expression at the onset of polarity remodelling. 12 of these genes had available RNAi TRiP lines (see **Appendix: Table 11**). None of these genes led to a phenotype in polarity remodelling when downregulated using RNAi in the fly pupal retina at 40% AFP or displayed a rough eye phenotype as adults. Moreover, no polarity remodelling phenotypes were observed even when the flies were maintained at 29°C to increase the expression of *GMR-Gal4*. In conclusion, from the genes I analysed, using RNAi, none seem to be involved in polarity remodelling or *ZA* morphogenesis within the fly retina. Further work will be required to confirm that these genes are indeed upregulated at the onset of photoreceptor *ZA* remodelling, and loss of function experiments will need to be complemented by using mutant alleles.

3.3.2 Gain-of-function analysis

Following from the loss-of-function analysis, I tested the genes that were expressed at low levels when polarity remodelling was initiated by gain-of-function analysis. 32 of the top 50 genes displayed low levels of expression at the onset of polarity remodelling when compared to earlier time points. 14 of these genes had available *Drosophila* EP lines (Rørth 1996), which I used to overexpress the genes prior to polarity remodelling (see **Appendix: Table 12**). Again, pupae were maintained at 18°C for 24 hours to reduce *GMR-Gal4* driver expression to suppress any earlier defects in development and then shifted to 25°C to increase *GMR-Gal4* expression. 4 of the 14 genes *(hlhmdelta, ovo, broad* and *glial cells missing)* led to defects in ommatidial morphogenesis including photoreceptor *ZA* remodelling (**Figure 3.4)**.

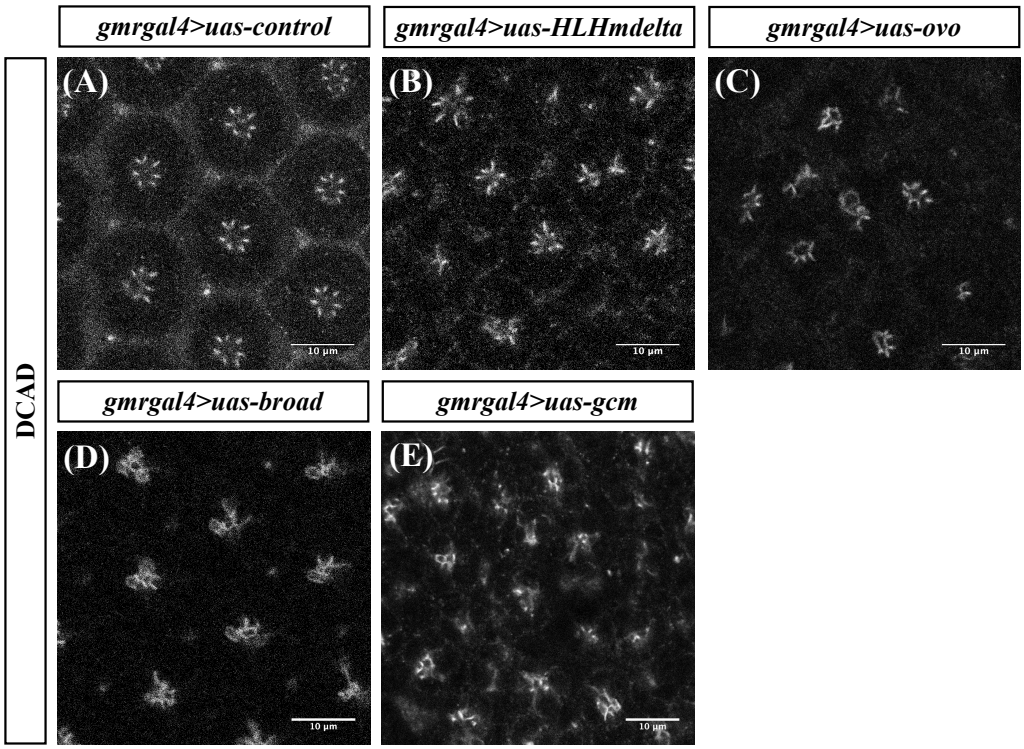

Figure 3.4: *ZA* morphogenesis defects result upon over-expression of transcription factor-related genes in fly pupal photoreceptors. Pupal retinas were dissected at 40% APF and stained with an antibody for DE-Cad in *GMRgal4* expressing *UAS-hlhmdelta* (**B**), *UAS-ovo* (**C**), *UAS-broad* (**D**) and *UAS-glial cells missing* (*gcm*; **E**). These experiments revealed defects in *ZA* remodelling compared to control (**A**).

hlhmdelta is involved in the regulation of R7-cell differentiation and in the development of cone cells, which are non-neuronal cells positioned above the photoreceptor. Using mutants that reduce *hlhmdelta* expression, cone cell development is delayed and R7-cells are replaced by R1-6 cells (Bhattacharya and Baker 2009). Overexpression of *hlhmdelta* also led to defects in photoreceptor morphogenesis (**Figure 3.4B**) suggesting that *hlhmdelta* may play an as yet unknown role in *ZA* remodelling within the fly photoreceptor. As a control, I maintained GMR-Gal4>*hlhmdelta* pupae at 18°C throughout development, however, I still observed defects in photoreceptor morphogenesis. Therefore, it is possible that in our study, suppressing expression levels of *GMRgal4* by maintaining flies at 18°C was not sufficient to suppress defects in early development of the photoreceptor. Consequently, overexpression of *hlhmdelta* expression may have led to defects in R7-cell and cone cell development, which could explain the photoreceptor morphogenesis defects observed in our study (**Figure 3.4B**).

Similarly, *broad* is required to maintain MF progression and R8-cell specification (Brennan et al. 2001), through an as yet unknown mechanism. Moreover, *broad* null mutant clones displayed aberrant photoreceptor numbers (Brennan et al. 2001), presumably as a consequence of defects earlier in development. Overexpression of *broad* led to defects in photoreceptor morphogenesis. As a control, I maintained *GMR-Gal4>UAS-broad* pupae at 18°C throughout development, however, I still observed defects in photoreceptor morphogenesis. This indicates that raising *GMR-Gal4>UAS-broad* expressing pupae at 18°C may not have been sufficient to suppress levels of *broad* at earlier stages in the development of the retina. Alternatively, *broad* plays an as yet unknown role in *ZA* remodelling within the fly photoreceptor. Taken together, further work is required to test whether *hlhmdelta* and *broad* play a role in the regulation of polarity remodelling and *ZA* morphogenesis in the fly pupal retina.

Moreover, it can be argued that some lamina remained attached to the isolated retina, which is why I identified *glial cells missing (gcm)* in our microarray. *gcm,* as the name suggests, regulates glial cell differentiation (Jones et al. 1995). However, overexpression of *gcm* leads to a rough eye phenotype and I see very severe defects in pupal photoreceptor morphogenesis. Further work is required to test whether *gcm* indeed plays a role in the regulation of polarity remodelling and *ZA* morphogenesis in the pupal retina.

The only other gene identified in our secondary screen is *ovo* (also known as *shavenbaby*). *ovo* encodes a family of zinc finger TFs (Mével-Ninio et al. 1991). *GMR-Gal4* driven *ovo* expression in the *Drosophila* eye leads to a reduction in size of the eye, as well as defects in ommatidial morphogenesis (Delon et al. 2003). Ectopic expression of *ovo* results in a strong increase in F-actin staining in fly pupal rhabdomeres (Delon et al. 2003), which could explain the ommatidial morphogenesis defects I observed in my study (**Figure 3.4C**). Our microarray analysis indicated that *ovo* transcription is greatly decreased following the onset of pupal photoreceptor polarity remodelling, suggesting that *ovo* transcription is regulated in a dynamic manner to allow photoreceptor morphogenesis, including polarity remodelling, to proceed optimally. The molecular network that coordinates photoreceptor morphogenesis through regulation of *ovo* is currently unknown and warrants further investigation.

3.4 Discussion

3.4.1 Using the whole fly retina as a model tissue

Over the past few decades, our understanding of the effectors that promote and regulate polarity remodelling has increased significantly (Tepass 2012). However, we know very little about the transcriptional regulations that govern these processes

during development. If we could understand what role this level of regulation plays during polarity remodelling *in vivo,* we could better evaluate the impact of this level of regulation for pathological situations such as cancer.

In this study, we carried out transcriptional profiling to try and discover transcriptional regulations that coordinate polarity remodelling within the fly retina. With this approach, I was able to uncover several genes that seem to be regulated during polarity remodelling. However, this approach is associated with a few limitations including the use of the whole retina. The retina is composed of several cell types, including the photoreceptor, cone and pigment cells. Consequently, any differences in gene regulation throughout the developmental time points that we chose may be due to a function of the gene in one of these three cell types. This is highlighted by the identification of genes, such as, *escargot,* which is only expressed in the interommatidial cells that lie between the developing photoreceptor cells (Lim and Tomlinson 2006) and *shaven,* which is expressed in cone and primary pigment cells (Fu and Noll 1997). In conclusion, it will be important to further analyse the hits identified in our microarray experiments to test whether they indeed play a role in polarity remodelling including *ZA* morphogenesis.

3.4.2 Untested genes identified in the microarray experiments

With our approach, I was able to identify *ovo* as a potential regulator of photoreceptor morphogenesis. However, so far I have only analysed a small number of the genes that were identified in the microarray analysis. This is largely due to the unavailability of RNAi or UAS lines that could be used to carry out gain or loss-of-function analysis. In future studies, analysis of these genes may help to discover novel genes that regulate photoreceptor morphogenesis. At present, the remaining gene families such as motor or cytoskeletal proteins that seem to be transcriptionally

regulated during retinal development have not been tested further. From these untested gene families, a number of candidates may be interesting to probe further. In the remainder of this section, I will discuss two of these hits (*dfer* and *prominin*) and the way in which they may regulate polarity remodelling/*ZA* morphogenesis.

3.4.3 A potential role for DFer in photoreceptor polarity remodelling

During dorsal closure in the fly embryo, epidermal sheets on either side of the embryo extend and meet at the dorsal midline, where they fuse to seal the embryo (Jacinto et al. 2002). Such morphogenetic movements require interplay between cell adhesion and cytoskeletal reorganisation. A similar interplay between cell adhesion and cytoskeletal reorganisation is likely to regulate polarity remodelling, making regulators of dorsal closure interesting candidates to investigate polarity remodelling. Our microarray analysis identified down-regulation of the non-receptor tyrosine kinase *fps85D/dfer* after the onset of photoreceptor polarity remodelling. *dfer* mRNA is specifically upregulated at the leading edge of the fly dorsal epidermis (Murray et al. 2006). DFer localises to the *AJ* and is required for the formation of the F-actin cable in the leading edge cells, which regulates dorsal closure (Murray et al. 2006). In $dfer^{\Delta 1}$ null mutants, the diameter of the F-actin cable is reduced, leading to slower rates of dorsal closure. Moreover, *dfer* gain-of-function $(dfer^{gof})$ embryos display increased levels of DFer and reduced levels of F-actin, with a large dorsal hole, indicative of severe dorsal closure defects (Murray et al. 2006). In $dfer^{\Delta 1}$ null mutants, Arm/β-Cat tyrosine phosphorylation is reduced almost five-fold with respect to controls. Conversely, Arm/β-Cat tyrosine phosphorylation is significantly increased in $dfer^{gof}$ mutant embryos, with much reduced levels of Arm/β-Cat, suggesting that hyper-phosphorylated Arm/β-Cat is removed from the *AJs* and degraded (Murray et al. 2006). DFer might contribute to the formation of the F-actin cable by phosphorylating Arm/β-Cat and thereby reducing its affinity for α-Cat. This

would lead to an increase in levels of cytoplasmic α-Cat, which favour the formation of F-actin bundles (Drees et al. 2005). In vertebrate mouse retinal cells, the mammalian homolog Fer, has the ability to both positively and negatively regulate stability of the E-Cad/Cat complex (Xu et al. 2004). Fer not only phosphorylates β-Cat but also targets the tyrosine phosphatase PTP1B, which dephosphorylates β-Cat, thereby stabilising the E-Cad/Cat complex (Xu et al. 2004). Whether Fer plays a similar role in the stability of the *ZA* during photoreceptor polarity remodelling remains to be tested. It is possible that reduced levels of *dFER* during polarity remodelling may correlate with reduced phosphorylation of Arm/β-Cat and therefore form more dynamic *AJs,* which might be more conducive for photoreceptor remodelling to occur (**Figure 3.5**).

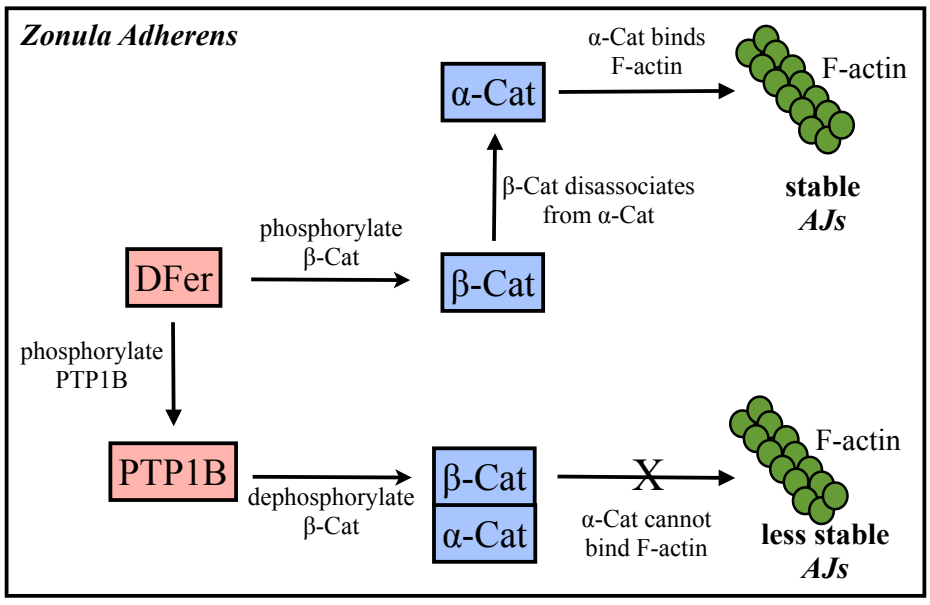

Figure 3.5: A potential role for DFer in regulating photoreceptor remodelling. The non-receptor tyrosine kinase, DFer phosphorylates β-Cat, which leads to the dissociation of α-Cat from β-Cat. Subsequently, levels of cytoplasmic α-Cat rise, leading to formation of actin bundles that stabilise *AJs*. DFer may also phosphorylate the tyrosine phosphatase PTP1B as shown in mammalian cells, where Fer dephosphorylates β-Cat, leading to α-Cat/β-Cat association. Therefore, resulting in decreased levels of cytoplasmic α-Cat, ultimately reducing the formation of actin bundles and destabilising *AJs*.

3.4.4 A potential role for Prominin in photoreceptor polarity remodelling

At the early stages of pupal photoreceptor development, the apical domains of all photoreceptor cells are initially attached to one other by the glycoprotein Chaoptin/Chp (Krantz and Zipursky 1990). At later stages of pupal photoreceptor development, apical membranes are separated by the action of Prominin/Prom and Eyes shut/Eys (Zelhof et al. 2006; Gurudev et al. 2014). Ommatidia lacking *prom* or *eys* have fused rhabdomeres (Zelhof et al. 2006), indicative of the failure to separate the apical membrane. Prom and Eys together antagonise the function of Chp to allow separation of apical membranes. This separation is followed by elongation of the apical microvilli. At this stage, Chp is required to maintain adhesion between apical microvilli. A reduction of Crb was shown to ameliorate the morphogenetic defects observed in photoreceptors mutant for *prom* and *eys* (Gurudev et al. 2014). These results suggest that *crb, chp, prom* and *eys* provide a balance of adhesion and anti-adhesion to maintain microvilli development and maintenance (Gurudev et al. 2014). As our microarrays indicate high levels of *prom* gene expression at the onset of photoreceptor polarity remodelling, it is possible that the anti-adhesion function of Prom is required to allow polarity remodelling to proceed. In the absence of *prom,* the balance between adhesion and anti-adhesion would shift towards adhesion, which would lead to defects in *ZA* morphogenesis and subsequent apical membrane separation. Further work will be required to underpin the transcriptional regulation of Prom during *ZA* morphogenesis or lumen formation.

3.5 Concluding remarks

With this part of my thesis work, we have begun to uncover potential transcriptional regulations that orchestrate photoreceptor polarity remodelling. Much work is still required to precisely underpin the molecular mechanisms that govern transcriptional control of polarity remodelling. These studies will be valuable to understand how cell

morphogenesis is regulated, which will help our understanding of when these processes malfunction leading to pathological events such as cancer.

Chapter 4. *rap1/dizzy* regulate *Adherens Junction* morphogenesis during *ZA* remodelling

The cellular and molecular pathways that promote *ZA* morphogenesis and remodelling during epithelial cell polarisation remain elusive. Recent published work from our lab identified *mbt,* as a regulator of *AJ* material accumulation at the developing *ZA* of fly pupal photoreceptors. However, in the absence of *mbt, AJ* material is only decreased by half at the developing photoreceptor *ZA*, indicating that other pathways must exist that regulate *AJ* accumulation at the developing photoreceptor *ZA*. Early studies on *rap1* implicated a role for this GTPase in *Drosophila* morphogenesis (Asha et al. 1999). Later studies confirmed a role for *rap1* in regulating cell-cell adhesion in fly wing and eye imaginal discs (Knox and Brown 2002; O'Keefe et al. 2009) and in mammalian cell culture (Hogan et al. 2004). Moreover, in the fly embryo, *rap1* and its GEF *dizzy* are required for the apical positioning of Baz and DE-Cad/Cat during the establishment of *AJs* (Spahn et al. 2012; Choi et al. 2013). However, the molecular mechanism underlying the function of Rap1 in *AJ* morphogenesis remains unclear.

The *Drosophila* embryo has been useful for the identification of key players involved in polarity establishment during cellularisation of the blastoderm. However, the cellularising embryo is less useful for understanding how polarity is remodelled during organogenesis. To test whether *rap1* plays a role during polarity remodelling, I first assessed its localisation using the *rap1::GFP* genomic rescue transgene (Knox and Brown 2002). With this approach, Rap1::GFP localisation should be identical to that of *wild-type* Rap1. These experiments show that Rap1 is colocalised with markers of the *ZA* in the developing fly eye disc, wing disc and notum (**Figure 4.1**). These findings are consistent with previous studies that also have shown a function

for *rap1* in regulating cell-cell adhesion between epithelial cells of imaginal wing (Knox and Brown 2002) and eye (O'Keefe et al. 2009) discs.

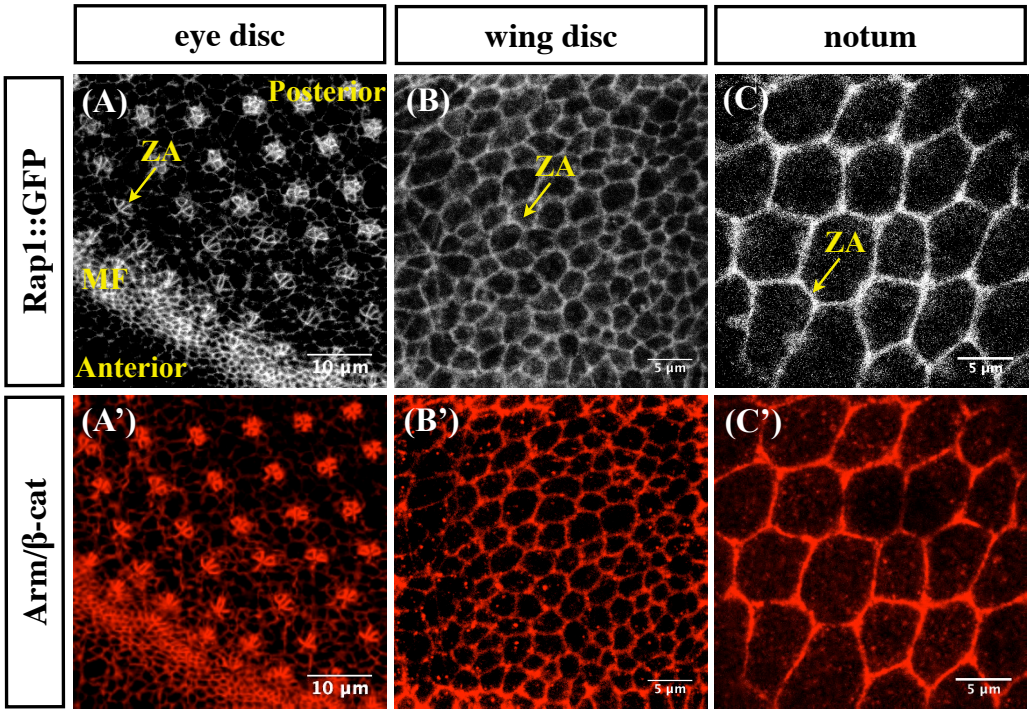

Figure 4.1: Rap1::GFP localisation in various developing *Drosophila* epithelia colocalise with the *AJ* marker Arm. Wild-type Rap1::GFP (grey) localisation was assayed using the *rap1::GFP* genomic rescue transgene (Knox and Brown 2002). Rap1::GFP localisation in *Drosophila* third instar eye imaginal disc (**A**), wing disc (**B**) and notum (**C**), which was dissected at 40% APF. The Morphogenetic Furrow (MF) has been labelled from which the ommatidial clusters emanate (from lower left to top right). The *ZA* has been annotated in all three tissues. Rap1GFP colocalises with Arm staining (**red**; **A'-C'**), suggesting a role for *rap1* in regulating *ZA* morphogenesis.

To test whether Rap1 regulates *ZA* remodelling during organogenesis, I examined two phases of photoreceptor morphogenesis: an early phase where the photoreceptor undergoes *AJ* remodelling during cell intercalation in the imaginal disc and a later phase where the cell remodels its *ZA* in pupal stages.

4.1 Rap1 regulates distribution of *AJ* material at early stages of photoreceptor development

At early stages of photoreceptor development, *rap1* mutant clones generated in the third instar eye imaginal discs revealed a function for Rap1 in DE-Cad localisation, with asymmetric or diffuse DE-Cad staining (O'Keefe et al. 2009). To confirm the function of *rap1* in early stages of retinal development, I made use of the hypomorphic *UAS-rap1*^{IR} line, expressed in most cells of the eye disc anterior and posterior to the MF using the *npGal4*^{2631} driver (O'Keefe et al. 2009). I then stained third instar eye imaginal discs with the *ZA* marker Arm. My data confirm that loss-of-function *rap1* leads to diffuse and asymmetric distribution of Arm (**Figure 4.2)**. Moreover, my data shows that *AJ* disruption is accompanied by an upregulation of activated non-muscle Myosin II (p-Myo II; **Figure 4.2E**). In *wild-type* photoreceptors, p-Myo II is mostly localised in the constricted cells of the MF, at the posterior edge of the MF where it forms an active actomyosin cable, and also around each ommatidial cluster (**Figure 4.2B;** Corrigall et al., 2007). An upregulation of p-Myo II in cells surrounding the ommatidial cluster rather than in the center of the cell might lead to decreased tension within the ommatidial cluster and therefore explain the defects in ommatidial morphogenesis.

It has been shown that Rap1 is required to recruit MyoIIB at the *ZA* of MCF-7 cells and therefore support contractile tension, which regulates morphological processes such as the formation of the epithelial *ZA* in MCF7 cells (Gomez et al. 2015). It is possible that Rap1 plays a similar role in the developing retina, with loss of *rap1* leading to mislocalisation of p-Myo II, resulting in aberrant tension and ommatidial morphogenesis defects. This hypothesis is supported by the observation that on average, ommatidial clusters are larger when *rap1* is decreased compared to *wild-*

type (n=85 junctions; **Figure 4.2I and K**). Moreover, *rap1* loss of function eye discs lead to the formation of cell 'strings' (**Figure 4.2H**), that are reminiscent of defects in *baz* and *rock* mutants, both of which are required for cell intercalation in the developing retina (Robertson et al. 2012).

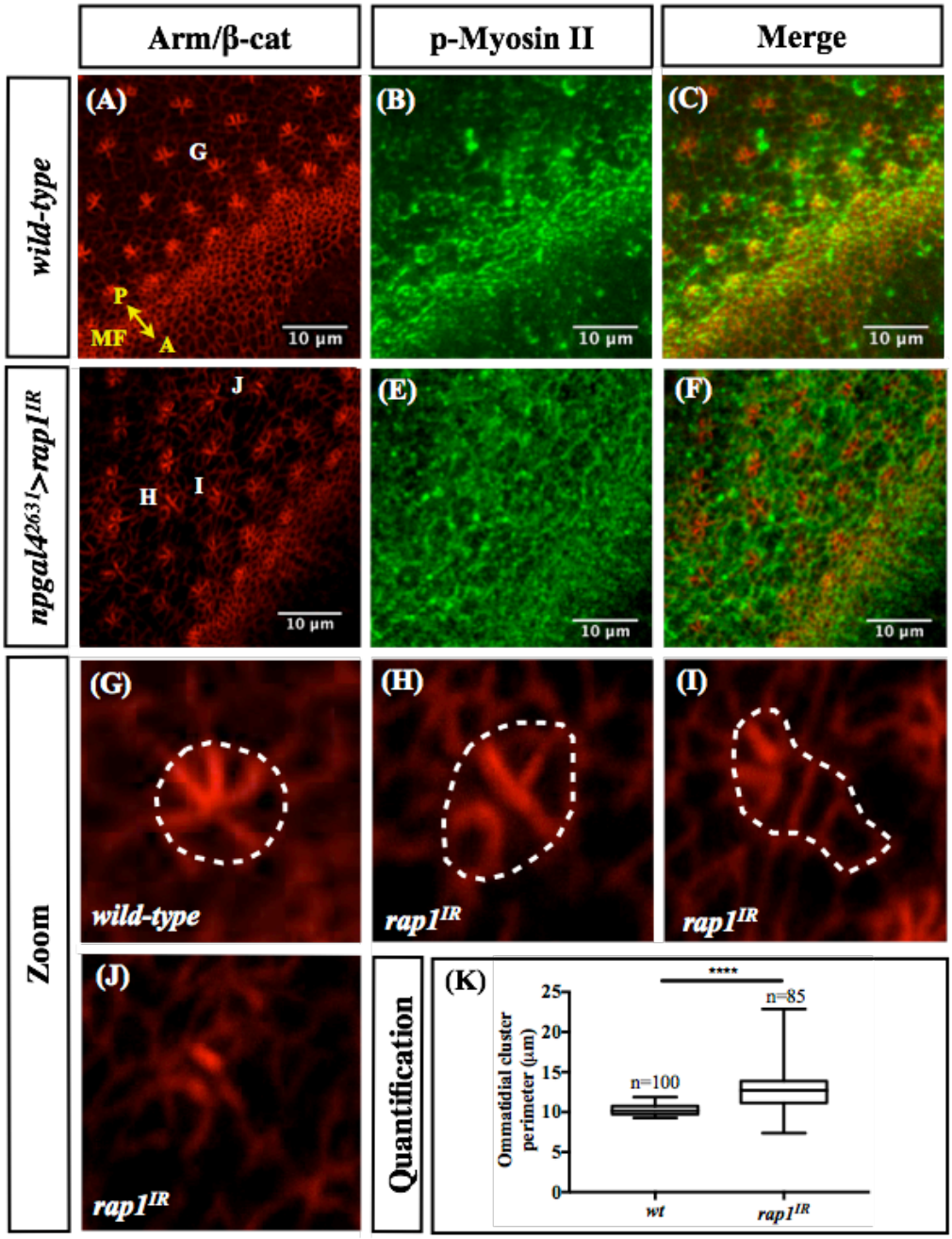

Figure 4.2: Defects in early stages of the development *of rap1^{IR}* eye imaginal discs. Morphogenetic Furrow (MF) is labelled along with the direction of the Anterior (A)/Posterior (P) axis in *wild-type* third instar eye imaginal discs stained for Arm (**A**) and active p-Myo II staining (**B**). Merge for *wild-type* is shown in (**C**). *rap1^{IR}* third instar eye imaginal discs display defects in patterning of the eye (**D**). An upregulation in p-Myo II staining (**E**) might explain the ommatidial morphogenesis defects observed. Merge for *rap1^{IR}* is shown in (**F**). Individual clusters have been enlarged to better illustrate the ommatidial patterning defects seen in *rap1^{IR}* discs compared to control (**G**). These defects include: ommatidial cluster enlargement (**H**), 'string' formation (**I**) and asymmetric Arm staining (**J**). The perimeter of ommatidial clusters was quantified using Arm stainings from both genotypes and shown as a graph in (**K**). 100 ommatidial clusters were measured for *wild-type* and 85 for *rap1^{IR}*. An unpaired t-test was carried out to confirm statistical relevance. **** represents a p-value of ≤0.0001.

In conclusion, I have identified a role for *rap1* in the accumulation and distribution of *AJ* material during early fly photoreceptor development, which may rely on the distribution of p-Myo II at the remodelling *ZA*. Moreover, Rap1 might regulate cell intercalation, alongside Baz and ROCK.

4.2 Dizzy regulates distribution of *AJ* material at early stages of photoreceptor development

My data are in agreement with previous work where *rap1* was shown to be required for the proper distribution of DE-Cad in the developing wing disc (Knox and Brown, 2002). However, the GEFs and GAPs that regulate the function of *rap1* in the distribution of *AJ* material are unknown. A screen previously carried out in the lab by Noelia Pinal (unpublished data), was used to identify GEFs and GAPs involved in apical membrane morphogenesis in the fly pupal photoreceptor. In this screen, around 60 GEFs and GAPs were tested for defects in apical membrane morphogenesis, using immunofluorescence staining in late pupal retina and positive hits were confirmed with EM. Using this candidate-based approach, Noelia identified the Rap1GEF *pdzgef/dizzy*, as a potential regulator of *ZA* morphogenesis, thus, making *dizzy* an ideal candidate to study the role of *rap1* in *ZA* morphogenesis in the developing photoreceptor. Indeed, using the rough eye modifier assay, I found that *rap1* genetically interacts with the *dizzy* loss-of-function allele ($dizzy^{A12}$; **Figure 4.3A-C**). A dose-dependent reduction of *dizzy* in the *rap1* RNAi $(rap1^{IR})$ background enhances the *rap1* rough eye phenotype, suggesting that *rap1* and *dizzy* function in the same or parallel cellular process. If *dizzy* functions as a Rap1-GEF during *ZA* remodelling, the *dizzy* loss-of-function phenotype should resemble that of loss-of-function *rap1*. In order to test this hypothesis, I first generated $dizzy^{A12}$ clones in fly

eye imaginal discs specifically in the eye using the FRT/FLP system (Xu and Rubin 1993).

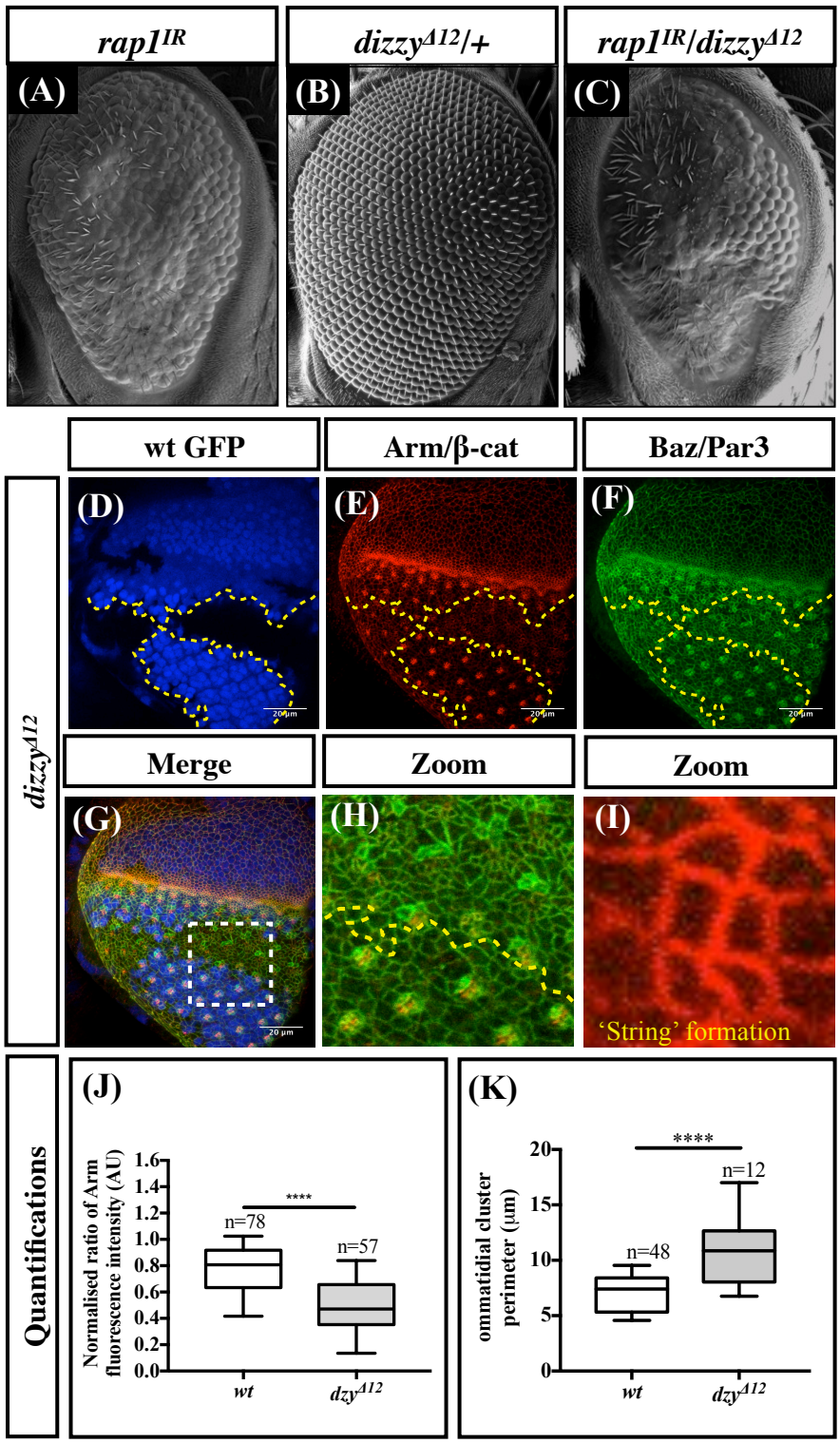

Figure 4.3: *dizzy*$^{\Delta 12}$ eye discs display defects in accumulation of *ZA* material. *Drosophila* genetics reveal an interaction between *npgal4>rap1*^{IR}, which leads to a mild rough eye phenotype (**A**) and the *dizzy* hypomorph *dizzy*$^{\Delta 12}$, shown by the enhanced rough eye phenotype (**C**). Removing one copy of the *dizzy*$^{\Delta 12}$ transgene results in a *wild-type* eye (**B**). Clones generated in third instar eye imaginal discs using the Eyflp/FRT system (Xu and

Rubin 1993), where *wild-type* cells are marked by GFP in **blue** and a yellow dotted line is used to outline the border between *wild-type* and mutant cells (**D**). Clones were stained for the *ZA* markers Arm (**E**) and Baz (**F**). $dizzy^{A12}$ cells reveal a marked reduction in the accumulation of Arm (**E**) and disorganisation of Baz (**F**). Merge is shown in (**G**) with a box outlining the enlargement panel shown in (**H**) to better illustrate the ommatidial morphogenesis defects caused by the loss of *dizzy*. *dizzy* loss-of-function also leads to the formation of 'strings' that are reminiscent of defects in cell intercalation (**I**). Arm intensity is measured in both genotypes and shown as a graph in (**J**). Average intensity of Arm was calculated per cell for 78 *wild-type* and 57 $dizzy^{A12}$ mutant ommatidia. The perimeter of ommatidial clusters was quantified using Arm stainings from both genotypes and shown as a graph in (**K**). 48 ommatidial clusters were measured for *wild-type* and 16 for $dizzy^{A12}$. An unpaired t-test was carried out to confirm statistical relevance. **** represents a p-value of ≤0.0001.

During ommatidial morphogenesis, *dizzy* loss-of-function leads to reduced staining of *AJ* material including Arm and Baz (n=57 junctions; **Figure 4.3D-J**). Moreover, *dizzy* loss-of-function also leads to the assembly of a 'string' of photoreceptors instead of ommatidial clusters (**Figure 4.3I**), which is accompanied by an enlargement of photoreceptor clusters (**Figure 4.3K**). In conclusion, *dizzy* loss-of-function leads to intercalation defects during ommatidial morphogenesis. These defects resemble the *rap1* loss-of-function, which together with our genetic interaction experiments is consistent with *dizzy* functioning as a GEF for *rap1* in the early stages of photoreceptor morphogenesis.

4.3 Rap1 colocalises with *AJ* markers in the remodelling pupal photoreceptor

My data have shown that *rap1* and its GEF *dizzy* regulate cell intercalation and the homogeneous distribution of *AJ* material at the remodelling *ZA* during early eye development. Next, I made use of the developing fly pupal photoreceptor, which undergoes a dramatic change in shape that requires remodelling of the epithelial *ZA*. In order to test where Rap1 localises in remodelling pupal epithelial cells, I made use of a *rap1::GFP* genomic rescue transgene (Knox and Brown 2002) and examined the localisation of Rap1. In the remodelling pupal photoreceptor, similar to early stages

of photoreceptor development, Rap1 colocalises with the *AJ* marker, Arm (**Figure 4.4A-E)**. Rap1 is also apically localised as shown by its colocalisation with the apical marker aPKC. Apical localisation of Rap1 suggests a potential function for Rap1 within the apical domain. This is consistent with a report, showing that Rap1 forms a complex with aPKC-Par6 in co-immunopreciptation experiments from fly embryo extracts (Carmena et al. 2011). Whether a similar complex exists in epithelial cells has not been examined.

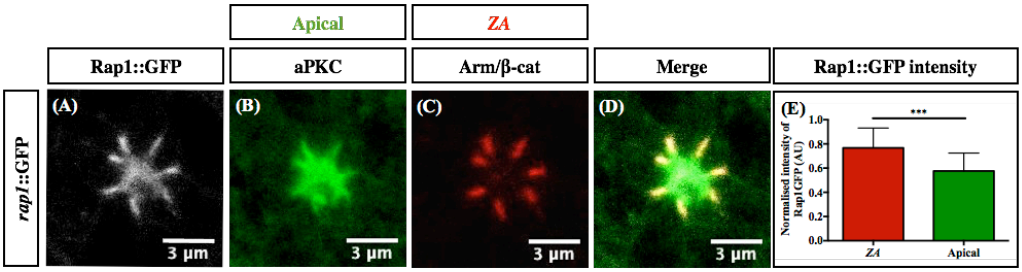

Figure 4.4: Rap1 localisation in developing *Drosophila* pupal photoreceptors. Rap1::GFP localisation is shown using the *rap1::GFP* genomic rescue transgene (Knox and Brown 2002) in *Drosophila* pupal photoreceptors dissected at 40% APF (**A**). Rap1::GFP colocalises with the apical marker aPKC (**B**) and *AJ* marker Arm (**C**). Merge is shown in (**D**) and quantification of normalised Rap1::GFP intensity in the *ZA* (**red bar**) and apical (**green bar)** compartments (**E**). 77 junctions and 11 ommatidia were analysed for the quantification. An unpaired t-test was carried out to confirm statistical relevance. *** represents a p-value of ≤0.001.

To test if the localisation of Rap1 depends on the apical epithelial gene network, I examined Rap1 localisation in baz^{XR11}, sdt^{XP96} double mutant cells, where the entire apical gene network is removed (Müller and Wieschaus 1996). It is important to note that Rap1::GFP is shown in the same channel as the weak nuclear signal of ubiGFP, used to mark *wild-type* cells. Consequently, I had to saturate levels of Rap1::GFP to determine which cells are *wild-type* and which are mutant. Nevertheless, I found that *ZA* domains, which contain Rap1, are still present in conditions where all apical determinants are removed (**Figure 4.5A-D**). These data indicate, that Rap1 localisation is not dependent on the apical gene network.

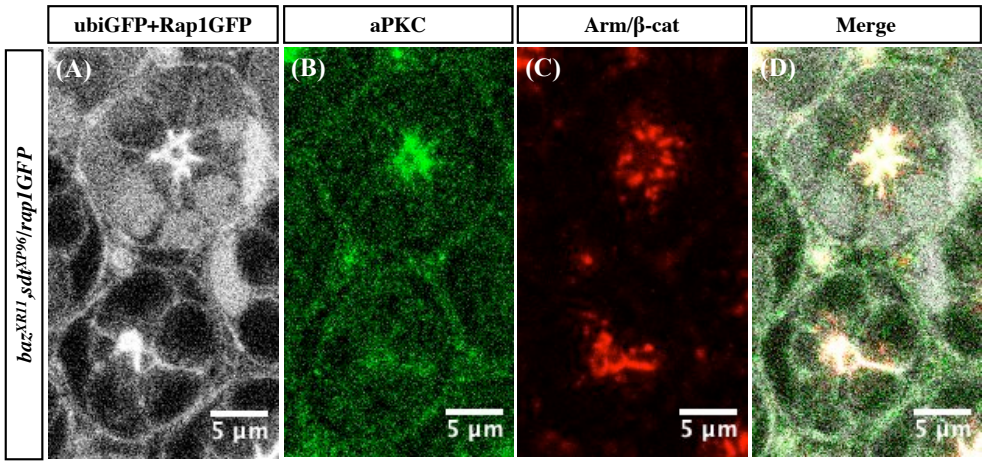

Figure 4.5: Rap1 localisation is not dependent on the apical gene network in fly pupal photoreceptors. *baz*^{XR11}, *sdt*^{XP96} double clones were made using the FLP/FRT system (Xu and Rubin 1993) in *Drosophila* pupal photoreceptors dissected at 40% APF. *Wild-type* cells are marked by ubiGFP (**grey; A**), with brighter nuclear signal indicating the twin spot. Rap1 localisation (also in **grey; A**) is shown using the *rap1::GFP* genomic rescue transgene (Knox and Brown 2002). Photoreceptors are stained for the apical marker aPKC (**B**) and the *ZA* marker Arm (**C**). Merge is shown in (**D**). Loss of aPKC in mutant cells confirms the loss of the apical gene network.

4.4 Dizzy colocalises with *AJ* markers in the remodelling pupal photoreceptor

So far, my data indicates that Rap1 is localised at the developing *ZA* of pupal photoreceptors and its localisation does not dependent on the apical gene network. In order to test if the localisation of Dizzy is consistent with regulating Rap1 during pupal photoreceptor remodelling, I made use of a *dizzy::GFP* genomic rescue transgene. This transgene is fully functional as it reverts all the dorsal closure defects associated with *dizzy* loss-of-function in the fly embryo (Boettner and Van Aelst 2007). Localisation of *dizzy::GFP* was mostly in the *ZA* (**Figure 4.6A-E**), which is consistent with its role as a Rap1-GEF during *ZA* remodelling in the pupal photoreceptor. However, as both Rap1 and Dizzy are localised in the apical region as well, I cannot rule out a potential function for *rap1/dizzy* in the apical domain.

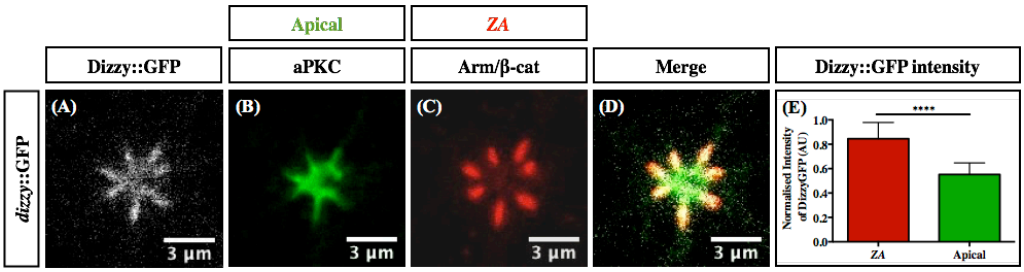

Figure 4.6:Dizzy is a potential GEF for Rap1 during *ZA* remodelling in the fly pupal photoreceptor. Dizzy localization (**A**) is examined in *Drosophila* pupal photoreceptors dissected at 40% APF using the *dizzy::GFP* genomic rescue transgene (Boettner and Van Aelst 2007). Dizzy colocalises with the apical marker aPKC (**B**) and *ZA* marker Arm (**C**). Merge is shown in (**D**). Quantification of normalised Dizzy::GFP intensity is shown within the *ZA* (**red bar**) and apical (**green bar)** compartments (**E**). 42 junctions and 6 ommatidia were analysed for the quantification. An unpaired t-test was carried out to confirm statistical relevance. **** represents a p value of ≤0.0001.

4.5 *rap1* regulates integrin-mediated cell signalling in the fly pupal photoreceptor

The localisation of Rap1/Dizzy at the remodelling *ZA* pupal photoreceptor suggests that Rap1/Dizzy are involved in *ZA* morphogenesis. To test if Rap1/Dizzy regulate *ZA* morphogenesis, I decided to use available null mutants for *rap1*. Loss of *rap1* is lethal to the fly (Hariharan et al. 1991), however, it is possible to generate *rap1* mutant clones specifically in the eye using the FRT/FLP system (Xu and Rubin 1993). Null mutant clones for the *rap1* null allele *($rap1^{CD5}$)* show that cells fall through the retinal floor (**Figure 4.7A-E**), a phenotype indicative of defects in integrin-mediated cell-cell adhesion. Indeed, I found that *rap1* genetically interacts with *myospheroid (mys),* which encodes for the beta subunit of the integrin complex, leading to a lethal interaction when both *rap1* and *mys* levels are reduced. These data are consistent with a report that describes a function for *rap1* in integrin–mediated adhesion during dorsal closure in the fly embryo (Ellis et al. 2013).

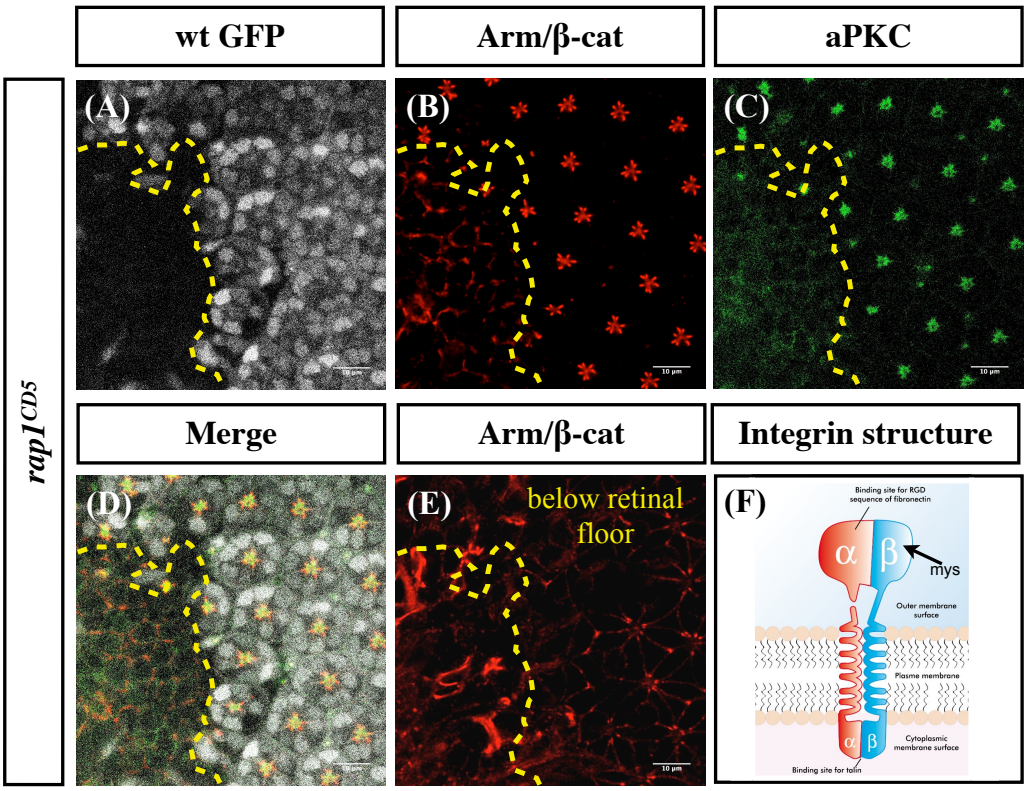

Figure 4.7: *rap1*^{CD5} null mutants display potential defects in integrin-mediated cell-cell adhesion. *rap1*^{CD5} null clones generated in the fly pupal eye using the FLP/FRT system (Xu and Rubin 1993). *Wild-type* cells are marked by GFP (**grey**) and separated from the mutant ommatidial clusters by a yellow dashed line (**A**). Photoreceptors are stained for the *ZA* marker Arm (**B**), apical marker aPKC (**C**) and merge is shown in (**D**). A *z* slice below the floor of the pupal retina shows aberrant accumulation of Arm in *rap1*^{CD5} mutant cells (**E**). A schematic image of α- and beta-subunits (*myospheroid* in flies) that comprise integrin molecules is shown in **F** (image adapted from http://www.amdbook.org/content/figure-3-alpha-and-beta-subunits-integrins-are-transmembrane-proteins).

Our data shows that *rap1* null mutants display a strong loss-of-function phenotype, leading to delamination of the photoreceptor. As a consequence, use of the *rap1* null allele might be more challenging in separating the role of Rap1 in integrin-mediated adhesion from *AJ*-mediated cell-cell adhesion. In this regard, I reasoned that the hypomorphic *rap1/dizzy* alleles might be more informative.

As integrin-dependent adhesion can drive delamination (Meghana et al. 2011), I first tested for delamination and positioning of integrins at the retinal floor using an antibody for Mys in *rap1*^{IR} and *dizzy*$^{\Delta 12}$ loss-of-function mutants. In hypomorphic *rap1* or *dizzy* photoreceptors, integrin remains positioned at the basal pole of the cell

(**Figure 4.8A-B**). Moreover, photoreceptors are mispositioned but do not delaminate as seen in *rap1* null cells. It is likely that *rap1*^{IR} does not lead to the complete loss of *rap1* expression and remaining *rap1* is able to mediate its effects on integrin-based cell-cell contacts.

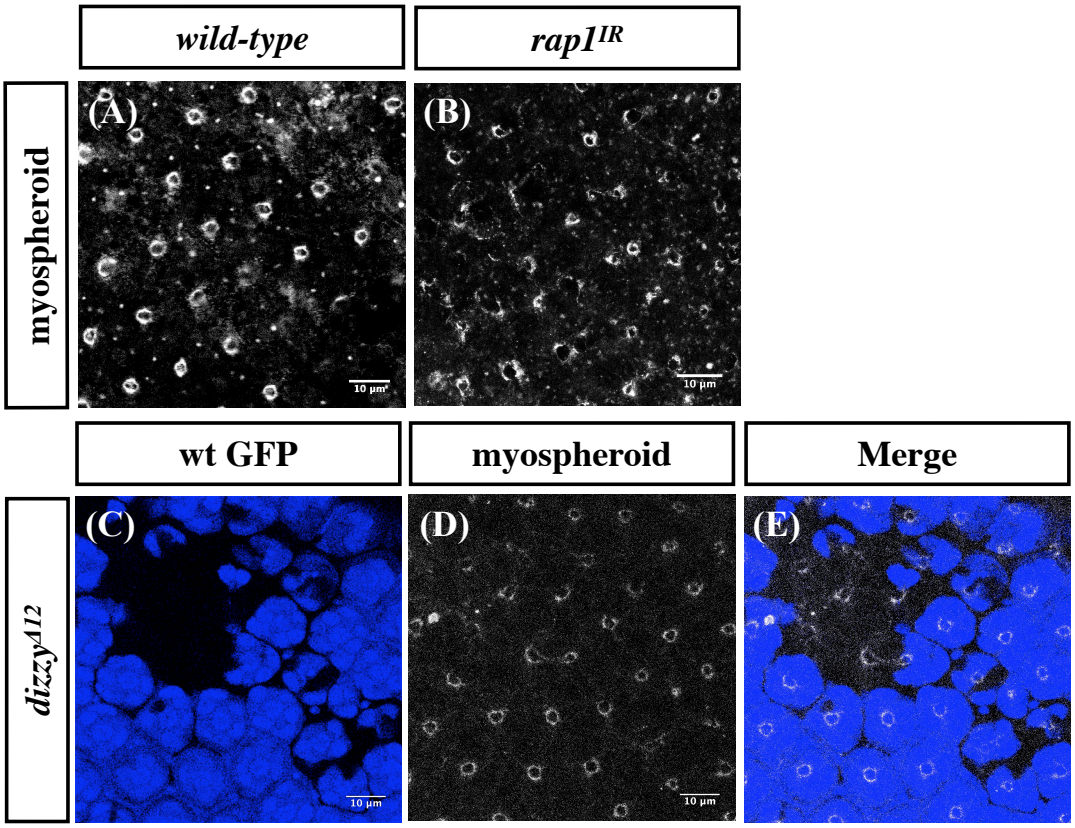

Figure 4.8: Integrin localisation in *rap1*^{IR} and *dizzy*$^{\Delta 12}$ loss-of-function mutants. Beta PS/myospheroid staining in *wild-type* (**A**) and *rap1*^{IR} pupal photoreceptors (**B**). *dizzy*$^{\Delta 12}$ clones were generated in the fly pupal eye using the FLP/FRT system (Xu and Rubin 1993). *Wild-type* cells are marked by GFP in **blue** (**C**) and photoreceptors are stained for the integrin marker Beta PS/myospheroid (**D**). Merge is shown in (**E**). Due to mispositioning of cells within the retina, integrin is located at various positions within the epithelium however, cells do not fall below the floor of the retina as seen in *rap1* null cells.

Similarly, the hypomorphic *dizzy*$^{\Delta 12}$ allele does not fully eliminate the function of *dizzy* and therefore only reduces levels of active Rap1. Presumably, in these mutants the residual active Rap1 is able to maintain integrin-based contacts with the ECM (**Figure 4.8C-E**). Taken together, these results indicate that *rap1*^{IR} and *dizzy*$^{\Delta 12}$ loss-of-function mutants might be more useful in understanding the role of *rap1/dizzy* in

polarity remodelling in the fly pupal photoreceptor, without complicating the analysis with defects in integrin-mediated cell adhesion.

4.6 Loss and gain-of-function *rap1* affects *ZA* remodelling in the developing pupal photoreceptor

Whether *rap1* gain or loss-of-function leads to defects in pupal photoreceptor development had previously not been tested. To this end, I raised *wild-type*, $rap1^{IR}$ and constitutively active $rap1^{V12}$ flies at 18°C to suppress any *ZA* morphogenesis defects in the developing eye disc. Subsequently, I shifted the pupae to 25°C at approximately 24 hours APF to allow $rap1^{IR}$ and $rap1^{V12}$ to be expressed prior to the onset of polarity remodelling. I then dissected the pupal retinas at 40% APF. In the remodelling pupal photoreceptor, the most striking effect of the loss of *rap1* was a reduction in the size of *ZA* by almost half. *ZA* length was measured using stainings for Arm and compared to control junctions (n=100 junctions; **Figure 4.9A-H**). Many pupal ommatidia were missing one cell, which is likely to be the R7 cell as *rap1* promotes apical accumulation of the sevenless receptor, which is required for R7 differentiation in the pupal photoreceptor (Baril et al. 2014). In the case of $rap1^{V12}$, *ZA* length was more varied with an overall increase in length (n=90 ommatidia; **Figure 4.9I-L**).

Moreover, in $rap1^{V12}$ pupal retina polarity remodelling defects were characterised by the invasion of *AJ* material to a more apical region of the cell. Invasion of *AJ* material was quantified by measuring the area of the apical membrane using stainings for aPKC that did not overlap with the *ZA* marker Arm (n=27 junctions; **Figure 4.9L)**. These experiments suggest that *rap1* might regulate polarity by

affecting *ZA* morphogenesis through the accumulation, distribution and stability of DE-Cad at the remodelling *ZA*.

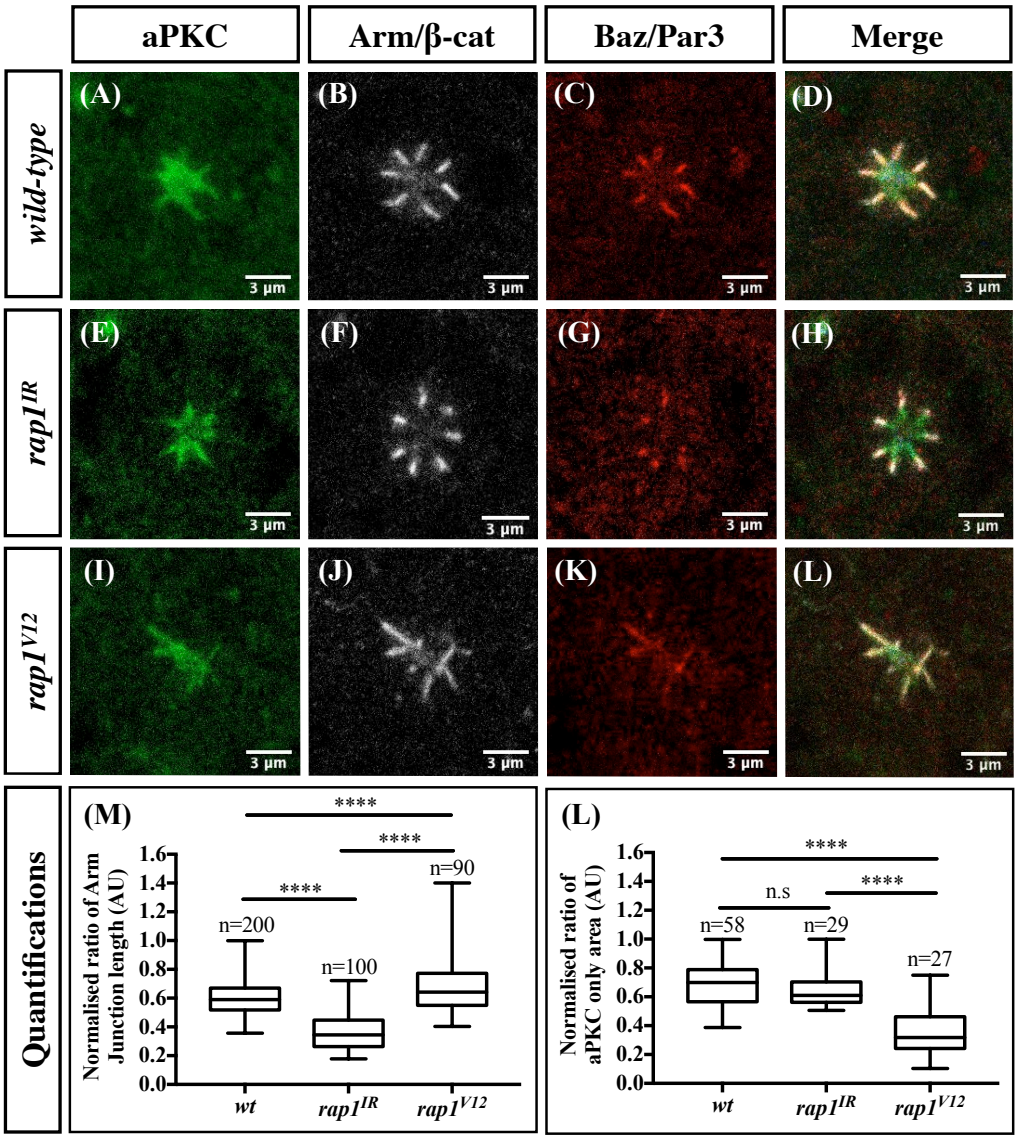

Figure 4.9: *rap1* loss and gain-of-function analysis reveals *ZA* morphogenesis and polarity remodelling defects in the pupal photoreceptor. *wild-type* pupal photoreceptors stained for aPKC (**A**), Arm (**B**) and Baz (**C**). Merge for *wild-type* pupal photoreceptors are shown in (**D**). Stainings on $rap1^{IR}$ pupal photoreceptors reveal *ZA* morphogenesis defects with the reduction in *ZA* length shown by *ZA* markers Arm (**F**) and Baz (**G**). Stainings on $rap1^{V12}$ pupal photoreceptors reveal polarity remodelling defects with the failure to properly separate the apical (**I**) and *ZA* (**J-K**) domains. *ZA* length in $rap1^{V12}$ pupal photoreceptors is more varied, with an overall increase in length. *ZA* length is measured in each genotype using stainings for Arm and shown as a graph (**M**). Apical only region was measured in each genotype using merged images of aPKC and Arm and shown as a graph (**L**), to illustrate a reduction in apical area in $rap1^{V12}$ pupal photoreceptors. All pupae were dissected at 40% APF. One-way Anova was carried out to confirm statistical relevance. **** represents a p-value of ≤0.0001. A p-value 0.4037 was deemed non-significant (n.s).

4.7 *dizzy* loss-of-function affects *ZA* remodelling in the developing pupal photoreceptor

If *dizzy* functions as a Rap1-GEF during later stages of photoreceptor morphogenesis, the *dizzy* loss-of-function phenotype should resemble that of *rap1* loss-of-function. In order to test this hypothesis, I generated $dizzy^{\Delta 12}$ clones in the pupal retina and stained for markers of polarity (**Figure 4.10**). *dizzy* loss-of-function leads to a decrease in *ZA* length (n=22 junctions; **Figure 4.10 A, C** and **E**) and loss of one photoreceptor cell from most ommatidial clusters. However, the loss of *dizzy* does not affect the accumulation of apical markers such as aPKC (n=8 ommatidia; **Figure 4.10B** and **F**). Other markers of polarity including Sdt, PatJ and Crb were also tested in *rap1* and *dizzy* loss-of-function cells, with no significant difference in accumulation (**See Appendix: Table 13**). Therefore, loss of *rap1/dizzy* leads to similar phenotypes in the remodelling photoreceptor, which is compatible with *dizzy* functioning as a Rap1-GEF during photoreceptor morphogenesis.

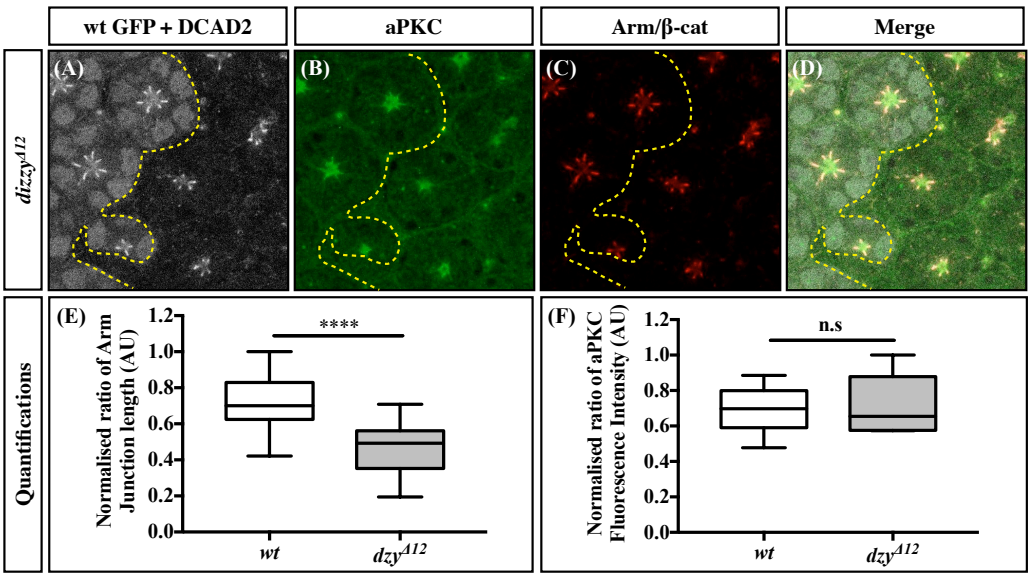

Figure 4.10: *dizzy*$^{\Delta 12}$ pupal photoreceptor reveal defects in accumulation of *ZA* material. Clones generated in the fly pupal photoreceptor using the FLP/FRT system (Xu and Rubin 1993) where *wild-type* cells are marked by GFP (grey) and separated from the mutant ommatidial clusters by a yellow dashed line (**A**). Pupal photoreceptors are stained for the *ZA* marker DCAD2 (**A**), the apical marker aPKC (**B**) and *ZA* marker Arm (**C**). Merge is shown in (**D**). *dizzy*$^{\Delta 12}$ mutant cells reveal a marked reduction in the length of the *ZA* as measured by Arm stainings (**E**). However, no difference in aPKC intensity was found (**F**). 45 *wild-type* and 22 *dizzy*$^{\Delta 12}$ mutant junctions were analysed for *ZA* length quantification. An unpaired t-test was carried out to confirm statistical relevance. **** represents a p-value of ≤0.0001. aPKC fluorescence intensity was measured in 20 *wild-type* and 8 *dizzy*$^{\Delta 12}$ mutant ommatidia. An unpaired t-test was carried out to confirm statistical relevance. With a p-value of 0.7428, the difference in aPKC intensity was not significant (n.s).

4.8 *rapgap1* affects *ZA* remodelling in the developing photoreceptor

Our data have shown that *dizzy* plays a role in the regulation of *rap1* during polarity remodelling in the developing fly pupal photoreceptor. Whether Rap1 activity is regulated by means of spatially localising its GEFs and GAPs is currently not clear. However, at present there is no antibody or rescue transgene for the only known fly Rap1-GAP (Rapgap1; Chen et al. 1999). In the gastrulating embryo, Rapgap1 has been shown to spatially modulate the activity of *rap1* (Wang et al. 2013). Rapgap1 reduces coupling of the *AJs* to the actin cytoskeleton, thereby allowing cells to shorten and form a deep fold during epithelial cell invagination. In contrast, reduced expression of *rapgap1*, leads to tight coupling of *AJs* to the actin cytoskeleton

thereby, preventing cells from shortening and invaginating and ultimately resulting in abnormal fold formation (Wang et al. 2013). Whether Rapgap1 also regulates the activity of *rap1* during pupal photoreceptor remodelling is not known. To this end, I repeated the same temperature shift assays on flies overexpressing *UAS-rapgap1* in the fly eye using the *GMRgal4* driver.

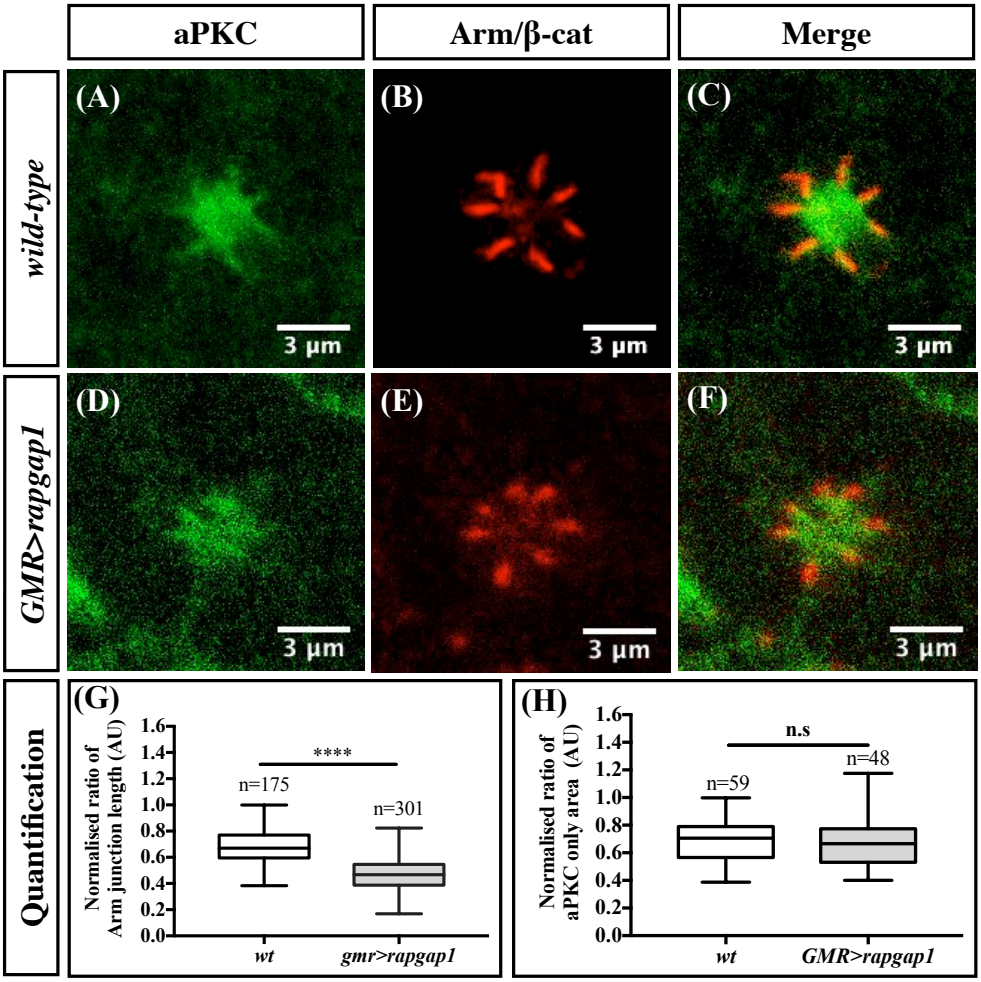

Figure 4.11: Gain-of-function *rapgap1* reveals *ZA* morphogenesis defects in the pupal photoreceptor resembling *rap1*^{IR}. *wild-type* pupal photoreceptor stained for aPKC (**A**), Arm (**B**) and a merge shown in (**C**). Stainings on *GMR>UAS-rapgap1* pupal photoreceptors revealed *ZA* morphogenesis defects with a reduction in *ZA* length shown by the *ZA* marker Arm (**D**). *ZA* length was measured in both genotypes using stainings for Arm and shown as a graph (**G**). Apical only region was measured in each genotype using merged images of aPKC and Arm and shown as a graph (**H**). Unpaired t-tests were carried out to confirm statistical relevance. **** represents a p-value of ≤0.0001 and a p-value of 0.5282 was deemed non-significant (n.s).

In the remodelling pupal photoreceptor, the size of the *ZA* is reduced by almost half in *GMR>UAS-rapgap1* (n=301 junctions) as measured by Arm staining compared to control junctions (n=175 junctions; **Figure 4.11A-G**). However, the aPKC only area is unchanged suggesting that Rapgap1 may not be required to separate the apical domain from the *ZA* (n=48 junctions; **Figure 4.11H**), but instead regulates the size of the *ZA*. Taken together, these experiments indicate that gain-of-function *rapgap1* resembles the $rap1^{IR}$ phenotype, which is consistent with *rapgap1* functioning as a Rap1-GAP during the regulation of *ZA* remodelling in the fly pupal photoreceptor.

4.9 *rap1* affects cell morphogenesis in the adult fly retina

To gain a more quantitative view of the function of *rap1* in photoreceptor morphogenesis, I carried out Electron Microscopy (EM) on 3-day old $rap1^{IR}$ adult retina (**Figure 4.12A-H**). The apical membrane of the adult fly photoreceptor consists of two membrane domains: the rhabdomere and the stalk membrane. The rhabdomere is an actin-rich organelle that has a characteristic spherical shape (Wolff and Ready 1993). I found that in $rap1^{IR}$ adult retina, photoreceptor clusters where cell number was reduced, rhabdomere shape elongates compared to controls (**Figure 4.12C, magnified in D**). Enlarged, elongated or split rhabdomeres are characteristic of defects in actin regulation (Bahri et al. 1997) and mutations that affect rhabdomere morphology usually result in a rough eye phenotype.

Moreover, EM analysis allowed me to precisely measure the length of the *ZA* (**Figure 4.12G**) and the size of the stalk membrane (**Figure 4.12H**). These experiments confirmed that *rap1* regulates the size of the apical membrane domain, in addition to regulating the size of the *ZA*. More specifically, these measurements indicate that the stalk membrane increases at the expense of the *ZA*. Other notable

morphogenetic defects include missing photoreceptor cells and fused ommatidial clusters (**Figure 4.12B**). It has been reported that in adult heterozygous *rap1*$^{rv(R)B1}$ flies, approximately 70% of ommatidia are missing one cell. In 70% of the cases, the missing photoreceptor is the R7 cell, but the remainder are missing one of the outer (R1/R6) cells (Hariharan *et al.,* 1991). Moreover, Hariharan *et al.,* showed that in approximately 10% of ommatidia, the secondary pigment cell that separates adjacent ommatidia is missing which, could partially explain the fusion of ommatidia and the irregular spacing between ommatidia in our experiments (**Figure 4.12B**). These data show that *rap1* regulates photoreceptor morphogenesis, in particular the length of the *ZA* and the stalk membrane.

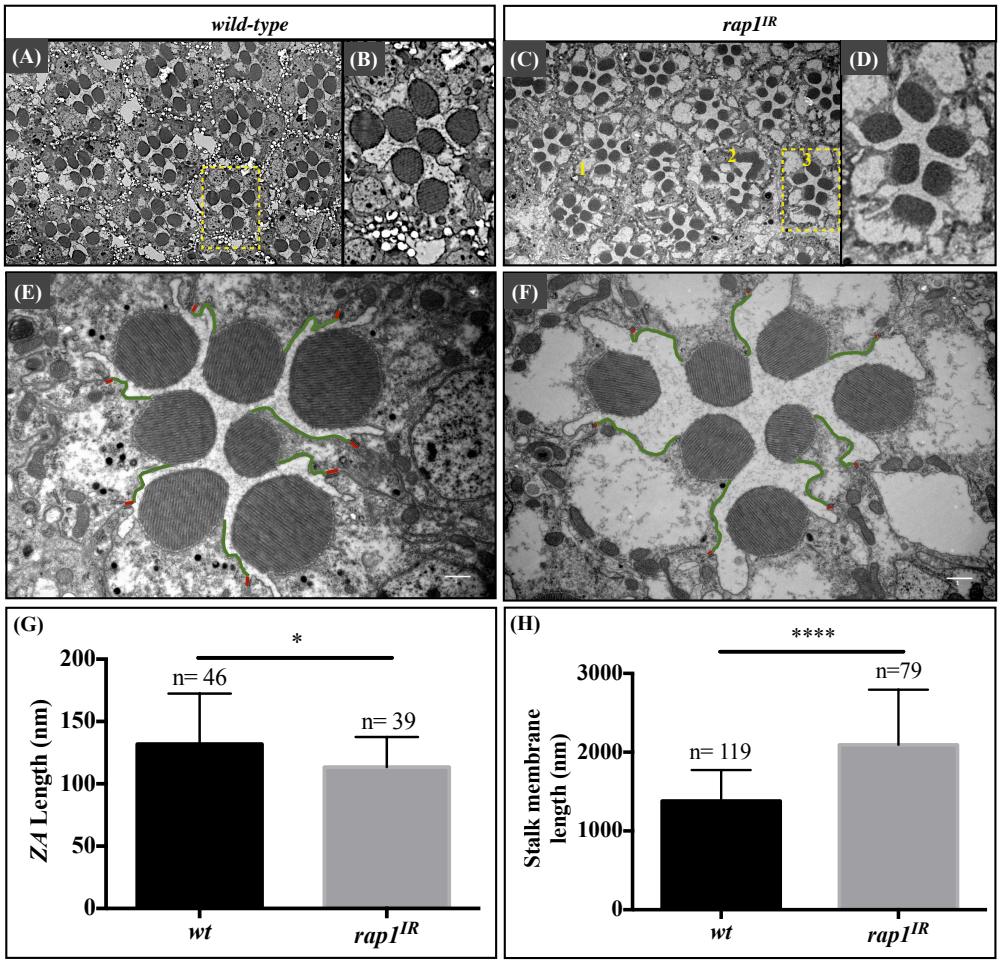

Figure 4.12: *rap1*^{IR} shows apical membrane and *ZA* morphogenesis defects in the adult fly retina. EM cross-sections on 3-day old female *wild-type* flies show characteristic morphology and localisation of the photoreceptors (**A**). *rap1*^{IR} expressing adult retina display various morphogenetic defects similar to those seen in the pupal retina (**C**). Many ommatidial clusters in *rap1*^{IR} adult flies are *wild-type* in appearance (**1**), whereas others have elongated or fused rhabdomers (**2**), or ommatidial clusters with missing cells (**3**). Individual clusters have been enlarged to better illustrate the ommatidial defects in and *rap1*^{IR} adult retina (**D**) compared to *wild-type* (**B**). Stalk membrane was measured by tracing the outline of the membrane shown in **green** (**E** and **F**). *ZA* length was by measured by tracing the outline of the electron dense region indicated in **red** (**E** and **F**). Graphs were made from measurements taken from both genotypes for *ZA* length (**G**) and stalk membrane length (**H**). N numbers for each genotype are indicated on the graphs. Measurements were analysed by unpaired t-tests to confirm statistical relevance. **** represents a p-value of ≤0.0001 and * represents a p-value of ≤0.05. Scale bar for EM images shown in (**E** and **F**) represents 1 µm.

4.10 rap1 and *baz* regulate epithelial morphogenesis at the remodelling *ZA*

So far, my data have shown that *rap1/dizzy* regulate *AJ* material accumulation at the remodelling pupal photoreceptor *ZA*. In the *Drosophila* gastrulating embryo, epithelial apical-basal polarity is established by the formation of the *ZA,* which separates the apical and basal compartments of the cells. In the absence of *AJs* (using arm^{XP33} mutants depleted of both *m/z* contributions cell-cell adhesion and polarity is lost in the cellularising fly embryo (Cox et al. 1996). In the cellularising embryo, Baz accumulates at the apical pole of the cell in the absence of *AJs* (Harris and Peifer 2004), suggesting that Baz positioning does not rely on *AJs* in this system. In *m/z baz* (baz^{Xi106}) mutants, DE-Cad loses its apical enrichment and redistributes along the lateral membrane (Harris and Peifer 2004). Therefore, Baz is required to direct apical accumulation of DE-Cad during cellularisation.

More recently, a study reported that *rap1 m/z* mutant embryos showed lateral spreading of Baz and *AJ* material, suggesting that *rap1* is required for the initial apical positioning of Baz and *AJs* during cellularisation (Choi et al. 2013). Altogether, these observations suggest that perhaps *rap1* regulates *AJ* morphogenesis through *baz*. To begin to test whether *rap1* might regulate *ZA* remodelling through *baz* in the pupal photoreceptor, I made use of the genetic rough eye modifier assay. This assay is based on generating a rough eye by reducing the expression of *rap1* and testing whether reducing the amount of other candidate genes enhances or suppresses the rough eye phenotype. Using this approach, I found that *baz* enhances the $rap1^{IR}$ rough eye phenotype (**Figure 4.13A-C**), suggesting that *baz* and *rap1* function as part of a common cellular process.

In order to investigate the genetic interaction between *baz* and *rap1*, I stained *Drosophila* pupal photoreceptors with a Baz antibody in $rap1^{IR}$ pupal photoreceptors. In this context, I found a reduction in Baz quantity at the developing *ZA* in $rap1^{IR}$ pupal photoreceptors (**Figure 4.13D-H**). As mentioned above, *rap1* has previously been shown to be required for Baz localisation in the *Drosophila* embryo, where cells polarise *de novo*. However, in this case, in the absence of *rap1* other unknown polarity cues partially restore Baz localisation (Choi et al. 2013). Our data shows that a similar situation is found during polarity remodelling in the fly pupal photoreceptor, where *rap1 is* required for the accumulation of Baz at the remodelling *ZA*. However, as some Baz is still localised at the remodelling *ZA*, other cues must regulate accumulation of Baz.

Mark Peifer's lab was able to show that *baz* functions downstream of *rap1* during the establishment of apical-basal polarity in the *Drosophila* embryo (Choi et al. 2013). To test whether this is also the case during photoreceptor polarity remodelling, I made use of *UAS-baz::GFP* to re-introduce additional *baz* in $rap1^{IR}$ photoreceptors. If ectopic *baz* supresses the *rap1* phenotype, it is likely that *baz* functions downstream of *rap1*. However, these flies displayed an enhanced rough eye phenotype (**Figure 4.13I-K)**. To examine the corresponding cells in more details, I carried out immunohistochemistry experiments on these flies and measured *ZA* length using stainings for Arm. These experiments showed that overexpressing *baz::GFP* in a $rap1^{IR}$ background does not suppress the shortened length of the *ZA* (**Figure 4.13L-X**). It is possible that the enhanced rough eye phenotype seen in *rap1*/*baz* double mutants is a consequence of other *rap1*/*baz*-dependent cellular processes within the eye such as axon guidance.

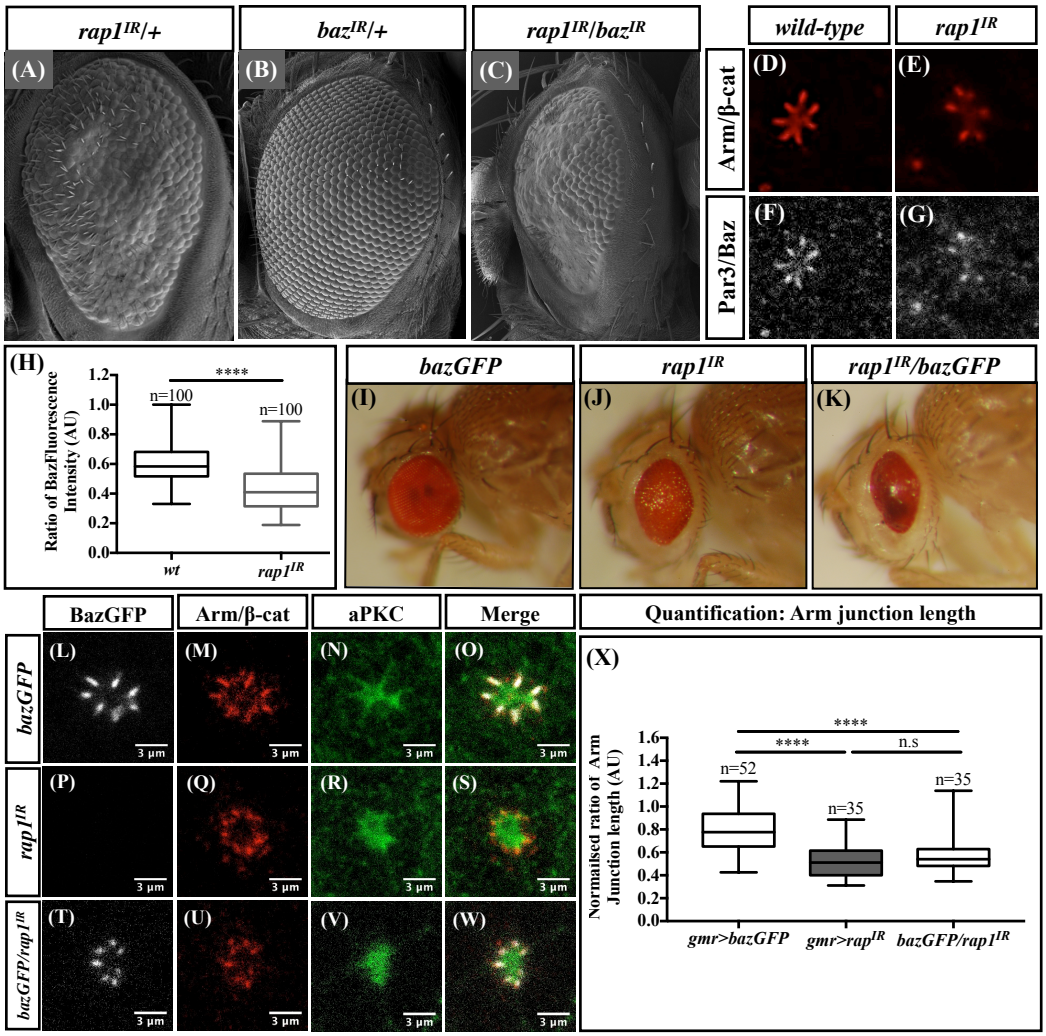

Figure 4.13: *rap1* and *baz* regulate epithelial morphogenesis in the *Drosophila* eye.
Classic *Drosophila* genetics reveal an interaction between $rap1^{IR}$, which exhibits a mild rough eye phenotype (**A**) with baz^{IR} (**C**). baz^{IR} alone has no rough eye phenotype (**B**). In *wild-type* pupal photoreceptors Baz colocalises with *ZA* marker Arm (**D-E**). $rap1^{IR}$ pupal photoreceptors reveal a reduction in the accumulation of Baz at the *ZA* (**F-G**). Reduction in Baz is quantified for both genotypes and is represented as a graph (**H**). Measurements were analysed by unpaired t-tests to confirm statistical relevance. **** represents a p-value of ≤0.0001. Reintroducing *baz* into the $rap1^{IR}$ background does not rescue the rough eye phenotype but rather enhances the phenotype (**I-K**). *bazGFP* alone does not induce a rough eye phenotype (**I**), whereas $rap1^{IR}$ is characterised by its mild rough eye (**J**). *bazGFP*/$rap1^{IR}$ double results in a glazed rough eye (**K**). Stainings on *bazgfp*/+ and *bazGFP*/$rap1^{IR}$ pupal photoreceptors reveal no further defects in ommatidial morphogenesis as measured by the length of the *ZA* using stainings for Arm (**L-X**). One-way Anova and Tukey's multiple comparison test was carried out to confirm statistical relevance. **** represents a p-value of ≤0.0001 and a p-value of 0.1965 was deemed non-significant (n.s).

Using a similar experiment, our lab previously showed that expression of *baz::GFP* in an *mbt* null mutant background led to lateral spreading of Baz (Walther et al. 2016). This suggested that *mbt* was required for retention of Baz at the *ZA*. My data indicate that unlike *mbt*, *rap1* is not required for retention of Baz at the *ZA*. However,

both *mbt* and *rap1* loss of function flies have reduced accumulation of *AJ* material at the developing *ZA* of pupal photoreceptors, suggesting a common function for both genes.

4.11 *rap1* functions with *mbt* to regulate *ZA* morphogenesis

Previous work from our lab has shown *mbt* regulates *ZA* morphogenesis by promoting *AJ* material stability in the developing fly photoreceptor (Walther et al. 2016). Using the rough eye modifier assay using an RNAi for *rap1*, I found that $rap1^{IR}$ can be enhanced by decreasing the dose of *mbt* (see **Appendix: Table 29)**. To test whether *rap1* and *mbt* function in the same pathway, I generated $rap1^{IR}/mbt^{P1}$ double mutants and compared the phenotype to $rap1^{IR}$ and mbt^{P1} single mutant cells (**Figure 4.14A-D**). As the length of the *ZA* was unaffected in the double mutants compared to the single mutants, *rap1* and *mbt* must function through the same pathway. Since mbt^{P1} is a null allele, my data are consistent with *mbt* functioning upstream or in parallel to *rap1*.

To further test the relationship between *rap1* and *mbt*, I generated flies where I overexpressed *wild-type mbt* (mbt^{wt}) in the $rap1^{IR}$ background. Unfortunately, overexpressing *mbt* was not able to rescue the *rap1* loss-of-function phenotype (**Figure 4.14E-G**), suggesting that either *mbt* does not function downstream of *rap1*, or that other factors may function with *mbt,* downstream of *rap1*.

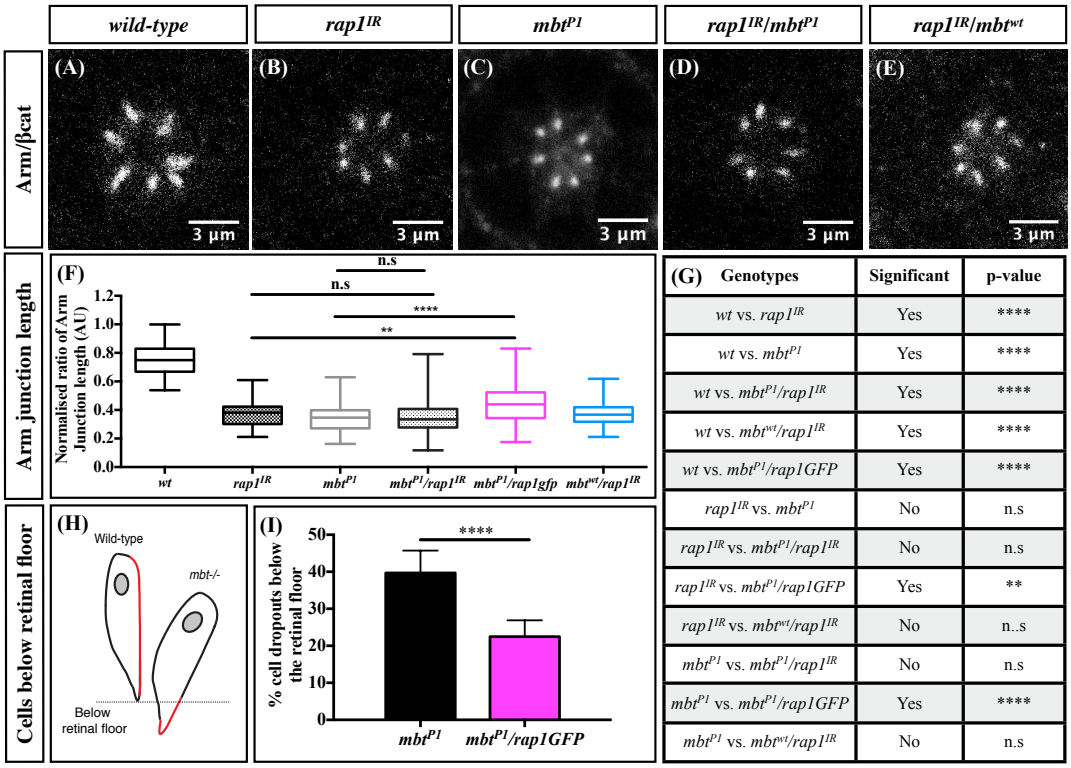

(G) Genotypes	Significant	p-value
wt vs. *rap1*^{IR}	Yes	****
wt vs. *mbt*^{P1}	Yes	****
wt vs. *mbt*^{P1}/*rap1*^{IR}	Yes	****
wt vs. *mbt*^{wt}/*rap1*^{IR}	Yes	****
wt vs. *mbt*^{P1}/*rap1GFP*	Yes	****
rap1^{IR} vs. *mbt*^{P1}	No	n.s
rap1^{IR} vs. *mbt*^{P1}/*rap1*^{IR}	No	n.s
rap1^{IR} vs. *mbt*^{P1}/*rap1GFP*	Yes	**
rap1^{IR} vs. *mbt*^{wt}/*rap1*^{IR}	No	n..s
mbt^{P1} vs. *mbt*^{P1}/*rap1*^{IR}	No	n.s
mbt^{P1} vs. *mbt*^{P1}/*rap1GFP*	Yes	****
mbt^{P1} vs. *mbt*^{wt}/*rap1*^{IR}	No	n.s

Figure 4.14: *mbt* functions upstream of *rap1*. Pupal photoreceptors stained for the *ZA* marker Arm in *wild-type* (**A**), *rap1*^{IR} single mutants (**B**), *mbt*^{P1} single mutants (**C**), *rap1*^{IR}/*mbt*^{P1} double mutants (**D**) and *rap1*^{IR}/*mbt*^{wt} (**E**). *rap1* loss-of-function resembles the *mbt* loss-of-function phenotype as shown by the junction lengths measured by Arm stainings (**F**). One-way Anova and Tukey's multiple comparison test was carried out to confirm statistical relevance **** represents a p-value of ≤0.0001, ** represents a p-value of ≤0.01 and a p-value of >0.05 is considered not significant (n.s). P-values for all genotypes where junction length was measured are shown in Table **G**. One of the phenotypes that characterise loss of *mbt* is the falling of cells below the retinal floor. A representation of *wild-type* and *mbt* null retina where apical and *ZA* components (shown in **red**) fall below the floor of the retina (adapted from Walther *et al.,* 2016; **H**). Re-introducing one copy of the *rap1* locus in the *mbt* mutant background leads to a small but significant increase in junction length (**F**) and a decrease in cells falling below the floor of the retina (**I**).

Intriguingly, I found that additional *rap1* was able to partially rescue the *mbt* loss-of-function phenotype (**Figure 4.14F-I**), suggesting that an excess of *rap1* can compensate for a lack of *mbt*. Therefore, *rap1* seems to function both upstream and downstream of *mbt*. Alternatively, *rap1* might function in a parallel pathway to *mbt* that is able to compensate for the decrease in *rap1* expression

4.12 Rap1 regulates DE-Cad mobility at the remodelling *ZA*

My data in eye imaginal discs, together with a previous study in wing discs (Knox and Brown 2002), indicate that Rap1 is required for the accumulation of *AJ* material at the remodelling *ZA*. It has been shown that in the fly embryo, DE-Cad exists in a mobile and immobile state depending on its association with Baz (Bulgakova et al. 2013), asymmetric distribution of mobile DE-Cad is regulated by Baz and dynamic MTs. In contrast to Baz, it is possible that Rap1 immobilises *AJ* material by linking the *AJ* to the underlying F-actin cytoskeleton, thereby regulating the stability of *AJs*. To begin to test this hypothesis, I carried out FRAP experiments on *wild-type* and *rap1*^{IR} pupae labelled with *ubi-DECad::GFP* to photo-bleach the basal half of the *ZA* and measure the recovery of DE-Cad over time (**Figure 4.15A**). Subsequently, I plotted the FRAP data using a double exponential as there seemed to be two phases of recovery: a short and fast recovery followed by a longer and slower recovery.

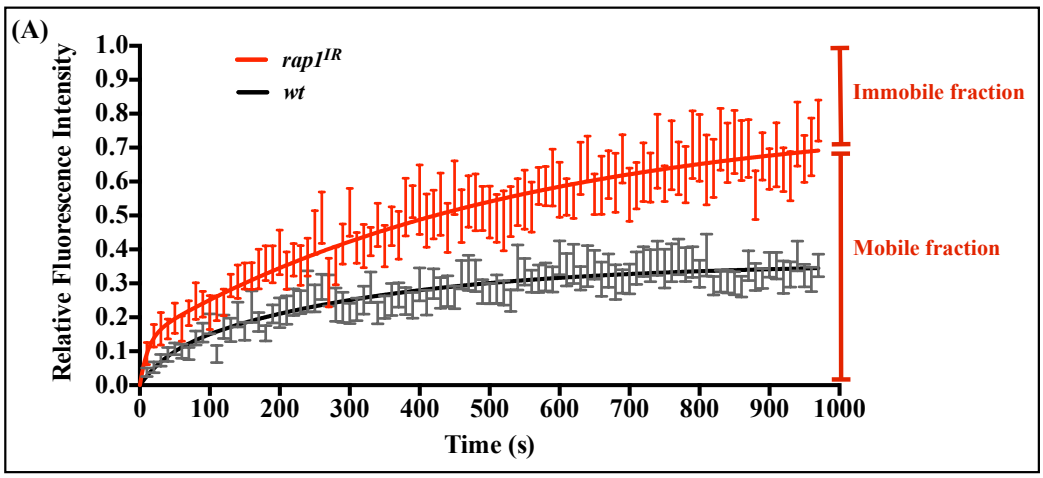

(B) FRAP data					
Genotype	Mobile fraction	SEM	n	Fast half-life (secs)	Slow half-life (secs)
wt	36%	0.020	14	27	219
rap1^{IR}	80%	0.065	12	8	366

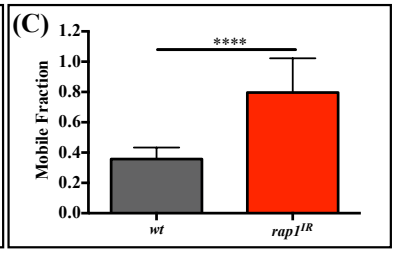

Figure 4.15: Rap1 regulates DE-Cad mobility at the remodelling *ZA*. FRAP on pupae labelled for *ubi-DEcad::GFP* (*wild-type*) shown in **black** and for *rap1*^{IR} labelled for *ubi-DEcad::GFP* in **red** (**A**). FRAP data reveals two pools of DE-Cad – a mobile and an immobile fraction; the former is enhanced in *rap1*^{IR} tissue and is highlighted on the graph. A table summarising the FRAP data is shown in (**B**) and a bar graph highlighting the difference

in mobile fractions of DE-Cad between the *wild-type* (**grey bar**) and *rap1*^{IR} tissue (**red bar**) is shown in (**C**). An unpaired t-test was carried out to confirm statistical relevance. **** represents a p value of ≤0.0001.

In *wild-type* pupae, DE-Cad recovery is rapid and plateaus after a few minutes (~220 seconds), suggesting that these *ZA* domains are very stable. However, in *rap1*^{IR} pupae, there is a delay in stabilisation of DE-Cad, as shown by the increase in time taken to plateau (~360 seconds). In addition, there is an increase in the mobile fraction of DE-Cad from 36% in *wild-type* to 80% in *rap1*^{IR} retina (**Figure 4.15B-C)**. This suggests that *rap1* stabilises DE-Cad, at the developing photoreceptor *ZA*. This data resembles FRAP data on *mbt* loss-of-function tissue (Walther et al. 2016), showing that *rap1* and *mbt* function is somewhat similar and is compatible with the notion that part of *mbt* function is mediated by *rap1*.

How Rap1 maintains *AJ* stability at the *ZA* is unclear. A possible mechanism that Rap1 may use to regulate *ZA* morphogenesis is by regulating the mobility of DE-Cad at the *ZA,* by linking DE-Cad to the underlying actin cytoskeleton via the actin linker, Cno. On the other hand, Rap1 might regulate DE-Cad turnover *via* modulating DE-Cad endocytosis or delivery.

4.13 *rap1* interacts with *cno* and functions to localize Cno at remodelling *Zonula Adherens*

As mentioned in **Chapter 1**, Cno is an F-actin binding protein shown to regulate *ZA* remodelling in part through positioning Baz in the fly embryo (Boettner et al. 2000; Boettner et al. 2003; Sawyer et al. 2009; Choi et al. 2013). Previous work has shown that Cno binds to Rap1 in a yeast two-hybrid screen (Linnemann et al. 1999) and that

these two proteins are functionally linked in both flies (Boettner et al. 2003) and mice (Hoshino et al. 2005). Indeed, I could confirm that the *cno* null allele, cno^{R2} genetically interacts with $rap1^{IR}$ in the adult fly retina (**Figure 4.16A-C**). This suggests that *cno* functions in the same cellular process as *rap1*. In $rap1^{IR}$ pupal photoreceptors and $dizzy^{\Delta 12}$ mutant clones, Cno expression is significantly reduced at the *ZA* of remodelling pupal photoreceptors (**Figure 4.16D-K**). Our data show that *rap1* promotes the accumulation of Cno at the remodelling photoreceptor *ZA*.

To test whether the *cno* loss-of-function resembles that of *rap1* I made use of cno^{R2} null allele that I have shown to genetically interact with *rap1* using the rough eye assay. Similar to the *rap1* null allele, cno^{R2} null allele leads to a very severe phenotype with all cells falling below the retinal floor (**Figure 4.16L-P**), which is indicative of an integrin phenotype. To test whether *cno* functions downstream of *rap1* in accumulating *AJ* material during *ZA* remodelling, I next re-introduced *cno* using *UAS-cno* in the background of $rap1^{IR}$ pupal photoreceptors. Re-introducing *cno* led to a small increase in the length of junctions but did not fully suppress the *ZA* to *wild-type* (*npgal4>control UAS*) lengths (**Figure 4.16Q**), suggesting that other factors may also function downstream of *rap1* in the regulation of *ZA* length.

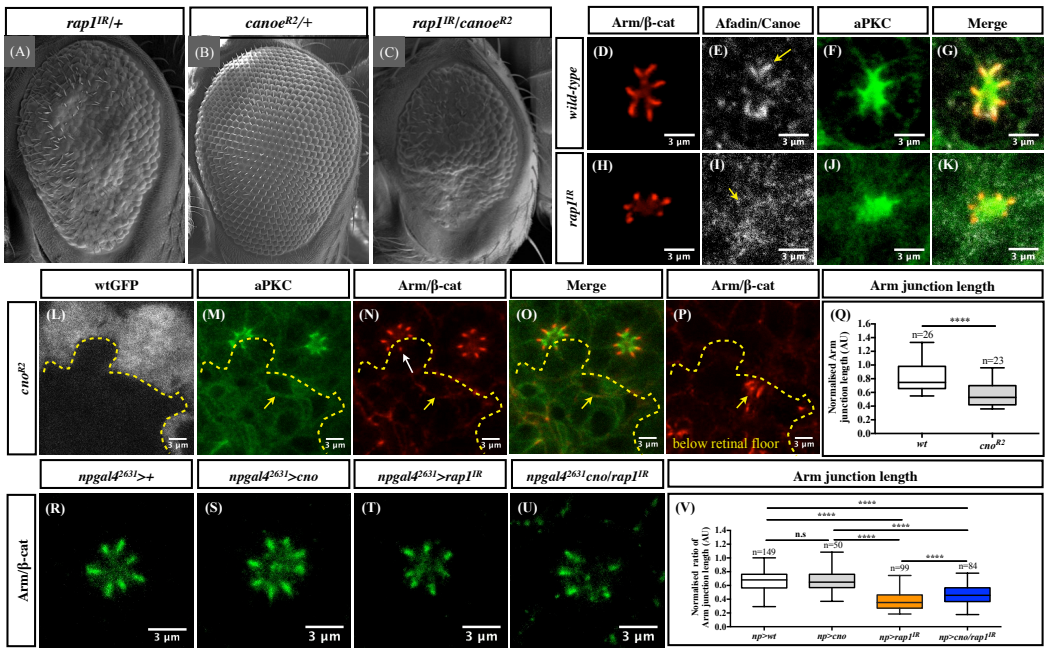

Figure 4.16:Cno mediates part of the function of Rap1 in regulating *ZA* morphogenesis. Classic *Drosophila* genetics reveal an interaction between *rap1*^{IR} (**A**) the *cno*^{R2} *null allele* (**C**). One copy of the *cno*^{R2} transgene has no rough eye phenotype (**B**). In *wild-type* pupal photoreceptors Cno colocalises with the *ZA* marker Arm (**D-G**). *rap1*^{IR} pupal photoreceptors reveal a reduction in the accumulation of Cno at the *ZA* (**I**). Arrows point to Cno staining in *wild-type* (**E**) and the remaining Cno staining at the *ZA* of *rap1*^{IR} cells (**I**). Reintroducing additional Cno using *UAS-cno* in the *rap1*^{IR} background leads to a partial recovery of *ZA* lengths**.** Pupal photoreceptors were dissected at 40% APF and stained for anti-Arm. Npgal4^{2631} driver was used to express *UAS-ctl* (**R**), *UAS-cno* **(S)** *UAS-rap1*^{IR} (**T**) and both *UAS-cno* and *UAS-rap1*^{IR} (**U**). Arm stainings were used to measure junction lengths in each genotype and normalised to control junctions. Data is shown as a graph (**V**). One-way Anova and Tukey's multiple comparison test was carried out to confirm statistical relevance. **** represents a p-value of ≤0.0001, a p-value of >0.05 is considered non-significant (n.s).

4.14 Canoe regulates DE-Cad mobility at the remodelling *ZA*

Our experiments have shown that Rap1 is required for the accumulation of Cno at the developing *ZA*, however, re-introducing Cno fails to restore *ZA* length in *rap1*^{IR} cells. If *cno* mediates part of *rap1* function, then it should also promote *AJ* stability. To test whether Cno regulates the mobility of DE-Cad at the remodelling *ZA,* I carried out FRAP experiments on *ubi-DECad::GFP* and *GMR>UAS-cno*^{IR} pupae labelled with *ubi-DECad::GFP* (**Figure 4.17**). These FRAP experiments revealed similar recovery of DE-Cad in *GMR>UAS-cno*^{IR} compared to *npgal4>UAS-rap1*^{IR} pupae, which is consistent with Rap1 and Cno functioning together during *ZA* morphogenesis. Thus,

my data provide correlative evidence for the existence of a *rap1*/*cno* pathway during *ZA* morphogenesis in the remodelling fly pupal photoreceptor.

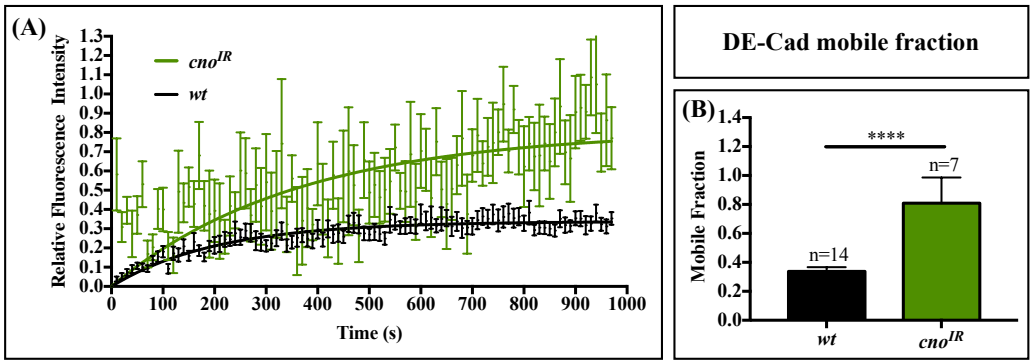

(C) FRAP data				
Genotype	**Mobile fraction**	**SEM**	**n**	**Half life (secs)**
wt	34%	0.007	14	143
cno^{IR}	81%	0.067	7	250

Figure 4.17: Cno regulates DE-Cad mobility at the remodelling *ZA*. FRAP on pupae labelled for *ubiDECad::GFP* (*wild-type*) shown in **black** and for *gmrgal4>cno^{IR}* labelled for *ubi-DECad::GFP* in **green**. FRAP data reveals two pools of DE-Cad – a mobile and an immobile fraction; the former is enhanced in *cno^{IR}* retinal tissue (**A**). A bar graph highlighting the difference in mobile fractions of DE-Cad between the *wild-type* (**black bar)** and *cno^{IR}* tissue (**green bar**) shown in (**C**). An unpaired t-test was carried out to confirm statistical relevance. **** represents a p value of ≤0.0001. A table summarising the FRAP data (**C**). Similar FRAP profiles suggest that Rap1 and Cno function in a complex.

4.15 Discussion

4.15.1 Rap1 and EGFR signalling regulate *ZA* remodelling in the developing retina.

Ommatidial formation in the developing fly eye imaginal discs is accompanied by increased DE-Cad-based cell-cell adhesion between nascent photoreceptors (Brown et al. 2006). My data shows that Rap1 is required for the accumulation of DE-Cad in the developing photoreceptor during ommatidia formation. Moreover, my data show that both the *rap1* and *dizzy* loss-of-function mutants lead to cell intercalation errors during ommatidia morphogenesis, with the formation of cell 'strings' that are reminiscent of mutants of cell intercalation regulators, *baz* and *rock* (Robertson et al. 2012). Further work is still required to underpin exactly how *rap1* interacts with

other members of the cell intercalation pathway including *baz* and *rock,* with the aim to regulate *AJ* remodelling during cell intercalation.

4.15.2 Rap1 and the apical polarity network.

Our data have shown that both Rap1 and its GEF Dizzy are mostly localised at the *ZA* of pupal photoreceptors but also at their apical membrane. At present it is unclear why Rap1 and Dizzy are localised at the apical membrane, as levels of apical determinants remain unchanged when levels of *rap1* and *dizzy* are reduced. As discussed in the **Chapter 1,** in the cellularising embryo, *AJs* are pre-assembled within the apical domain of the cells before being captured by Baz at the developing *ZA*. It is therefore possible that Rap1 functions at the apical pole of the cell to pre-assemble *AJ* material prior to its capture by Baz to assemble the *ZA*.

At later stages of photoreceptor development, Rap1 is required to regulate apical membrane morphogenesis with an increase in stalk membrane length in $rap1^{IR}$ adult photoreceptors. Whether this phenotype could be explained by the possible interaction between Rap1 and aPKC-Par6 in co-immunopreciptation is unclear (Carmena et al. 2011). Even though our data indicates that Rap1 does not rely on the apical gene network to be localised in the developing photoreceptor, whether Rap1 is for example required for the activation of the Par complex through activation of Cdc42 during polarity remodelling is not known.

4.15.3 Rap1 stabilises DE-Cad at the remodelling *ZA*

My data indicates that Rap1 stabilises DE-Cad at the remodelling pupal photoreceptor *ZA*. In fly embryos at segment boundaries, Baz links the *AJ* to MTs, thereby mobilising *AJs* (Bulgakova et al. 2013). Similar to the embryo, in

remodelling pupal photoreceptors, Baz might function to mobilise DE-Cad, whereas Rap1 functions to stabilise DE-Cad to ensure a balance between mobile and immobile DE-Cad and regulate the strength of adhesions during polarity remodelling. In this way, the developing *ZA* can be remodelled without disrupting the integrity of the epithelial cell.

My genetic experiments using additional *baz (bazGFP)* in the $rap1^{IR}$ background enhanced the $rap1^{IR}$ phenotype, suggesting that increasing *baz* levels might shift the balance towards more mobile DE-Cad. However, reducing *baz* (using baz^{IR}) in the $rap1^{IR}$ background also enhanced the $rap1^{IR}$ phenotype, suggesting that simply reducing *baz* levels does not shift the balance towards more immobile DE-Cad. In conclusion, maintaining a balance between mobile and immobile DE-Cad requires both Rap1 and Baz to be present at optimal levels.

4.15.4 Regulation of Rap1 during *AJ* remodelling

Previous data showed that *mbt* null photoreceptors show a reduction in *AJ* material at the remodelling *ZA* (Walther et al. 2016). My data showed that $rap1^{IR}$ loss-of-function photoreceptors also display a reduction in *AJ* material at the remodelling *ZA*. Considering, that lack of both *baz* and *mbt* leads to the total absence of *AJ* material at the photoreceptor cell cortex and *rap1*/*mbt* double mutants does not enhance the *mbt* null phenotype, indicate that *mbt* is most likely upstream or parallel of *rap1*. Whether *rap1* function is linked to that of *baz* remains to be investigated, for example by examining baz^{null}, $rap1^{IR}$ double mutant cells.

Our findings also highlight the complex nature of the polarity network, where it is often an over-simplification to describe genes as upstream or downstream of one another. Additional work will required to support the genetic experiments between

rap1, *mbt* and *baz* to clarify the function of polarity genes during remodelling of epithelial cells.

4.16 Concluding remarks

Using a candidate-based approach, I have identified *rap1* as an important regulator of *AJ* morphogenesis during *ZA* remodelling in the developing fly photoreceptor. My results indicate that loss of *rap1* leads to reduced *AJ* material at the *ZA* of cells undergoing cell intercalation, which is concomitant with an increase in acto-myosin in cells surrounding the photoreceptor. Moreover, in another instance of polarity remodelling within the photoreceptor, when the cell builds its *ZA*, loss of *rap1* leads to a decrease in *AJ* material accumulation. This correlates with defects in overall cell morphogenesis and apical membrane differentiation. Interestingly, FRAP experiments using a *DE-Cad::GFP* transgene indicate a function for *rap1* in stabilising DE-Cad at the developing *ZA*. We propose that *rap1* may stabilise DE-Cad at the developing *ZA* through the recruitment of the actin cytoskeleton. Lack of both *baz and mbt* has previously been shown to lead to the total absence of *AJ* material at the photoreceptor cell cortex (Walther et al. 2016). Whether *rap1* contributes to *baz or mbt* function in this process remains to be tested.

Chapter 5. Large-scale genetic modifier screen

Currently, little is known about how *rap1* regulates polarity specification and remodelling. In addition, it is not clear how *rap1* fits within the core epithelial polarity gene network. One way to discover new genes and mechanisms that might link *rap1* to the epithelial gene network is to perform a genetic modifier screen. As mentioned earlier, loss-of-function *rap1* using $rap1^{IR}$ presents a rough eye phenotype (O'Keefe et al. 2009). I decided to capitalise on this mild rough eye phenotype and conduct a large-scale genetic modifier screen.

As $rap1^{IR}$ leads to a mild rough eye phenotype, enhancers and suppressors can be identified *in vivo*. I decided to carry out a small candidate-based screen used to assess genetic interactions between *rap1* and known regulators of polarity and morphogenesis (see **Appendix: Table 14**). Using this candidate-based screen, I found that *rap1* genetically interacts with several known regulators of polarity such as *baz, rock* and *cno*, which is consistent with our findings in **Chapter 4**. To further expand on the small candidate-based screen, I decided to conduct a large-scale genetic modifier screen in the *Drosophila* eye. Here, I screened genes from the following families, which are likely to be involved in polarity remodelling and *ZA* morphogenesis:

- Kinases and Phosphatases (564 strains)
- Transmembrane proteins (1730 strains)
- Transcription factors (964 strains)
- Ubiquitin pathway (458 strains)

- Trafficking (91 strains)
- Actin cytoskeletal remodelling (567 strains)
- Polarity-related (50 strains)

In our screen, certain genes displayed a rough eye phenotype on their own and therefore were not investigated further as they could not be used to assay for a genetic interaction with the polarity genes we selected (Crb, Par1, aPKC and Rap1).

5.1 Genetic enhancers and suppressors of *rap1*

I screened 2694 candidate genes and identified 58 suppressors (2.15%; **Figure 5.1A**) and 312 enhancers (11.58%; **Figure 5.1B**) of the $rap1^{IR}$ rough eye phenotype. The suppressors are listed in **Tables 14-20** and enhancers in **Table 21-28**. Using this approach, many more enhancers than suppressors were identified. Nevertheless, the $rap1^{IR}$-genetic modifier screen identified a number of interesting hits, several of which I will discuss in this chapter. In addition, in order to identify the most important hits and also to confirm the validity of our approach, I will compare the $rap1^{IR}$-genetic modifier screen to other screens completed by members of the Pichaud lab and to screens previously published (Shao et al., 2010; Toret et al., 2014).

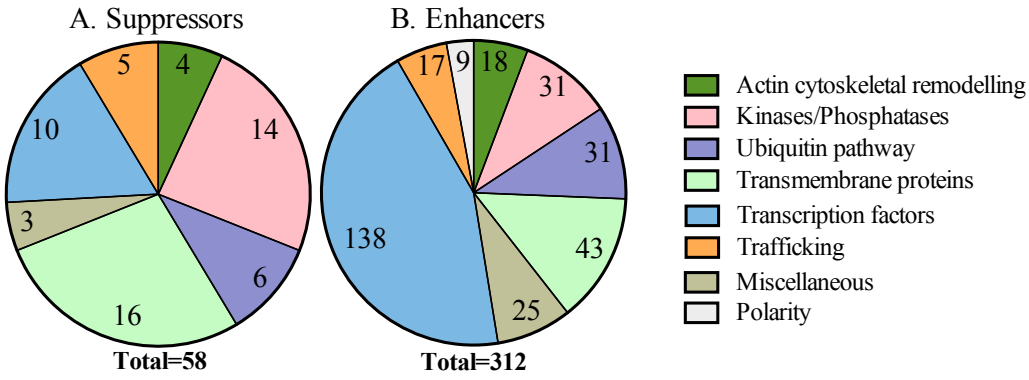

Figure 5.1: Large-scale *rap1*^{IR}-genetic modifier screen. 58 suppressors (**A**) and 312 enhancers (**B**) were identified in the *rap1*^{IR}-genetic modifier screen. All hits are organised by the different families the genes belong to and shown as pie charts.

5.2 Genetic links between the *rap1* and known polarity genes

The large-scale *rap1*^{IR}-genetic modifier screen together with a candidate-based screen identified a number of genetic interactions between *rap1* and genes already known to be involved in polarity remodelling. These hits have been summarised in **Figure 5.2** using String analysis (String, 2000). These hits further support the notion that *rap1* is involved in polarity remodelling and validates our screen approach. Many of the interactions between *rap1* and known polarity determinants are novel, as they have not been identified in any model organism and no experimental evidence exists as yet to support these interactions.

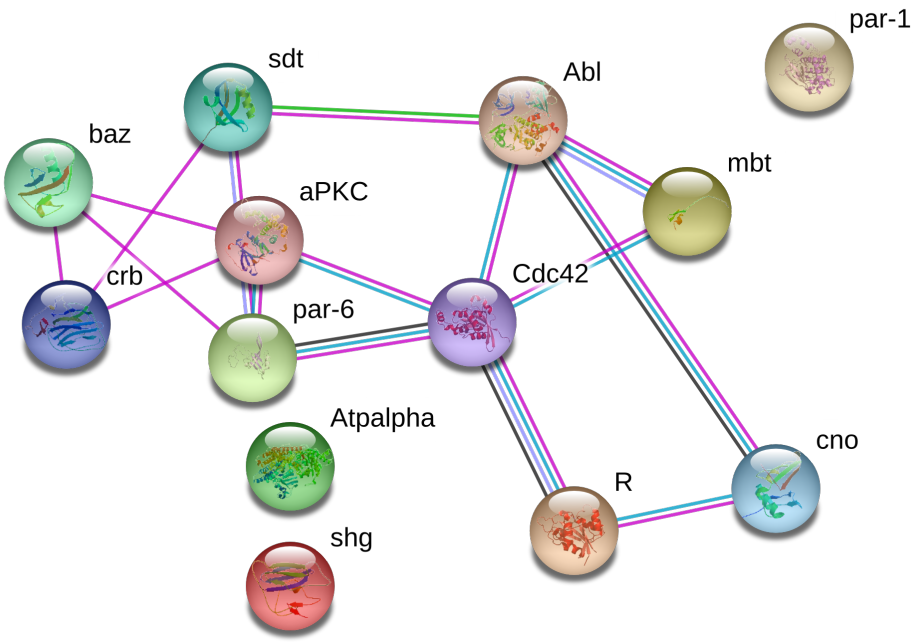

Figure 5.2: Genetic interactions between *rap1* and polarity-related genes. *rap1* genetically interacts with several genes associated with polarity remodelling. **Magenta** lines indicate known interactions from experimental data. **Blue** lines indicate known interactions curated from databases. **Green** lines indicate groups of genes that are frequently observed in each other's genomic neighbourhood. **Black** lines indicate genes that are co-expressed in *Drosophila*. **Purple** lines indicate protein homology. Gene inputs for this analysis include: *shotgun (shg), rap1 (R), mushroom bodies tiny (mbt), par-6, Na pump alpha subunit (Atpalpha), bazooka (baz), stardust (sdt), canoe (cno), Cdc42, atypical protein kinase C (aPKC), Abl tyrosine kinase (Abl), par-1* and *crb* (String, 2000).

5.3 Overlap between the *rap1*^{IR} and *aPKC*^{CAAX}-genetic modifier screens

As part of our lab effort to identify new genes regulating epithelial polarity during development, the kinase *aPKC* was overexpressed in the eye using the *aPKC*^{CAAX} allele. This led to a gain of function phenotype, whereby the flies develop a very strong rough eye phenotype. This allowed Laura Blackie in the lab to screen for genes that may interact with *aPKC*. The same gene families were screened as in the *rap1*^{IR}-genetic modifier screen. Laura identified 45 (3.2%) suppressors and 410 (29.3%) enhancers. To investigate the interaction between *rap1* and *aPKC*, I made use of the *rap1::GFP* genomic rescue transgene (Knox and Brown 2002) to express *rap1* in the *aPKC*^{CAAX} overexpression background. Overexpression of *rap1* partially suppresses the *aPKC*^{CAAX} rough eye phenotype. The *aPKC*^{CAAX} rough eye alone is very strong and pupal retina could not be dissected as a consequence. These preliminary results further support the idea that cross-talk between apical and *ZA* determinants exist during establishment and remodelling of polarity (**Figure 5.3**). As a result, I reasoned that identifying common hits between the *aPKC*^{CAAX} and *rap1*^{IR}-genetic modifier screens, might lead to the identification of novel genes that are required for apical-basal polarity.

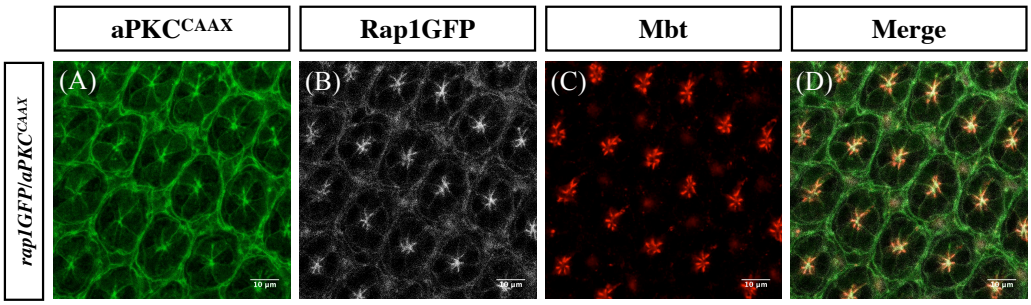

Figure 5.3: An extra copy of the *rap1* gene locus partially suppresses the *aPKC*^{CAAX} rough eye phenotype. *aPKC*^{CAAX} rough eye phenotype is very strong and pupal retina could not be dissected as a consequence. However, one extra copy of the *rap1* gene partially suppresses the *PKC*^{CAAX} phenotype. This allowed me to perform immunohistochemistry on 40% APF retina. The *aPKC*^{CAAX} transgene causes the spreading of aPKC from its usual apical location to all around the membrane cortex (**A**). *rap1* transgene is labelled with GFP (Knox and Brown 2002), antibody against Mbt labels the *ZA* (**C**) and the merge is shown in (**D**).

Curating the list of modifiers from these screens revealed 31 common candidate genes between the two modifier screens. These candidates have been summarised in **Table 30**. Candidate genes that have been previously known to regulate polarity in various model organisms, such as *par-3/baz* (Izumi et al. 1998; Benton and St Johnston 2003) and the *actin-related protein 2/3 (Arp2/3) complex* (Georgiou et al. 2008; Harris and Tepass 2008; Leibfried et al. 2008; Bernadskaya et al. 2011), help to validate the screens. However, what remains unclear is whether the Arp2/3 complex functions with Rap1 in stabilising *AJs* during polarity remodelling.

It is important to note that identifying a gene, as a modifier might not necessarily mean that this gene is involved in polarity remodelling. Such false positives might arise as rough eye phenotypes can be induced by defects in other cellular processes. This is highlighted by the identification of genes such as the histone acetyltransferase *Tat interactive protein 60kDa (Tip60),* the RNA binding *Prp31* and the netrin receptor *frazzled (fra)*. Arguably, Tip60 and Prp31 are more likely to play roles in protein expression (i.e. transcription, translation, splicing, ribosome assembly and other housekeeping pathways). These hits should be excluded from the screen as modified rough eye phenotypes may arise due to the loss of generic pathways involved in protein expression and not polarity remodelling.

fra however, is classically known as a regulator of axon guidance in the *Drosophila* CNS (Kolodziej et al. 1996). Interestingly, *fra* was identified in a yeast two-hybrid screen performed previously in the lab to identify genes that interact with *baz* (unpublished data). Baz (Spindler and Hartenstein 2011) aPKC (Wolf et al. 2008) and Rap1 (Yang et al. 2016) have been proposed to be involved in axon guidance in the fly CNS. Whether like *fra, baz, aPKC* and *rap1* play role in axon guidance within the fly retina is not clear. Alternatively, *fra* may play a role in polarity remodelling. In support of this hypothesis, Fra has been shown to regulate epithelial cell

dissociation, a process that relies on loss of apical-basal polarity and *AJs*, thereby allowing cells to become migratory and invasive in the *Drosophila* wing (Manhire-Heath et al. 2013). Fra overexpression leads to a block in disc eversion, whereas fra^{RNAi}, accelerates eversion in cultured *Drosophila* wing discs. As *fra* mutant clones display a loss of epithelial polarity, the authors suggested that *fra* may play a role in epithelial cell maintenance. It will be interesting to test whether *fra* plays a similar role during *ZA* remodelling.

5.4 Overlap between the $rap1^{IR}$ and $crumbs^{intra}$-genetic modifier screens

To further our lab effort to identify new genes regulating epithelial polarity during development, we overexpressed the intracellular and transmembrane domain of *crumbs (*$crumbs^{intra}$*)*, which led to a very mild rough eye phenotype. This allowed Rhian Walther in the lab to identify genes that enhance or suppress the $crumbs^{intra}$ rough eye phenotype from the gene families listed above. She identified 69 (2.4%) suppressors and 520 (18%) enhancers. As my candidate-based screen identified that *rap1* interacts with many components of the polarity pathway including *crumbs* (**Figure 5.2**), I reasoned that identifying common hits between the two modifier screens might lead to the identification of novel genes that are required for apical-basal polarity.

There were 43 hits found to be common between my screen and the Crb screen. These hits have been summarised in **Table 31.** Hits common between the two screens that have been previously known to regulate polarity in flies such as *baz* (Benton and St Johnston 2003), *sdt* (Bachmann et al. 2001; Hong et al. 2003) and *par6* (Petronczki and Knoblich 2001) help to validate our approach.

Of particular interest are the genes that have not previously been known to be involved in polarity remodelling. These genes include *puffyeye,* a thiol-dependent ubiquitin-specific protease, *lesswright*, a ubiquitin-activating enzyme involved in dorsal closure (Miles et al. 2008) and *CG3473*, a ubiquitin protein transferase. Several ubiquitin-related genes were identified in the *rap1*-genetic modifier screen (37 genes in total; **Figure 5.1**). Very little is known about the role of the ubiquitin pathway in regulating polarity remodelling and the lab has started to investigate the potential role of genes such as *puffyeye, lesswright* and *CG3473* in polarity remodelling in flies. Recent studies have shown that the conserved E3 ubiquitin ligase Neuralised (Neur) is a regulator of epithelial polarity in the fly embryo (Chanet and Schweisguth 2012), suggesting a role for ubiquitin ligases in the regulation of apical basal polarity. Increased Neur activity leads to destabilisation of the apical domain as a consequence of increased apical endocytosis. High levels of Neur correlate with low levels of Crumbs, which might explain loss of *AJ* stability. Increased endocytosis has been reported during apical constriction in gastrulating *Xenopus* embryos (Lee and Harland 2010) and *Cdc42*-compromised *Drosophila* embryos, where increased apical endocytosis correlates with *AJ* destabilisation (Harris and Tepass 2008). Whether Neur activity affects the balance between endocytosis and recycling of apical determinants is not known. Also, whether Neur counteracts the function of Crb is not known. Interestingly, Rap2A function is negatively regulated by the ubiquitin ligase Nedd4-1 during mammalian neurite outgrowth (Kawabe et al. 2010). Whether a similar inhibitory mechanism regulates Rap1 function and potentially other polarity determinants during apical-basal polarity is not known.

5.5 Overlap between the *rap1^{IR}*, *aPKC^{CAAX}* and *crb^{intra}*-genetic modifier screens

There are 17 hits in common between the *rap1^{IR}*, *aPKC^{CAAX}*, *crb^{intra}* genetic modifier screens. These hits have been summarised in **Table 32**. These genes are of high interest as all three screens identified these screens as modifiers, suggesting that they are more likely to be related to polarity remodelling. It may be argued that these genes would interact with any gene and therefore have been picked up in all three screens. As there are only a small number of hits common to all these three screens, we could stain the photoreceptors with polarity markers to confirm whether the interaction is indeed a consequence of regulating polarity remodelling.

Of particular interest are the genes that have not previously been known to be involved in polarity remodelling, such as *CG8237* and *fasciclin 2 (fas2)*. Currently, very little is known regarding *CG8237* other than the fact that it has an RDD domain, which suggests it is a transmembrane protein. Interestingly, *fas1* was picked up in a yeast two-hybrid screen performed previously in the lab to identify genes that interact with *baz* (unpublished data). Several studies have implicated a role for *fasciclins* in axon guidance (Snow et al. 1989). However, *fasciclins* have roles in other cellular functions such as cell migration (Araújo and Tear 2003). Dynamic Fas2 expression and polarity regulates Dlg and Lgl localisation during *Drosophila* border cell cluster migration (Szafranski and Goode 2004). Interestingly, Fas3 is highly enriched in *SJs* but excluded from the *AJs* of *Drosophila* wing imaginal discs (Woods et al. 1997). *SJ* determinants including Scrib (Bilder and Perrimon 2000), Dlg (Woods et al. 1996), Yurt (Laprise et al. 2009) and Neuroglian (Genova and Fehon 2003) play a key role in regulating apical-basal polarity. Whether all *fasciclins* are key components of the *SJ* and whether they play a role during polarity remodelling is unclear.

Interestingly, *roadblock*, which encodes for the dynein light chain was identified as a modifier in all three screens. Dynein has been shown to be a key regulator of apical-basal polarity (Harris and Peifer 2005; Horne-Badovinac and Bilder 2008). At the onset of polarity establishment in the fly embryo, Baz recruits the Cad/Cat complex and promotes *AJ* assembly in a MT-Dynein-dependent manner (Harris and Peifer 2005). Moreover, Dynein regulates apical-basal polarity by apical targeting of *sdt A* mRNA, which subsequently localises Crb apically (Horne-Badovinac and Bilder 2008) More recently, MT-Dynein-dependent apical restriction of recycling endosomes was shown to maintain the localisation of Baz and E-Cad at the *AJ* (Le Droguen et al. 2015), thereby, maintaining adhesion in *Drosophila* tracheal cells. Whether dynein targets other polarity determinants in a similar manner is not known.

5.6 Overlap between $rap1^{IR}$-genetic modifier screen and enhancers of the baz^{zyg} mutant cuticle phenotype

As mentioned in the introduction, Baz is a molecular scaffold protein that binds to apical determinants such as Par6 (Lin et al. 2000) and aPKC (Nagai-Tamai et al. 2002). However, Baz has been shown to function separately from the apical determinants in *Drosophila* and *c. elegans* (Harris and Peifer 2005; Beers and Kemphues 2006). Baz interacts directly with several proteins that are functionally linked to Rap1. For this reason, common hits between the $rap1^{IR}$-genetic modifier screen and the baz^{zyg} screen (Shao et al. 2010) may help uncover genes required for the function of Rap1 in *AJ* remodelling.

To this end, I decided to compare the $rap1^{IR}$-genetic modifier screen to a screen performed by the Harris lab to identify additional players that function with Baz to regulate epithelial structure in the *Drosophila* embryo (Shao et al. 2010). Zygotic *baz* mutants have a maternal supply of *baz* and display a mild cuticle phenotype, which is

indicative of defects in epidermal structure and patterning. Reducing levels of proteins that function with Baz can reduce the activity of the maternal supply and lead to an enhanced cuticle phenotype. Using this genetic assay, the Harris lab screened molecularly defined deficiencies of chromosome 2 and 3 to identify new regulators of polarity.

From the deficiencies tested 37 showed an enhancement of the *baz*^{zyg} mutant phenotype. Subsequently, the authors used deficiency mapping, bioinformatics and available single gene mutations to identify 17 interacting genes. The loss of these genes revealed enhanced *AJ* defects in *baz*^{zyg} mutant background, whereas, individual cuticle phenotypes for these genes were relatively mild. 3 hits from this screen were common to the *rap1*^{IR}-genetic modifier screen: Rho1, DE-Cad and Par1. Rap1 was also identified as one of the candidates shown to enhance the *baz* mutant phenotype, but was not analysed further due to lack of null allele stocks at the time. Although a low number of hits were identified between the two screens, there are some similar hits such as the clathrin adaptor protein *AP-1 sigma* was identified in the *baz*^{zyg} screen, whereas *AP-2 alpha* was identified in the *rap1*^{IR}-genetic modifier screen. AP2 has been shown to regulate DE-Cad endocytosis during epithelial morphogenesis in the fly embryo (Levayer et al. 2011). It will be interesting to confirm whether Baz and Rap1 function together with clathrin adaptor proteins in the regulation of E-Cad endocytosis during *ZA* morphogenesis. Similarly, *cullin-5* was identified in the *baz*^{zyg} screen, whereas, *cullin-3* and *-4* were identified in the *rap1*^{IR}-genetic modifier screen. Roles for cullin proteins have not been established in the context of *ZA* morphogenesis or polarity remodelling. To this end, it would be interesting to test whether Baz and Rap1 function to regulate polarity remodelling through ubiquitination and therefore protein stability.

5.7 Overlap between *rap1*^{IR}-genetic modifier screen and *Drosophila* E-Cad-S2 cell adhesion screen

The Nelson lab published a genome-wide (~14,000 genes) RNAi screen to identify proteins and pathways that are required for DE-Cad-mediated cell-cell adhesion (Toret et al. 2014). To this end, they established an inducible *Drosophila* S2 cell adhesion assay that restricted analysis to Ca^{2+}-dependent, DE-Cad-mediated cell adhesion. In this way, they could exclude other adhesion processes such as ECM adhesion, cell spreading and migration. Thus, defining the important regulatory hubs and pathways regulating DE-Cad-mediated cell-cell adhesion.

Selected hits from the primary screen were subsequently confirmed in both the *Drosophila* oocyte and mammalian MDCK cells. This screen is highly relevant considering that *rap1* has been linked to the regulation of DE-Cad based cell-cell contacts in cell culture (Hogan et al. 2004) and *Drosophila* wing discs (Knox and Brown 2002). Therefore, I reasoned that comparative hits between the *rap1*^{IR}-genetic modifier screen and the *Drosophila* S2 cell adhesion screen could help uncover genes required for the function of Rap1 in cell-cell contact formation.

Toret et al. identified 378 proteins that formed 17 interconnected regulatory hubs including adhesion, regulation of actin cytoskeleton, trafficking and kinases/phosphatases. 27 hits (7.14%) were common between the two screens and are summarised in **Table 32.** Surprisingly, *ran* and the Ran binding protein *CAS/CSE1 segregation protein* were identified in both screens. Ran has been shown to bind directly to the Cno RA domain in *Drosophila* neural stem cells leading to activation of the Pins/Mud/dynein spindle orientation pathway during mitosis (Wee et al. 2011). It is through this RA domain that Rap1 interacts with Cno (Boettner et al. 2003) raising the possibility that there is competition between Rap1 and Ran for binding to Cno during apical-basal polarity remodelling.

Using the *Drosophila* S2 cell adhesion assay, Toret et al. identified 373 positive hits displaying defective cell aggregation phenotypes and around 100 displayed similar phenotypes to that of the loss of DE-Cad, α-Cat and β-Cat. This included Cno, which leads to a decrease in DE-Cad expression, suggesting that loss of Cno affects stabilisation of DE-Cad. This finding is consistent with our FRAP data shown in **Chapter 4**. Surprisingly, loss of Cno led to an increase in α-Cat expression, indicating that other mechanisms may be in place that stabilise α-Cat other than Cno.

Interestingly, most of the RNAi lines (52.6%) tested affected levels of α-Cat only, indicating that regulatory mechanisms exist to control levels of α-Cat that are independent of E-Cad and β-Cat. This group of proteins included the F-actin severing protein Cofilin (known as Twinstar in *Drosophila*), which was identified in both the $rap1^{IR}$-genetic modifier screen and the DE-Cad-S2 cell aggregation screen. Cofilin is involved in the establishment of neuronal polarity in mice and in cell culture (Garvalov et al. 2007). Cofilin knockdown exhibits defects similar to that following Cdc42 ablation, which results in increased phosphorylation and subsequent inactivation of Cofilin (Garvalov et al. 2007). Cofilin/Twinstar also becomes phosphorylated upon activation of Mbt in HEK293 cells (Menzel et al. 2007). At present, it is not clear what the exact function of Cofilin during polarity remodelling is and whether Rap1 function is affected by the activity of Cofilin.

5.8 Discussion

AJs are fundamental to multi-cellularity, which complicates loss-of-function analysis (Toret et al. 2014). Moreover, only studying single cells or unicellular organisms may risk oversimplifying the role of *AJs* in Biology. To this end, it is important to find a model system in which gene function can be analysed in a high-throughput manner without compromising survival. The *Drosophila* retina represents such a

system and I used this to carry out genetic screens to identify novel components of the polarity pathway. In this Chapter, I have outlined the key findings from the *rap1*^{IR}-genetic modifier screen and overlaps between this screen and several other polarity-related screens, which support the general usefulness and specificity of this screen.

The main potential caveat of our genetic approach using RNAi lines for screening is the problem of false negatives and false positives. False negatives may arise as a consequence of insufficient gene knock down, which may hinder the identification of a genetic interaction. False negatives and positives may also be a consequence of off target effects (Mohr and Perrimon 2012). We have tried to increase our chance of identifying relevant genes by comparing our data with that of other screens. Moreover, carrying out secondary screens to experimentally confirm the positive hits can narrow down the possibility of false positives. In our screen, certain genes displayed a rough eye phenotype on their own and therefore were not investigated further as they could not be used to confirm a genetic interaction with the polarity genes we selected. However, the genes that lead to a phenotype on their own may be involved in polarity remodelling without being genetically linked to *aPKC, rap1 or crb.* Despite these caveats, RNAi screening remains a powerful genetic tool in flies for elucidating the genetic basis and mechanisms regulating cellular processes such as epithelial apical-basal polarity.

5.9 Concluding remarks

From our screen it is clear that *rap1* interacts with several components of the *AJ* and polarity network. Moreover, overlaps between the *rap1*^{IR}-genetic modifier screen and other polarity-related screens have allowed us to increase our chances of identifying relevant genes for further analysis. These include several ubiquitin-related genes; of

which very little is known about in regards to the regulation of polarity and therefore warrants further investigation. From the *Drosophila* S2 cell adhesion assay it is clear that stable accumulation of the core Cad/Cat complex is a fundamental mechanism in the regulation cell-cell adhesion. Stabilisation is key in the early stages of cell-cell contact formation and later in development during the maintenance of cell-cell contacts. Rap1 may play a role in the stabilisation of cell-cell contacts at later stages during the maintenance of contacts by linking the *AJ* to the actin cytoskeleton.

Chapter 6. Discussion and future directions

6.1 Transcriptional regulation of polarity remodelling and *ZA* morphogenesis

During my thesis, I have carried out transcriptional profiling of the *Drosophila* pupal retina to try and uncover the transcriptional regulations that coordinate polarity remodelling in this developing neuroepithelium. With this approach, I was able to uncover several genes whose transcription is regulated at the onset of photoreceptor polarity remodelling. This includes, *ovo* a zinc finger TF that might regulate *ZA* morphogenesis, through regulation of the actin cytoskeleton. *ovo* is known to upregulate F-actin levels in the fly eye (Delon et al. 2003). However, the exact molecular mechanism remains unclear. In this thesis, I have shown that *ovo* is transcriptionally repressed at the onset of polarity remodelling. It is possible that reduced levels of *ovo* lead to reduced levels of *G-actin*, which subsequently reduces the stability of *AJ* material allowing the polarity of the cell to be remodelled. Whether *ovo* promotes direct expression of *G-actin* or indirectly through actin-associated genes, which could be involved in the accumulation of F-actin has not yet been tested. To this end, I could use qPCR to measure RNA levels of actin-associated genes before, during and after polarity remodelling to test whether up or downregulation regulation of *ovo* correlates with expression of these genes.

During my thesis, I only rescreened the top most variable TFs that seemed to be transcriptionally regulated at the onset of photoreceptor polarity remodelling. However, the remaining gene families such as the cytoskeleton-associated genes were not analysed by immunohistochemistry. Similar to the approach carried out in this part of my thesis, it would be interesting to carry out a secondary screen whereby genes were up or downregulated by means of available UAS or RNAi lines. However, there are a large number of genes that do not have available RNAi or UAS

lines. In future studies, analysis of these genes may be vital to discover novel genes that regulate photoreceptor morphogenesis. To this end, it might be useful to generate RNAi lines or CRISPR/Cas9 mutants to determine whether these genes are required for photoreceptor morphogenesis.

Our approach to uncover transcriptional regulations that coordinate polarity remodelling in the developing pupal retina is associated with a number advantages and limitations. Even though microarray analysis serves as a powerful tool for the study of gene expression as they are easy to use, do not require large-scale RNA sequencing and allow quantitative comparisons between gene expression levels amongst different samples. However, there are a number of limitations associated with our microarrays experiments. The main caveat to our approach is the use of the whole fly retina, which is composed of several cell types, including the photoreceptor, cone and pigment cells. Consequently, any differences in gene regulation throughout the chosen developmental time points might be due to a function of the gene in one of the these three cell types.

6.2 Rap1 and its GEF Dizzy regulate *ZA* morphogenesis in the remodelling fly pupal photoreceptor

Using a candidate-based approach, I have identified the small GTPase protein Rap1 as an important regulator of *AJ* morphogenesis at the remodelling fly photoreceptor *ZA*. My results indicate that loss of *rap1* leads to a decrease in *AJ* material at the *ZA* of cells undergoing cell intercalation, which is concomitant with an increase in acto-myosin in cells surrounding the photoreceptor. Moreover, I have found that during *ZA* remodelling in the pupal photoreceptor, loss of *rap1* leads to a decrease in *AJ* material accumulation. This correlates with defects in overall cell morphogenesis and apical membrane differentiation, indicating a pre-eminent role for *rap1* in regulating

AJ morphogenesis. Interestingly, FRAP experiments using a *DE-Cad::GFP* transgene indicate a function for Rap1 and Cno in stabilising DE-Cad at the developing *ZA,* presumably by linking the *AJ* to the underlying cytoskeleton (**Figure 6.1**).

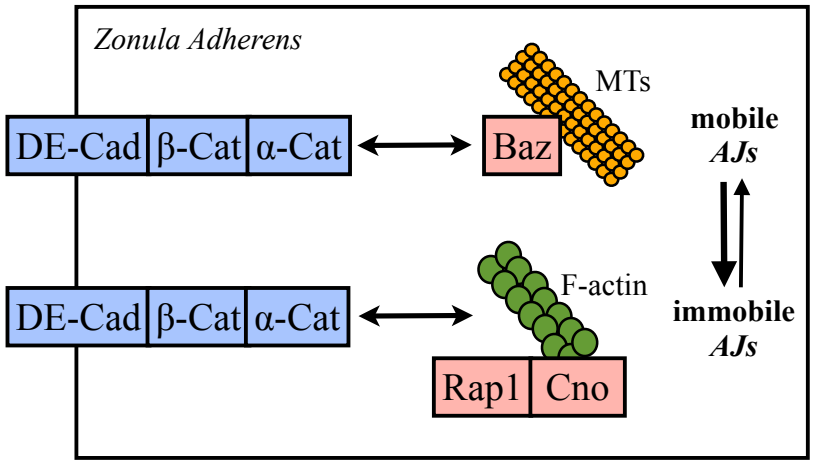

Figure 6.1: A balance between mobile and immobile *AJs.* A schematic diagram of the *ZA* representing the balance between mobile and immobile DE-Cad depending on its binding partners. Baz links DE-Cad to dynamic MTs, thus ensuring more mobile *AJs*, whereas Rap1/Cno anchors DE-Cad to the F-actin cytoskeleton and therefore ensure that *AJs* remain immobile. It is possible that DE-Cad is maintained in the immobile states independently of MTs.

It has previously been shown that in the embryo, Baz links the *AJ* to MTs, thereby promoting *AJs* mobility in fly embryos (Bulgakova et al. 2013). Therefore, it is possible that in remodelling pupal photoreceptors, Baz functions similarly to mobilise DE-Cad, whereas Rap1/Cno function to stabilise DE-Cad. In this way, a balance between mobile and immobile DE-Cad can be maintained, which might dynamically regulate the strength of adhesions during morphogenetic processes such as polarity remodelling. Considering that Baz engages with E-Cad/Cat molecules at a ratio of 1:7 in the embryo during formation of the *ZA* (McGill et al. 2009), not all E-Cad/Cat molecules are complexed with Baz and instead might interact with other factors including Rap1/Cno.

The hypothesis that DE-Cad/Cat might be complexed with other molecules is supported by my FRAP data in *wild-type* pupae, where the fraction of immobile DE-Cad (Rap1-dependent) is higher than the mobile fraction (Baz-dependent). It is likely that as a consequence of this equilibrium between immobile and mobile *AJs*, the *ZA* can be remodelled without disrupting the integrity of the epithelial cell. To support this hypothesis, it will be useful to test the ratio at which Rap1/Cno:DE-Cad exist at the developing *ZA*. If the ratio for Rap1/Cno:DE-Cad is higher than the ratio for Baz:DE-Cad, it is possible that DE-Cad is mostly in an immobile state due to the higher concentration of Rap1/Cno compared to Baz.

At present it is unclear whether binding of Rap1 to Cno is required to maintain DE-Cad in an immobile state. To test this, I could generate mutants for *cno* that lack the RA domain, which is required to mediate binding of Cno to Rap1. Subsequently, I could test whether Rap1 can still associate with the *AJ* and whether stability of *AJ* material is affected as a consequence of this uncoupling. Moreover, I could mutate the actin-binding domain of *cno* to confirm whether binding of *AJs* to the actin cytoskeleton is responsible for its immobile state.

In *rap1*^{IR} loss-of-function photoreceptors, whether an increase in the mobile fraction is a consequence of increased lateral diffusion or turnover at the PM is currently unclear (**Figure 6.2**).

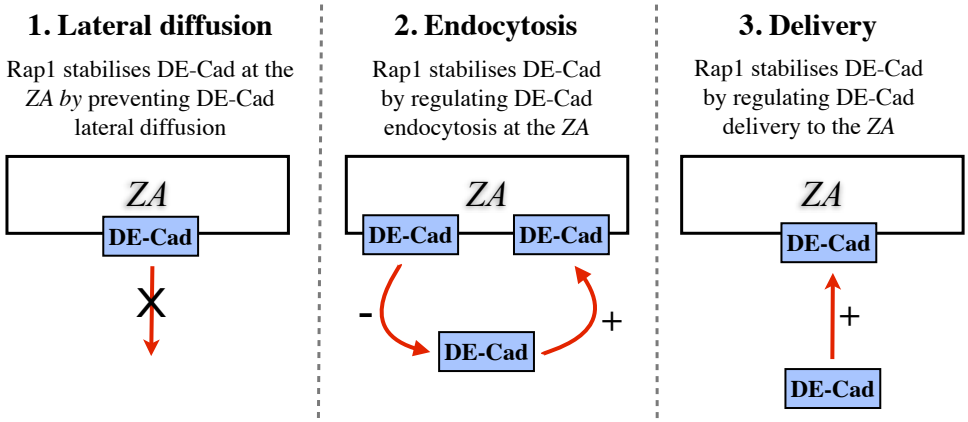

Figure 6.2: Potential molecular mechanisms employed by Rap1 to regulate immobility of DE-Cad. Rap1 may regulate the stability of DE-Cad through different mechanisms: (**1**) by regulating lateral diffusion of DE-Cad, (**2**) or by regulating the rate of endocytosis of DE-Cad, (**3**) or through regulating the delivery of DE-Cad to the PM.

In the embryo, the formin, diaphanous, promotes Clathrin (AP2)-dependent endocytosis of DE-Cad during germband extension, a process that supports *AJ* remodelling in the developing fly epidermis (Levayer et al. 2011). Interestingly, using the *rap1*^{IR} rough eye genetic modifier assay, I was able to identify an interaction between *rap1* and several regulators of the endocytosis pathway (**see Appendix**), including the *adaptor protein 2 alpha* (*ap2*α), a component of the AP2 complex. This interaction suggests that Rap1 might be involved in the regulation of DE-Cad endocytosis. To test this, I have tried to carry out endocytosis assays in the fly retina. This assay relies on the comparison between surface DE-Cad to levels of internalised DE-Cad, thereby, allowing us to establish whether reducing *rap1* function by RNAi leads to enhanced DE-Cad endocytosis. However, the retina has proven difficult to work with, as the apical membranes of the photoreceptors in both the larvae and the pupal retina are not readily accessible due to the presence of the

peripodial membrane and cone cells respectively. In my experience, this made it very difficult for the DCAD2 antibody to label the apical membrane without permeabilisation of the tissue. Consequently, these assays should probably be carried out in other developing tissues with a more accessible epithelium.

To support data from the endocytosis assays, I could carry out FRAP on mutants for *dynamin* (*shibire* in flies), to block endocytosis and assay whether the increase in mobility observed in *rap1* loss-of-function photoreceptors is lost when endocytosis is blocked. In this way, I could further probe the role of Rap1 during *ZA* remodelling in the fly pupal photoreceptor.

My data have shown that both Rap1 and its GEF Dizzy are mostly localised at the *ZA* but also at apical membranes of pupal photoreceptors. At present it is unclear why Rap1/Dizzy are localised at the apical membrane. When levels of *rap1* and *dizzy* are reduced, levels of apical determinants remained unchanged, suggesting that Rap1 is required primarily for the accumulation of *AJ* material at developing *ZA*. However, at later stages of photoreceptor development Rap1 is required to regulate apical membrane morphogenesis with an increase in stalk membrane length in adult photoreceptors. A possible explanation for a function of Rap1 at the apical membrane might be found in previous studies, showing that Rap1 can form a complex with aPKC-Par6 in co-immunopreciptation experiments from fly embryo extracts (Carmena et al. 2011). Whether Rap1 also forms a similar complex in epithelial photoreceptor cells and how this interaction would lead to promoting Par6-aPKC activity is during apical membrane morphogenesis is however not clear.

It will also be interesting to test where Rap1 is active at the apical membrane, as it is

possible that the pool of Rap1 that localises at the apical membrane is largely inactive due the presence of a Rap1-GAP. To this end, Rap1-Raichu FRET reporters (Mochizuki et al. 2001) might be useful to address changes in Rap1 activity within the photoreceptor. Furthermore, as *AJ* remodelling is an active process, live imaging may prove a more insightful method to address the regulation of *ZA* remodelling in the developing epithelial cells.

Data from the Mark Peifer's lab showed that Rap1 is involved in the positioning of Baz and *AJ* material during the establishment of apical-basal polarity (Choi et al. 2013). It is possible that Rap1 plays a similar role in apical pre-assembly of *AJs,* during *ZA* morphogenesis (**Figure 6.4**).

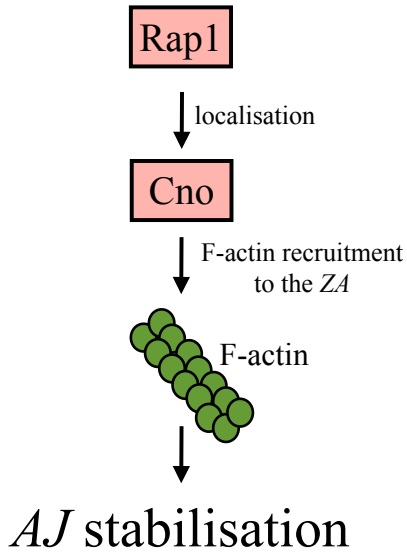

Figure 6.3: Model for the role of Rap1 in apical pre-assembly followed by *AJ* material stabilisation. A schematic diagram of the apical membrane, where Rap1 stabilises DE-Cad/Cat complexes through the localisation of Cno. Cno subsequently recruits the F-actin cytoskeleton to stabilise the *AJ*. Baz then captures the DE-Cad/Cat complexes and positions them at the interface between the apical and lateral membrane to form the *ZA*.

Previous work from our lab has shown that *mbt* regulates *ZA* morphogenesis by promoting *AJ* material stability by phosphorylating β-Cat/Arm in the developing fly photoreceptor (Walther et al. 2016). Phosphorylation of β-Cat/Arm is required for the

retention of Baz at the remodelling *ZA* so it does not accumulate at the lateral membrane. My data indicate that accumulation of DE-Cad also depends on *rap1* and *cno*. How the *rap1/cno* pathway relates to *mbt* function during *ZA* morphogenesis is not clear and requires more work. In conclusion, regulation of apical-basal polarity and *ZA* morphogenesis in the pupal photoreceptor requires the function of *baz, mbt* and *rap1/cno*.

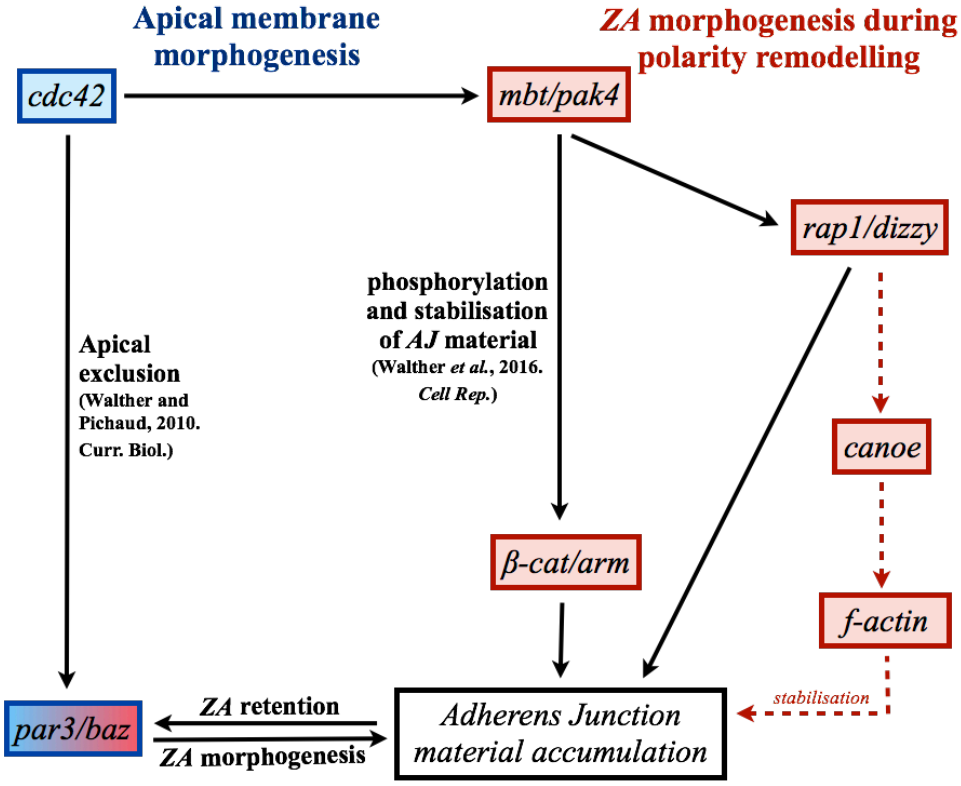

Figure 6.4: Model for the role of *rap1*, *mbt* and *baz* in polarity remodelling. A schematic diagram highlighting apical membrane morphogenesis with the apical exclusion of Baz by a pathway downstream of Cdc42. Mbt is responsible for the retention of Baz at the developing *ZA* through phosphorylation of β-Cat/Arm. Rap1 functions to stabilise *AJ* material at the *ZA*, through the accumulation of Cno, which recruits the F-actin cytoskeleton and ultimately stabilises the *ZA*. *rap1* and *mbt* pathways are partially redundant, with *mbt* functioning either upstream or in parallel to *rap1* during the process of *AJ* material accumulation.

6.3 Large scale *rap1*-genetic modifier screen

I have uncovered a role for *rap1* in the stabilisation of *AJ* material at the remodelling

photoreceptor *ZA*. Therefore, genes that genetically interact with *rap1* might also be involved in *ZA* morphogenesis and by extension in epithelial apical-basal polarity.

To identify genetic interactors of $rap1^{IR}$, I made use of the mild rough eye phenotype associated with the $rap1^{IR}$ to carry out a genetic-modifier screen. In this way, I was able to identify suppressors and enhancers of *rap1,* which are potentially involved in the same or parallel pathway as *rap1*. Comparaison of my screen with our *crb* genetic-modifier screen, revealed a strong connection between *rap1*/*crb* and protein ubiquitination. At present, the role of ubiquitin-related genes in polarity remodelling remains unclear and warrants further investigation. First, these genes will need to be rescreened by immunohistochemistry to confirm whether they are indeed involved in the regulation of epithelial polarity. Secondly, why these genes interact with *rap1* will need to be investigated in order to understand how they fit into the epithelial polarity network.

Although genetic screens can be very fruitful, they are associated with several limitations. Firstly, although analysing only a subset of interesting gene families, rather than the entire genome allows completion of the screen more rapidly and hits are more likely to be of interest. It can be argued that the most interesting hits may also be the unexpected hits, which would be missed by not analysing the entire genome. As for our screen, the main caveat of the rough eye screening approach is the problem of false negatives and false positives. False negatives may arise as a consequence of insufficient gene knock down, which may hinder the identification of a genetic interaction. False negatives and positives may also be a consequence of off target effects (Mohr and Perrimon 2012). For this reason, making use of loss of function alleles to retest genetic interactions should be done whenever possible.

Appendix

Table 1:Primary antibodies

Primary	Species	Dilution	Source
aPKCζ	Rabbit	1/200	Santa Cruz Biotechnology
Arm (N27-A1)	Mouse	1/200	DSHB (Wieschaus, E)
Avalanche	Chicken	1/500	Bilder, D
Bazooka	Chicken	1/2,000	Walther, R
Integrin Beta-PS	Mouse	1/10	DSHB (Brower, D)
Canoe	Guinea pig	1/20	Walther, R
CNN	Guinea pig	1/1000	Dobbelaere, J
Crumbs	Rat	1/200	Walther, R
DCAD2	Rat	1/50	DSHB (Uemura, T)
Gamma tubulin	Mouse	1/50	Sigma
Lgl	Guinea pig	1/50	Walther, R
Mbt	Guinea pig	1/500	Walther, R
Moesin	Rabbit	1/500	Kiehart, D
Par1	Rat	1/100	Walther, R
Par6	Guinea pig	1/500	Wodarz, A
PatJ	Guinea pig	1/500	Walther, R
p-SER19MRLC	Rabbit	1/10	Cell signalling
Rab5	Rabbit	1/500	Abcam
Rab11	Mouse	1/100	BD Transduction Laboratories
Rhodopsin-1/4C5	Mouse	1/100	DSHB (de Couet, H. G/ Tanimura, T)
Sec15	Guinea pig	1/200	Tepass, U
Stardust	Rabbit	1/50	Knust, E

Table 2: Secondary antibodies

Secondary	Species	Dilution	Source
AlexaFluor 488	anti-guinea pig	1/200	AlexaFluor
AlexaFluor 555	anti-guinea pig	1/200	AlexaFluor
AlexaFluor 647	anti-guinea pig	1/200	AlexaFluor
AlexaFluor 405	anti-mouse	1/200	Jackson ImmunoResearch
AlexaFluor 405	anti-rabbit	1/200	Jackson ImmunoResearch
AlexaFluor 488	anti-chicken	1/200	Jackson ImmunoResearch
AlexaFluor 488	Anti-rat	1/200	Jackson ImmunoResearch
AlexaFluor 488	anti-mouse	1/200	Jackson ImmunoResearch
Cy3	anti-rabbit	1/200	Jackson ImmunoResearch
Cy3	anti-mouse	1/200	Jackson ImmunoResearch
Txr	anti-mouse	1/200	Jackson ImmunoResearch
AlexaFluor 647	anti-rat	1/200	Jackson ImmunoResearch
AlexaFluor 647	Anti-rabbit	1/200	Jackson ImmunoResearch
Phalloidin	n/a	1/200	Thermo Fischer Scientific

Table 3: FRAP acquisition settings

	Pre-bleach	Bleach	Post-bleach
Frames	2	1	98
Time/frame (s)	1.293	1.293	10

Table 4: Transmembrane proteins identified in the microarray experiments on the developing fly retina.

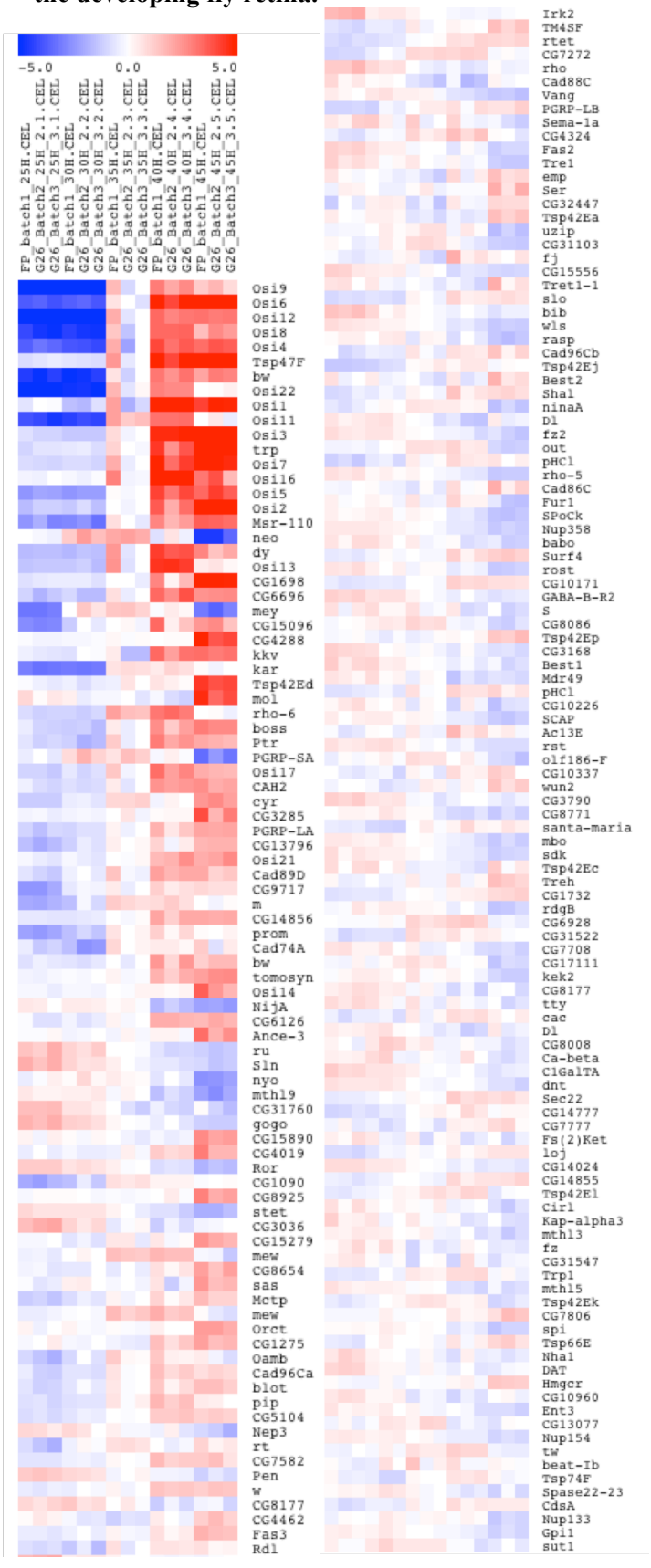

Table 5: Cytoskeleton-related genes identified in our microarray experiments on the developing fly retina

Table 6: Trafficking-related genes identified in our microarray experiments on the developing fly retina

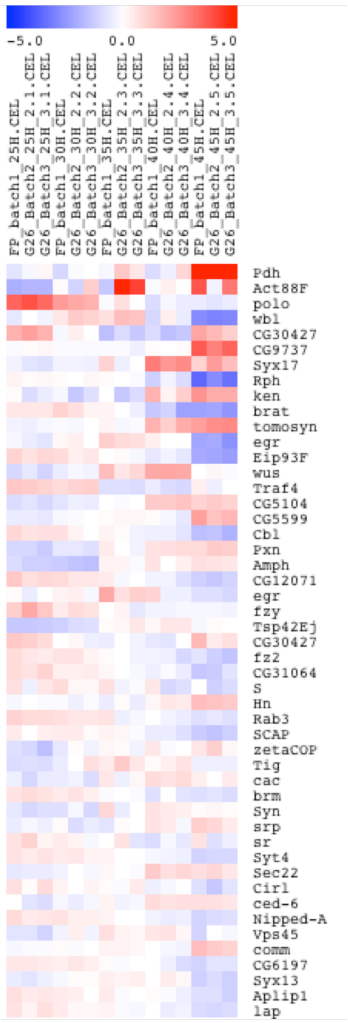

Table 7: Kinase encoding genes identified in our microarray experiments on the developing fly retina.

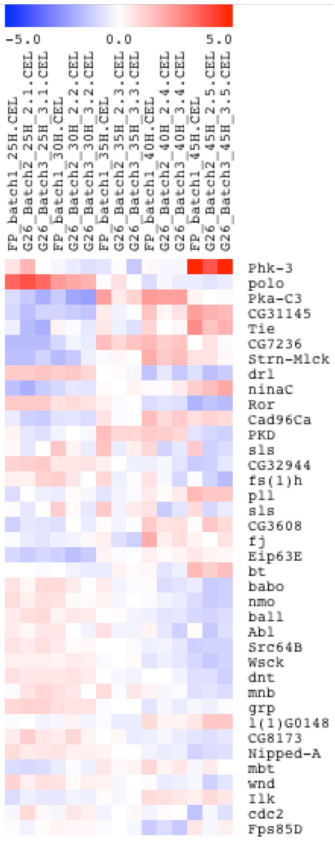

Table 8: Phosphatase encoding genes identified in our microarray experiments on the developing fly retina.

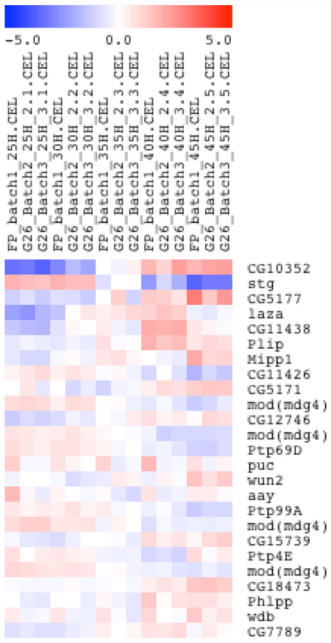

Table 9: Motor protein encoding genes identified in our microarray experiments on the developing fly retina.

Table 10: Transcription factor-related genes identified in our microarray experiments on the developing fly retina.

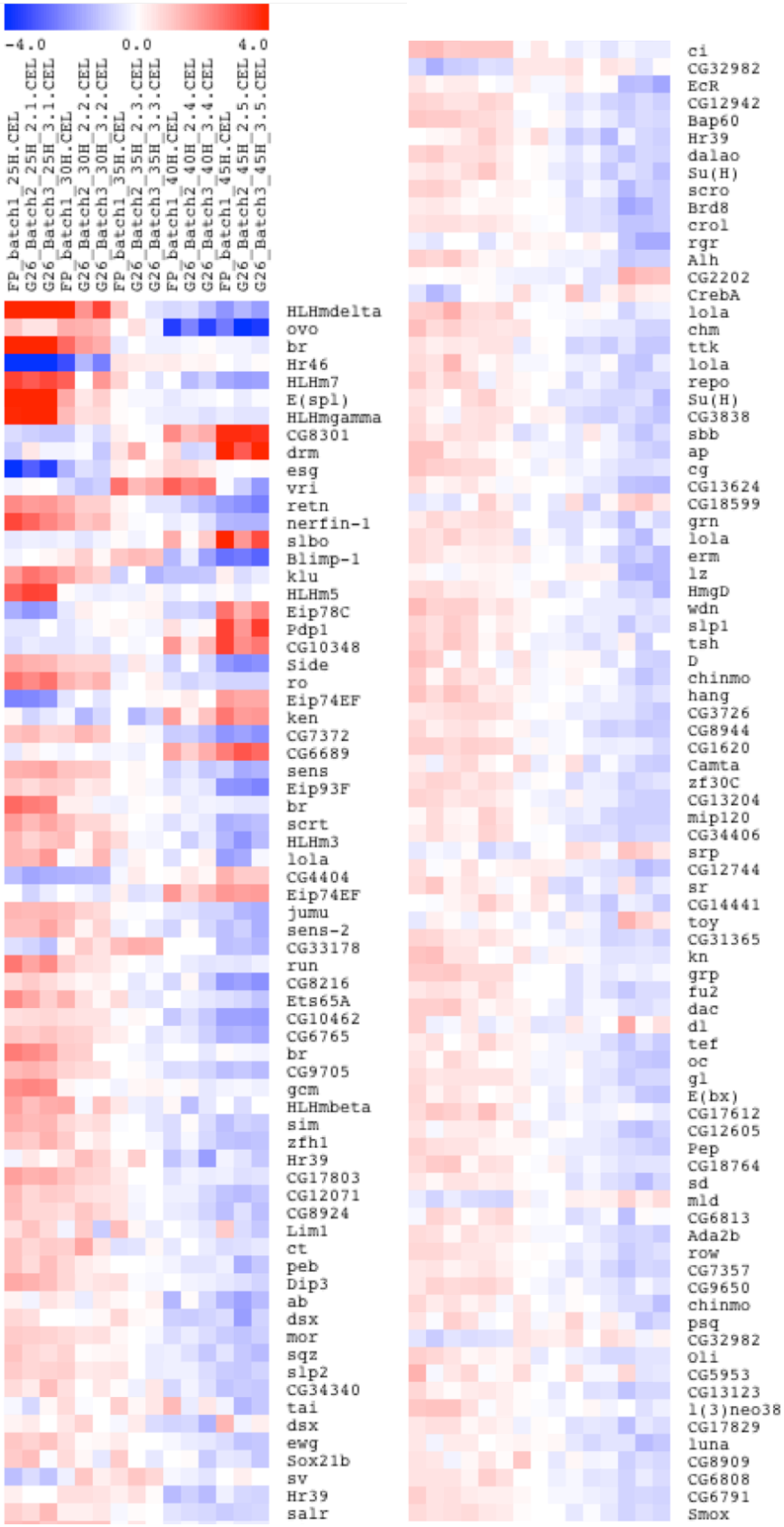

Table 11: TF-related genes that were expressed at high levels at the onset of polarity remodelling in the developing fly retina.

Gene	Name
Hr46	Hormone receptor-like in 46
CG8301	
drm	Drumstick
esg	Escargot
vri	Vrille
slbo	slow border cells
Eip78C	Ecdysone-induced protein 78C
Pdp1	PAR-domain protein 1
CG10348	lincRNA.186
Eip74EF	Ecdysone-induced protein 74EF
ken	ken and barbie
CG4404	

Table 12: TF-related genes that were expressed at low levels at the onset of polarity remodelling in the developing fly retina.

Gene	Name
HLHmdelta	Enhancer of split mδ, helix-loop-helix
Ovo	Also known as shavenbaby
Br	Broad
HLHm7	Enhancer of split m7, helix-loop-helix
HLHm5	Enhancer of split m5, helix-loop-helix
Side	Sidestep
CG7372	
Sens	Senseless
Eip93F	Ecdysone-induced protein 93F
Lola	longitudinals lacking
Jumu	Jumeau
CG33178	
Gcm	glial cells missing
HLHmbeta	Enhancer of split mβ, helix-loop-helix

Table 13: A summary of markers tested for defects in accumulation in *rap1* and *dizzy* loss-of-function mutants.

3A	Genotype	
Apical	***rap1*^{IR}**	***dizzy*$^{\Delta 12}$**
aPKC	no	no
Stardust	no	no
Crumbs	no	no
PatJ	no	no
Par6	no	no

3B	Genotype	
ZA	***rap1*^{IR}**	***dizzy*$^{\Delta 12}$**
Armadillo	↓	↓
DCAD2	↓	↓
Bazooka	↓	↓
Mbt	↓	↓
Canoe	↓	↓

3C	Genotype	
Basal	***rap1*^{IR}**	***dizzy*$^{\Delta 12}$**
Lgl	no	-
Par1	-	↓

3D	Genotype	
Cytoskeletal	***rap1*^{IR}**	***dizzy*$^{\Delta 12}$**
Actin	no	↑
p-Myosin II	↑	↑
Moesin	-	↓

3E	Genotype	
Trafficking	***rap1*^{IR}**	***dizzy*$^{\Delta 12}$**
Avalanche	no	no
Rab5	no	-
Rab8	no	-
Rab11	no	no
Sec15	no	no

3F	Genotype	
Other	***rap1*^{IR}**	***dizzy*$^{\Delta 12}$**
Gamma tubulin	no	-
CNN	no	-
Beta PS	no	no

Table 14: Candidate–based genetic modifier assay

Gene	Stock number	Allele/Insertion	Genetic interaction
Alpha catenin	33430	Chromosome 3	No
AP2	12319	Chromosome 2	No
AP2	27322	Chromosome 3	Enhancer
AP2	42155	Chromosome 2	No
Bazooka	35002	Chromosome 3	No
Bazooka	35122	Chromosome 2/CG3955	Enhancer
Bazooka	35123	Chromosome 2/CG17124	Enhancer
Bazooka	38213	Chromosome 2	No
Bazooka	39072	Chromosome 2	No
Canoe	38194	Chromosome 2	Enhancer
Canoe	33367	Chromosome 3	Enhancer
Canoe	-	Cno^{R2}	Enhancer
Canton S	-	Chromosome 2	No
Diaphanous	9138	Chromosome 2/dia^{5}	No
Diaphanous	102532	Chromosome 2/K07135	No
Diaphanous	28541	Chromosome 3	No
Dizzy	-	Chromosome 2/ $Delta^{12}$	Enhancer
Dizzy	-	Chromosome 2/ $Delta^{10}$	No
E-Cadherin	27802	Chromosome 3	Enhancer
E-Cadherin	-	?	Enhancer
E-Cadherin	103962	Chromosome 2/KK line	Enhancer
E-Cadherin	-	Chromosome 2	Enhancer
Myosin II	-	sqh^{EE}	No
Rab4	33757	Chromosome 3	Enhancer
Rab5	30518	Chromosome 3	Enhancer
Rab5	34832	Chromosome 3	No
Rab5	51847	Chromosome 2	No
Rab7	27051	Chromosome 3	Enhancer
Rab8	34373	Chromosome 3	No
Rab11	27730	Chromosome 3	Enhancer
RalA	105296	Chromosome 2/KK line	Enhancer
Rho Kinase	28797	Chromosome 3	Enhancer
Rho Kinase	34324	Chromosome 3	No
Rho Kinase	35305	Chromosome 3	No
Star	-	48-5	Enhancer
Ubi Cadherin GFP	-	Chromosome 2	No
UAS control	-	Chromosome 2	No
Vps26	38937	Chromosome 2	No
Vps33B	44006	Chromosome 3	Enhancer

Table 15: Transmembrane proteins that suppress the *rap1* phenotype in the large-scale genetic modifier screen

Number	CG number	Gene	Predicted function
1	CG14744		Calcium channel activity; integral component of the membrane
2	CG33282		Monosaccharide transmembrane transporter activity
3	CG16974		Neuron projection morphogenesis
4	CG5820	Gp150	Transmembrane receptor protein tyrosine phosphatase signaling pathway
5	CG42611	Megalin	Low-density lipoprotein receptor activity; regulation of endocytosis
6	CG8090	Golgi pH Regulator	Golgi organization
7	CG4585		CDP-alcohol phosphatidyltransferase class-I family
8	CG31006	slow termination of phototransduction	Deactivation of rhodopsin mediated signalling
9	CG30106	CCHamide-1 receptor	Neuropeptide signalling pathway
10	CG42235		Sodium-dependent multivitamin transmembrane transporter activity; sodium:iodide symporter activity
11	CG31860	Zinc transporter 33D	Zinc ion transmembrane transporter activity
12	CG7740	prominin-like	Integral component of membrane; neuron projection morphogenesis
13	CG31962	Scavenger receptor class C, type III	Scavenger receptor activity
14	CG31020	Sanpodo	Integral component of membrane; Notch signalling; protein binding; cell division;
15	CG14808	Sarcoglycan δ	Structural constituent of muscle; cytoskeletal anchoring at plasma membrane
16	CG43224	Glial cell line-derived neurotrophic family receptor-like	Cell adhesion molecule binding; anchored component of external side of plasma membrane

Table 16: Actin cytoskeletal proteins that suppress the *rap1* phenotype in the large-scale genetic modifier screen.

Number	CG number	Gene	Predicted function
17	CG10923	Klp67A	Microtubule motor activity; cell division
18	CG15097		Actin binding
19	CG7664	Cropped	Myosin binding; sequence-specific DNA binding
20	CG17927	Myosin heavy chain	Microfilament motor activity; epithelial cell migration; muscle myosin complex

Table 17: Kinases and phosphatases that suppress the *rap1* phenotype in the large-scale genetic modifier screen.

Number	CG number	Gene	Predicted function
21	CG7094		Serine threonine protein kinase
22	CG1362	Cdc2-related kinase	Serine threonine protein kinase
23	CG32849	Hex-t2	Hexokinase; glycolysis
24	CG7335		Ketohexokinase activity
25	CG42327		Protein tyrosine phosphatase activity
26	CG3573	Oculocerebrorenal syndrome of Lowe	Phosphatidylinositol bisphosphate phosphatase activity
27	CG3980	Cep97	Protein phosphatase type 1 regulator activity; centriole replication
28	CG17027		Inositol monophosphate 1-phosphatase activity
29	CG2699	Pi3K21B	Phosphatidylinositol 3-kinase regulator activity
30	CG34099	MAP kinase-specific phosphatase	MAP kinase tyrosine/serine/threonine phosphatase activity
31	CG3324	cGMP-dependent protein kinase 21D	cGMP-dependent protein kinase activity
32	CG1228	Protein tyrosine phosphatase Meg	Protein tyrosine phosphatase activity; cytoskeletal protein binding; EGFR signaling
33	CG12306	polo	Protein serine/threonine kinase activity; cell division

34	CG1107	auxillin	Protein serine/threonine kinase activity; Notch signalling pathway

Table 18: TFs that suppress the *rap1* phenotype in the large-scale genetic modifier screen.

Number	CG number	Gene	Predicted function
35	CG2120		Metal ion binding; nucleic acid binding
36	CG17835	invected	Sequence-specific DNA binding transcription factor activity
37	CG12299		Nucleic acid binding
38	CG4875	Receptor component protein	DNA-directed RNA polymerase activity; G-protein coupled receptor activity
39	CG17686	DISCO Interacting Protein 1	Double-stranded RNA binding; pre-miRNA binding; protein binding
40	CG7439	Argonaute 2	Translation initiation factor activity; autophagic cell death; RNA interference
41	CG11990	hyrax	Transcription factor binding; compound eye morphogenesis; smoothened/wnt signalling
42	CG6352	Ods-site homeobox	Sequence-specific DNA binding; transcription factor activity
43	CG11518	pygopus	RNA polymerase II transcription co-activator activity; wnt signalling
44	CG7292	Rrp6	Nucleotide binding; mRNA polyadenylation

Table 19: TFs that suppress the *rap1* phenotype in the large-scale genetic modifier screen.

Table 4.1E Rap1 suppressors - Rab GTPases/signalling			
Number	**CG number**	**Gene**	**Predicted function**
45	CG4168		G-protein coupled receptor activity
46	CG32475	methuselah-like 8	G-protein coupled receptor activity
47	CG32547		G-protein coupled receptor activity; neuropeptide receptor activity
48	CG8024	Lightoid/Rab32	GTPase activity; regulation of autophagy; sequence similarity to rab11
49	CG2041	legless	Beta catenin binding; wnt signalling

Table 20: Ubiquitin pathway components that suppress the *rap1* phenotype in the large-scale genetic modifier screen.

Number	CG number	Gene	Predicted function
50	CG7656		Ubiquitin-protein ligase activity
51	CG3455	Regulatory particle triple-A ATPase 4	Proteasome regulatory particle; microtubule associated complex
52	CG2944	gustavus	Protein binding; intracellular signal transduction; Cul5-RING ubiquitin ligase complex
53	CG1736	Proteasome α3 subunit, Testis-specific	Threonine-type endopeptidase activity; proteasome-mediated ubiquitin-dependent protein catabolic process
54	CG4166	Non-stop	Thiol-dependent ubiquitin-specific protease activity; axon guidance; transcription regulation
55	CG11942	SKP1-related E	Protein ubiquitination

Table 21: Miscellaneous components that suppress the *rap1* phenotype in the large-scale genetic modifier screen.

Number	CG number	Gene	Predicted function
56	CG16910	Kenny	Immune response
57	CG31997		Single domain Von Willebrand factor type C domain
58	CG32812		Calcium ion binding; negative regulation of phosphatase activity; pebble suppressor

Table 22: Membrane proteins that enhance the *rap1* phenotype in the large-scale genetic modifier screen.

Number	CG number	Gene	Predicted function
1	CG3936	Notch	Cell adhesion; compound eye morphogenesis; actin filament organization
2	CG33090		Integral component of membrane
3	CG12839	Tetraspanin 42En	Integral component of membrane
4	CG12317	JhI-21	Amino acid transmembrane transporter activity
5	CG4589	LETM1	Calcium:sodium antiporter activity; mitochondrion morphogenesis
6	CG3564	CHOp24	Integral component of membrane; ER to Golgi vesicle-mediated transport; wnt signalling
7	CG1751	Spase 25-subunit	Integral component of membrane; signal peptide processing
8	CG7625	Vacuolar H^+ ATPase M9.7 subunit b	Plasma membrane proton-transporting V-type ATPase complex
9	CG6625	α Soluble NSF attachment protein	SNARE binding; ER to Golgi vesicle-mediated transport; compound eye morphogenesis
10	CG10808	Synaptogyrin	Synaptic vesicle transport
11	CG9943	Surfeit 1	Heme transporter activity; neurogenesis
12	CG14239	pickpocket 15	Integral component of membrane; sodium channel activity
13	CG7309		Dicarboxylic acid transmembrane transporter activity
14	CG12327	Bestrophin 3	Integral component of plasma membrane; chloride transport
15	CG33110		Integral component of membrane; fatty acid elongase activity
16	CG7627		ATPase activity, coupled to transmembrane movement of substances

17	CG3619	Delta	Notch binding; actin filament organization; compound eye development; lateral inhibition
18	CG12366	O-fucosyltransferase 1	Integral component of Golgi membrane; Notch binding; endocytosis; lateral inhibition
19	CG18734	Furin 2	Serine-type endopeptidase activity; regulation of glucose metabolic process
20	CG9355	dusky	Integral component of membrane; genetic interaction with miniature
21	CG2507	stranded at second	Integral component of plasma membrane; receptor activity; axon guidance
22	CG31741		Integral component of plasma membrane; scavenger receptor activity; cell adhesion
23	CG12127	almondex	Spanning component of plasma membrane; lateral inhibition; notch signalling
24	CG33289	pickpocket 5	Integral component of membrane; sodium channel activity
25	CG7000	Sensory neuron membrane protein 1	Integral component of plasma membrane; scavenger receptor activity; cell adhesion
26	CG4977	Kekkon-2	Integral component of plasma membrane
27	CG3033	Glycosylphosphatidylinositol anchor attachment 1	Regulation of Golgi to plasma membrane protein transport; rhabdomere membrane biogenesis; GPI-anchor transamidase complex
28	CG5429	Autophagy-related 6	Autophagy cell death; endocytosis; neuron remodeling;
29	CG17664		Integral component of membrane; transmembrane transport
30	CG8581	frazzled	Integral component of membrane; netrin receptor activity; axon guidance
31	CG5474	Signal sequence receptor β	Integral component of membrane; signal sequence binding; protein retention in ER lumen;
32	CG10369	Inwardly rectifying potassium channel 3	Integral component of membrane; inward rectifier potassium channel activity
33	CG11190	attachment of GPI anchor to protein	
34	CG5677	Spase 22/23-subunit	Integral component of membrane; signal peptide processing
35	CG9501	pickpocket 14	Integral component of membrane; sodium channel activity
36	CG3665	Fasciclin 2	Integral component of membrane; protein binding; cell morphogenesis involved in neuron differentiation;
37	CG30394		Amino acid transmembrane transporter activity
38	CG33196	dumpy	Extracellular matrix structural constituent; lateral inhibition
39	CG5183	KDEL receptor	Integral component of membrane; KDEL sequence binding; protein retention in ER lumen; trans-Golgi network transport vesicle

40	CG17762	Tomosyn	SNARE binding; exocytosis; establishment or maintenance of cell polarity;
41	CG11500	Spase 12-subunit	Integral component of membrane; signal peptide processing
42	CG10367	HMG Coenzyme A reductase	Integral component of membrane; hydroxymethylglutaryl-CoA reductase (NADPH) activity; ERK signaling;
43	CG3456	Monocarboxylate transporter 1	Integral component of membrane; monocarboxylic acid transmembrane transporter activity;

Table 23: Actin cytoskeletal proteins that enhance the *rap1* phenotype in the large-scale genetic modifier screen.

Number	CG number	Gene	Predicted function
44	CG9423	karyopherin α3	Myosin binding; contain Armadillo repeats
45	CG1913	α-Tubulin at 84B	GTPase activity; mitotic spindle organization
46	CG1560	myospheroid	Actin filament organization; integrin-mediated cell adhesion
47	CG10541	Tetkin C	Microtubule binding
48	CG4254	twinstar	Actin filament organization; compound eye development; genetic interaction with *mbt*
49	CG7507	Dynein heavy chain 64C	Microtubule motor activity; establishment of epithelial cell apical/basal polarity; mitosis
50	CG6292	Cyclin T	Cyclin-dependent protein serine/threonine kinase regulator activity; actin filament organization; cell shape regulation
51	CG33106	multiple ankyrin repeats single KH domain	Structural constituent of cytoskeleton; compound eye photoreceptor cell differentiation; positive regulation of JAK-STAT cascade;
52	CG8978	Actin-related protein 2/3 complex, subunit 1	Actin binding; structural constituent of cytoskeleton; Arp2/3 complex-mediated actin nucleation; integrin-mediated cell adhesion; compound eye morphogenesis;
53	CG2092	scraps	Actin/microtubule binding; cell division;
54	CG6831	rhea	Structural constituent of cytoskeleton; integrin binding; integrin-mediated cell adhesion
55	CG2096	flapwing	Myosin phosphatase activity; protein serine/threonine phosphatase activity; JNK signaling; regulation of actomyosin

			contractile ring contraction; cell adhesion
56	CG10540	capping protein alpha	Actin cytoskeleton organization; cell morphogenesis; JNK signaling;
57	CG10751	roadblock	Dynein intermediate chain binding; microtubule-based movement; microtubule associated complex
58	CG32156	Myosin binding subunit	Myosin phosphatase activity; imaginal disc morphogenesis; dorsal closure
59	CG8440	Lissencephaly-1	Dynein binding (physical interaction with Dhc64C)
60	CG1977	α Spectrin	Actin/microtubule binding; cytoskeleton organization; epithelium development;
61	CG4869	β-Tubulin at 97EF	Structural constituent of cytoskeleton; GTPase activity;

Table 24: Phosphatases and kinases that enhance the *rap1* phenotype in the large-scale genetic modifier screen.

Number	CG number	Gene	Predicted function
62	CG3954	Corkscrew	Protein tyrosine phosphatase activity; EGFR signaling; sevenless signaling; mitotic cell cycle
63	CG18214	Trio	Protein serine/threonine kinase activity; actin cytoskeleton organization; Rho GEF
64	CG12019	Cdc37	Protein tyrosine kinase; ERK signaling
65	CG2049	Pkn	Protein serine/threonine kinase activity; actin cytoskeleton reorganization; dorsal closure
66	CG8874	FER	Protein tyrosine kinase activity; actin filament bundle assembly; dorsal closure
67	CG7525	Tie-like receptor tyrosine kinase	Protein tyrosine kinase activity
68	CG7597	Cyclin-dependent kinase 12	RNA polymerase II carboxy-terminal domain kinase activity; ERK/Ras signaling
69	CG3292		Alkaline phosphatase activity
70	CG14992	Activated Cdc42 kinase	Protein tyrosine kinase activity; dorsal closure; cellular protein localization
71	CG15218	Cyclin K	Cyclin-dependent protein serine/threonine kinase regulator activity; neurogenesis

72	CG13369		Ribokinase activity
73	CG7850	Puckered	JUN kinase phosphatase activity; MAP kinase tyrosine/serine/threonine phosphatase; actin filament organization; cell shape; dorsal closure
74	CG5150		Alkaline phosphatase activity
75	CG1395	String	Protein tyrosine phosphatase activity; mitosis
76	CG9774	Rho kinase	Protein serine/threonine kinase activity; Rho GTPase binding; actin cytoskeleton organization; regulation of cell junction assembly; dorsal closure; planar cell polarity
77	CG1098	MLF1-adaptor molecule	Protein serine/threonine kinase activity; cell proliferation; cell size
78	CG4634	Nucleosome remodeling factor - 38kD	Inorganic diphosphatase activity; ecdysone receptor-mediated signaling pathway;
79	CG5974	Pelle	Protein serine/threonine kinase activity; dorsal/ventral axis specification;
80	CG4006	Akt1	Protein serine/threonine kinase activity
81	CG8866		Protein serine/threonine kinase activity
82	CG17029		Inositol monophosphate 1-phosphatase activity
83	CG6620	aurora B	Protein serine/threonine/tyrosine kinase activity; mitosis
84	CG32019	Bent	Protein serine/threonine/tyrosine kinase activity; structural constituent of cytoskeleton
85	CG34412	Tousled-like kinase	Protein serine/threonine/tyrosine kinase activity; cell cycle regulation
86	CG12252	TFIIF-interacting CTD phosphatase	CTD phosphatase activity; neurogenesis;
87	CG5179	Cyclin-dependent kinase 9	Cyclin-dependent protein serine/threonine kinase activity; cell adhesion
88	CG14217	Tao	Protein serine/threonine kinase activity; hippo signaling;
89	CG1810	mRNA-capping-enzyme	Protein tyrosine/serine/threonine phosphatase activity
90	CG3938	Cyclin E	Cyclin-dependent protein serine/threonine kinase regulator activity; cell adhesion; cell proliferation involved in compound eye morphogenesis;
91	CG1609	Gcn2	Elongation factor-2 kinase activity
92	CG17090	Homeodomain	Protein serine/threonine kinase activity; compound eye development; hippo signaling; wnt signaling

		interacting protein kinase	

Table 25: Transcription factors that enhance the *rap1* phenotype in the large-scale genetic modifier screen.

Number	CG number	Gene	Predicted function
93	CG5591	Lost PHDs of trr	Chromatin binding; phagocytosis; ecdysone receptor holocomplex
94	CG14029	Vrille	Transcription repressor activity; RNA polymerase II core promoter proximal region sequence-specific DNA binding
95	CG3314	Ribosomal protein L7A	Structural constituent of ribosome; mitotic spindle and centrosome organization
96	CG32211	TBP-associated factor 6	Transcription factor activity; positive regulation of transcription of Notch receptor target
97	CG13867	Mediator complex subunit 8	RNA polymerase II transcription cofactor activity
98	CG4602	Srp54	mRNA binding; neurogenesis
99	CG8415	Ribosomal protein S23	Structural constituent of ribosome; centrosome organization
100	CG18497	CG18497	Nucleic acid binding; wnt signaling
101	CG10582	Sex-lethal interactor	DNA-directed RNA polymerase activity
102	CG8614	Neosin	mRNA binding; precatalytic spliceosome
103	CG9075	Eukaryotic initiation factor 4a	Translation initiation factor activity; Mitotic spindle and centrosome organization
104	CG4878	eIF3-S9	Translation initiation factor activity
105	CG4954	eIF-3S8	Translation initiation factor activity
106	CG10267	Zinc-finger protein	DNA binding; establishment or maintenance of neuroblast polarity

107	CG31256	Brf	Transcription factor binding; TBP-class protein binding
108	CG7508	Atonal	Transcription factor activity; EGFR/MAPK signalling; R8 cell fate specification
109	CG17436	Verthandi/cohesin	Chromatin binding; mitosis
110	CG10811	eukaryotic translation initiation factor 4G	Translation initiation factor activity; mitosis
111	CG42698	pou domain motif 3	Transcription factor activity, sequence-specific DNA binding; axon guidance; axonogenesis
112	CG3281		Nucleic acid binding; positive regulation of JAK-STAT cascade
113	CG8068	Suppressor of variegation 2-10	DEAD/H-box RNA helicase binding; JAK/STAT signaling; compound eye development
114	CG11901	translation elongation factor activity	Translation elongation factor activity; microtubule associated complex
115	CG42632	mitochondrial ribosomal protein L37	Structural constituent of ribosome
116	CG7413	Retinoblastoma-family protein	Transcription factor binding; cell death and proliferation
117	CG12296	klumpfuss	Nucleic acid binding; positive regulation of compound eye retinal cell programmed cell death
118	CG7035	cap binding protein 80	RNA cap binding; gene silencing by miRNA
119	CG8053	Eukaryotic initiation factor 1A	Translation initiation factor activity; mitotic spindle organization
120	CG1249	Small ribonucleoprotein particle protein SmD2	Poly(A) RNA binding; mitotic spindle organization
121	CG6121	Tat interactive	Histone acetyltransferase activity;

		protein 60kDa	
122	CG3395	Ribosomal protein S9	Structural constituent of ribosome; mitotic spindle organization
123	CG1406	U2A	mRNA binding; mitotic spindle organization
124	CG17489	Ribosomal protein L5	Structural constituent of ribosome
125	CG9305		DNA binding; transcription factor activity; sequence-specific DNA binding
126	CG4918	Ribosomal protein LP2	Structural constituent of ribosome; translational elongation
127	CG2158	Nucleoporin 50kD	Nuclear pore complex; neurogenesis; phagocytosis; ran-binding domain
128	CG13109	taiman	Transcription coactivator activity; ligand-dependent nuclear receptor transcription coactivator activity; steroid hormone receptor binding
129	CG4035	Eukaryotic initiation factor 4E	Translation initiation factor activity; mitosis; microtubule associated complex
130	CG3195	Ribosomal protein L12	Cytosolic large ribosomal subunit
131	CG33473	luna	Transcription factor activity, sequence-specific DNA binding
132	CG9638	transcriptional Adaptor 2b	Chromatin remodeling
133	CG4654	DP transcription factor	DNA binding; mitosis
134	CG6876	Prp31	Poly(A) RNA binding; ribonucleoprotein complex binding; spliceosomal complex; neurogenesis
135	CG17077	pointed	Transcription factor activity, sequence-specific DNA binding; cell fate commitment; neurogenesis; EGFR/Ras signaling
136	CG14543		Pre-rRNA-processing protein TSR2; neurogenesis
137	CG3193	crooked neck	Poly(A) RNA binding; neurogenesis
138	CG11902		Nucleic acid binding; zinc ion binding
139	CG4185	Negative Cofactor 2β	Transcription factor activity, RNA polymerase II core promoter sequence-specific binding involved in preinitiation complex assembly
140	CG12864	Su(var)2-HP2	DNA binding; gene silencing; neurogenesis;
141	CG10652	Ribosomal protein	Structural constituent of ribosome; mitotic spindle organization;

		L30	
142	CG34419	H6-like-homeobox	Transcription factor activity, sequence-specific DNA binding
143	CG4184	Mediator complex subunit 15	RNA polymerase II transcription cofactor activity;
144	CG7467	osa	DNA binding; photoreceptor cell differentiation; wnt signaling
145	CG10377	Heterogeneous nuclear ribonucleoprotein at 27C	Single-stranded DNA binding;
146	CG7055	Brahma associated protein 111kD	Chromatin remodeling; positive regulation of transcription, DNA-templated;
147	CG10754		Poly(A) RNA binding; mitotic spindle organization; ERK/Ras signaling
148	CG6197	fandango	Regulation of alternative mRNA splicing, via spliceosome; phagocytosis
149	CG7162	Mediator complex subunit 1	RNA polymerase II transcription cofactor activity;
150	CG13773		RNA polymerase I activity;
151	CG31992	gawky	Nucleic acid binding; gene silencing by miRNA;
152	CG31224		Nucleic acid binding
153	CG8427	Small ribonucleoprotein particle protein SmD3	Poly(A) RNA binding; mitotic spindle organization
154	CG33936		DNA binding; zinc ion binding
155	CG4211	no on or off transient A	mRNA binding; nucleotide binding
156	CG6189	lethal (1) 1Bi	DNA binding
157	CG11397	gluon	DNA binding; mitosis
158	CG33213		Nucleic acid binding
159	CG7726	Ribosomal protein L11	Structural constituent of ribosome; mitotic spindle organization;
160	CG9310	Hepatocyte nuclear factor 4	RNA polymerase II transcription factor activity, ligand-activated sequence-specific DNA binding; steroid hormone mediated signaling pathway

161	CG5057	Mediator complex subunit 10	RNA polymerase II transcription cofactor activity; mediator complex
162	CG3278	Tif-IA	Ribosome biogenesis; regulation of transcription from RNA polymerase I promoter
163	CG13628	Rpb10	DNA-directed RNA polymerase activity;
164	CG5147		DNA-directed RNA polymerase activity
165	CG8274	Megator	Chromatin DNA binding; mitosis
166	CG13849	Nop56	Small nuclear ribonucleoprotein complex; neurogenesis
167	CG11121	sine oculis	Transcription factor activity, RNA polymerase II distal enhancer sequence-specific binding; compound eye morphogenesis;
168	CG15532	headcase	RNA interference; axon extension; neurogenesis
169	CG11607	Homeodomain protein 2.0	Transcription factor activity, sequence-specific DNA binding
170	CG10281	Transcription factor IIFα	TFIIF-class transcription factor binding; neurogenesis
171	CG8332	Ribosomal protein S15	Structural constituent of ribosome; mitotic spindle organization
172	CG15697	Ribosomal protein S30	Structural constituent of ribosome; mitotic spindle organization
173	CG4807	abrupt	Transcription factor activity, sequence-specific DNA binding;
174	CG5271	Ribosomal protein S27A	Structural constituent of ribosome; microtubule associated complex; protein ubiquitination
175	CG11132	DNA methyltransferase 1 associated protein 1	Histone acetylation; chromatin remodeling
176	CG32121		Metal ion binding
177	CG4759	Ribosomal protein L27	Structural constituent of ribosome; mitotic spindle organization
178	CG5605	eukaryotic release factor 1	Translation release factor activity; autophagic cell death; smoothened signaling pathway
179	CG9091	Ribosomal protein L37a	Structural constituent of ribosome
180	CG10415	Transcription factor IIEα	Sequence-specific DNA binding; positive regulation of transcription from RNA polymerase II promoter
181	CG6251	Nucleoporin 62kD	Nucleocytoplasmic transporter activity; structural constituent of nuclear pore

182	CG12740	Ribosomal protein L28	Structural constituent of ribosome; mitotic spindle organization; neurogenesis
183	CG11352	jim	Metal ion binding; transcription factor activity, sequence-specific DNA binding; dendrite morphogenesis; regulation of chromatin silencing
184	CG18001	Ribosomal protein L38	Structural constituent of ribosome
185	CG7843	Ars2	Conversion of ds siRNA to ss siRNA involved in RNA interference
186	CG3644	bicaudal	Intracellular mRNA localization involved in anterior/posterior axis specification; microtubule associated complex
187	CG7757	Precursor RNA processing 3	Poly(A) RNA binding; regulation of chromatin silencing;
188	CG11491	broad	RNA polymerase II regulatory region sequence-specific DNA binding; compound eye photoreceptor fate commitment;
189	CG1603		Metal ion binding; ERK/Ras signaling
190	CG5595	Sex combs extra	Zinc finger; chromatin silencing; ubiquitin-protein transferase activity; neurogenesis
191	CG8491	kohtalo	RNA polymerase II transcription cofactor activity; compound eye development; mediator complex
192	CG17183	Mediator complex subunit 30	RNA polymerase II transcription cofactor activity; mediator complex
193	CG7424	Ribosomal protein L36A	Structural constituent of ribosome; mitotic spindle organization
194	CG17420	Ribosomal protein L15	Structural constituent of ribosome
195	CG12031	Mediator complex subunit 14	RNA polymerase II transcription cofactor activity; mediator complex
196	CG11522	Ribosomal protein L6	Structural constituent of ribosome; mitotic spindle organization
197	CG1821	Ribosomal protein L31	Structural constituent of ribosome; mitotic spindle organization
198	CG32180	Ecdysone-induced protein 74EF	Transcription factor activity, sequence-specific DNA binding; cell death
199	CG2063		Regulation of transcription, DNA-templated; neurogenesis
200	CG12396	Nnp-1	rRNA metabolic process; mitotic spindle elongation;
201	CG2009	Bip2	Chromatin binding; transcription factor binding; positive regulation of transcription from RNA polymerase II promoter
202	CG8759	Nascent polypeptide	Protein binding; regulation of pole plasm oskar mRNA localization; neurogenesis

		associated complex protein alpha subunit	
203	CG6884	Mediator complex subunit 11	RNA polymerase II transcription cofactor activity; mediator complex
204	CG5352	Small ribonucleoprotein particle protein SmB	Poly(A) RNA binding;
205	CG3423	stromalin	Chromatin binding; neuron remodeling; cohesin complex
206	CG1070	Alhambra	Transcription factor activity, sequence-specific DNA binding;
207	CG1017	Microfibril-associated protein 1	mRNA splicing, via spliceosome
208	CG33152	homeobrain	Transcription factor activity, sequence-specific DNA binding
209	CG9797	Motif 1 Binding Protein	RNA polymerase II core promoter sequence-specific DNA binding
210	CG8103	Mi-2	DNA binding; regulation of transcription from RNA polymerase II promoter
211	CG7939	Ribosomal protein L32	Structural constituent of ribosome; mitotic spindle organization
212	CG12352	separation anxiety	Histone acetyltransferase activity; fatty acid binding; lateral inhibition; neuron projection morphogenesis
213	CG1245	Mediator complex subunit 27	RNA polymerase II transcription cofactor activity; cellular response to ecdysone; regulation of JAK-STAT cascade;
214	CG43284		Transcription factor activity, sequence-specific DNA binding;
215	CG6376	E2F transcription factor 1	Transcriptional activator activity, RNA polymerase II core promoter proximal region sequence-specific binding;
216	CG5249	Blimp-1	Transcriptional repressor activity, RNA polymerase II core promoter proximal region sequence-specific binding; cellular response to ecdysone
217	CG1064	Snf5-related 1	Protein binding; regulation of transcription from RNA polymerase II promoter
218	CG5193	Transcription factor IIB	Transcription factor binding; transcriptional start site selection at RNA polymerase II promoter
219	CG7776	Enhancer of Polycomb	Regulation of transcription from RNA polymerase II promoter; regulation of transcription from RNA polymerase II promoter
220	CG1527	Ribosomal protein S14b	Structural constituent of ribosome;

221	CG5119	pAbp	mRNA 3'-UTR binding; poly(A) binding; microtubule associated complex
222	CG32120	senseless	Transcription factor activity, RNA polymerase II distal enhancer sequence-specific binding; compound eye photoreceptor development; R8 cell differentiation
223	CG3949	hoi-polloi	mRNA binding;
224	CG13900		Damaged DNA binding; mitotic spindle organization; neurogenesis
225	CG9854	hiiragi	Polynucleotide adenylyltransferase activity
226	CG8882	Trip	Translation initiation factor activity; microtubule associated complex
227	CG1676	cactin	Poly(A) RNA binding; neuron projection morphogenesis;
228	CG18783	Kruppel homolog 1	Transcription factor activity, sequence-specific DNA binding; compound eye photoreceptor development
229	CG10955	Rtf1	DNA binding; positive regulation of transcription, DNA-templated
230	CG11049	shaven	Transcription factor activity, RNA polymerase II distal enhancer sequence-specific binding; regulation of R7 cell differentiation

Table 26: Rab GTPase/signalling proteins that enhance the *rap1* phenotype in the large-scale genetic modifier screen.

Number	CG number	Gene	Predicted function
231	CG3171	Trapped in endoderm 1	G-protein coupled receptor activity
232	CG8416	Rho1	Actin cytoskeleton organization; compound eye morphogenesis; dorsal closure; EGFR signaling; planar polarity
233	CG2848	Transportin-Serine/Arginine rich	Ran GTPase binding; neurogenesis; regulation of mRNA splicing, via spliceosome
234	CG9811	Rad, Gem/Kir family member 1	GTPase activity; negative regulation of voltage-gated calcium channel activity
235	CG11561	smoothened	G-protein coupled receptor activity; eye morphogenesis; notch signalling
236	CG8385	ADP ribosylation factor at 79F	GTPase activity; cell adhesion; compound eye development; endocytosis
237	CG1404	Ran	GTPase activity; actin filament organization; cell adhesion; mitosis
238	CG13345	tumbleweed	GTPase activator activity; cell fate; mitosis; Rho signaling; neurogenesis
239	CG18627	β subunit of type II geranylgeranyl transferase	Rab geranylgeranyltransferase activity; Rab-protein geranylgeranyltransferase complex
240	CG11448		JNK/Rab-associated protein-1, N-terminal; neuron projection morphogenesis
241	CG3269	Rab2	Protein binding; GTPase activity (structural similarity to Rab11); Rab protein signal transduction
242	CG3983	Nucleostemin 1	GTPase activity; insulin signaling; mitotic spindle assembly; ribosome biogenesis
243	CG3664	Rab5	GTPase activity; protein binding; vesicle-mediated transport; establishment or maintenance of apical/basal cell polarity; dorsal closure
245	CG6033	downstream of receptor kinase	Ras protein signal transduction; protein binding; sevenless signalling; Torso signaling; SH3/SH2 adaptor activity; actin filament organization; EGFR signalling
246	CG9375	Ras oncogene at 85D	GTPase activity; establishment or maintenance of apical/basal cell polarity;
247	CG13281	CAS/CSE1 segregation protein	Ran GTPase binding; protein export from nucleus

Table 27: Ubiquitin pathway components that enhance the *rap1* phenotype in the large-scale genetic modifier screen.

Number	CG number	Gene	Predicted function
248	CG16983	SKP1-related A	Ubiquitin-protein transferase activity; negative regulation of insulin receptor and JNK signaling pathway; positive regulation of mitotic cell cycle
249	CG9952	Partner of paired	SCF-dependent proteasomal ubiquitin-dependent protein catabolic process
250	CG6720	Ubiquitin conjugating enzyme 2	Ubiquitin-protein transferase activity
251	CG10800	Regulator of cyclin A1	Ubiquitin-protein transferase activity; lateral inhibition; mitosis
252	CG8392	Proteasome β1 subunit	Proteasome-mediated ubiquitin-dependent protein catabolic process
253	CG7528	Ubiquitin activating enzyme 2	Ubiquitin activating enzyme binding; protein sumoylation
254	CG11981	Proteasome β3 subunit	Threonine-type endopeptidase activity; proteasome-mediated ubiquitin-dependent protein catabolic process
255	CG9324	Pomp	Positive regulation of proteasomal ubiquitin-dependent protein catabolic process; Cell proliferation; mitosis
256	CG8439	T-complex Chaperonin 5	ATPase activity; unfolded protein binding; mitotic spindle organization; microtubule associated complex
257	CG7425	Effete	Ubiquitin protein ligase activity; compound eye morphogenesis; microtubule associated complex
258	CG42797		Ubiquitin protein ligase activity
259	CG10679	Nedd8	Regulation of ubiquitin-protein transferase activity; protein neddylation; smoothened signaling pathway; neuron projection morphogenesis;
260	CG3473		Ubiquitin-protein transferase activity
261	CG2960	Ribosomal protein L40	Structural constituent of ribosome; ubiquitin-dependent protein catabolic process; microtubule associated complex
262	CG32221		Ubiquitin-protein transferase activity; SCF ubiquitin ligase complex
263	CG42616	Cullin-3	Ubiquitin protein ligase binding; compound eye morphogenesis;
264	CG31633		Ubiquitin-protein transferase activity

265	CG12000	Proteasome β7 subunit	Threonine-type endopeptidase activity; proteasome-mediated ubiquitin-dependent protein catabolic process; mitotic spindle organization
266	CG7828	β-Amyloid precursor protein binding protein 1	NEDD8 activating enzyme activity; ubiquitin activating enzyme activity; protein neddylation
267	CG3329	Proteasome β2 subunit	Threonine-type endopeptidase activity; proteasome-mediated ubiquitin-dependent protein catabolic process
268	CG5003		Ubiquitin-protein transferase activity;
269	CG8711	Cullin 4	Ubiquitin protein ligase binding; Cul4-RING E3 ubiquitin ligase complex
270	CG9153	SUMO-related HECT repeat protein for Toll pathway activation	Ubiquitin-protein transferase activity
271	CG5794	puffyeye	Thiol-dependent ubiquitin-specific protease activity;
272	CG3416	Regulatory particle non-ATPase 8	Proteasome-mediated ubiquitin-dependent protein catabolic process; mitotic spindle organization;
273	CG3018	lesswright	SUMO ligase activity; ubiquitin activating enzyme binding; dorsal closure
274	CG3889	COP9 signalosome subunit 1b	Cullin deneddylation; COP9 signalosome; lateral inhibition; neurogenesis; regulation of G-protein coupled receptor protein signaling pathway
275	CG1242	Heat shock protein 83	Unfolded protein binding; actin filament organization; R7 cell fate commitment;
276	CG42641	Regulatory particle non-ATPase 3	Zinc ion binding; proteasome-mediated ubiquitin-dependent protein catabolic process
277	CG5798	Ubiquitin specific protease 8	Thiol-dependent ubiquitin-specific protease activity; wnt signaling; smoothened signaling;
278	CG4673	Npl4	Structural constituent of nuclear pore; ubiquitin-dependent protein catabolic process

Table 28: Miscellaneous components that enhance the *rap1* phenotype in the large-scale genetic modifier screen.

Number	CG number	Gene	Predicted function
279	CG1709	Vacuolar H^+ ATPase 100kD subunit 1	Calmodulin binding; autophagosome maturation; photoreceptor activity
280	CG1109		Neuron projection morphogenesis
281	CG5785	three rows	Mitosis; epithelial morphogenesis
282	CG32204		Unknown function
283	CG8610	Cell division cycle 27	Mitosis
284	CG8765		Lateral inhibition
285	CG9238	Glycogen binding subunit 70E	Protein phosphatase 1 binding
286	CG2938		Lateral inhibition
287	CG5052	pimples	Mitosis; epithelial cell development; neurogenesis
288	CG42322		Solute carrier family 35 member F3/F4
289	CG9300		
290	CG5844		Dodecenoyl-CoA delta-isomerase activity; phagocytosis
291	CG2691		Armadillo-type fold; neuron projection morphogenesis;
292	CG8374	dalmatian	Sororin protein; mitosis
293	CG9012	Clathrin heavy chain	Endocytosis; compound eye development;
294	CG13917		Pebble suppressor
295	CG8237		
296	CG7334	Sugar baby	Major facilitator superfamily associated domain
297	CG5586	Tusp	Intracellular signal transduction

298	CG12404		Yip1 domain
299	CG8213		Serine-type endopeptidase activity
300	CG17255	no circadian temperature entrainment	Entrainment of circadian clock
301	CG10583	Seperase	Peptidase activity; neurogenesis; phagocytosis
302	CG11451	Spc105-related	Mitotic spindle organization
303	CG6687	Serpin 88Eb	Serine-type endopeptidase inhibitor activity

Table 29: Polarity and cell adhesion proteins that enhance the *rap1* phenotype in the large-scale genetic modifier screen.

Number	CG number	Gene	Predicted function
304	CG31605	Basigin	Cell-cell adhesion; cytoskeleton of presynaptic active zone; photoreceptor cell morphogenesis
305	CG4032	Abl tyrosine kinase	Non-membrane spanning protein tyrosine kinase activity; compound eye development; dorsal closure; epithelial cell morphogenesis
306	CG3921	Bark beetle	Carbohydrate binding; cell-cell junction maintenance
307	CG3722	Shotgun/DE-Cad	Protein binding; cell adhesion molecule binding; apical protein localization; cell morphogenesis; compound eye morphogenesis
308	CG5884	Par6	Protein binding; apical protein localization; establishment or maintenance of epithelial cell apical/basal polarity
309	CG18582	mushroom bodies tiny	Protein serine/threonine kinase activity; compound eye development; lateral inhibition; cytoskeleton organization; cell-cell adherens junction morphogenesis
310	CG5055	Bazooka	Protein binding; apical protein localization; establishment of apical/basal cell polarity; zonula adherens assembly
311	CG5670	Na pump α subunit	Sodium:potassium-exchanging ATPase activity; septate junction assembly
312	CG32717	Stardust	Guanylate kinase activity; apical/basal polarity

Table 30: Common hits between the *rap1* and *aPKC*-genetic modifier screens

Number	CG number	Gene	Predicted function
1	CG6720	Ubiquitin conjugating enzyme 2	Ubiquitin-protein transferase activity
2	CG7525	Tie-like receptor tyrosine kinase	Protein tyrosine kinase activity
3	CG3292		Alkaline phosphatase activity
4	CG7625	Vacuolar H^+ ATPase M9.7 subunit b	Plasma membrane proton-transporting V-type ATPase complex
5	CG6121	Tat interactive protein 60kDa	Histone acetyltransferase activity;
6	CG7309		Dicarboxylic acid transmembrane transporter activity
7	CG7507	Dynein heavy chain 64C	Microtubule motor activity; establishment of epithelial cell apical/basal polarity; mitosis
8	CG12366	O-fucosyltransferase 1	Integral component of Golgi membrane; Notch binding; endocytosis; lateral inhibition
9	CG7850	puckered	JUN kinase phosphatase activity; MAP kinase tyrosine/serine/threonine phosphatase; actin filament organization; cell shape; dorsal closure
10	CG6876	Prp31	Poly(A) RNA binding; ribonucleoprotein complex binding; spliceosomal complex; neurogenesis
11	CG8978	Actin-related protein 2/3 complex, subunit 1	Actin binding; structural constituent of cytoskeleton; Arp2/3 complex-mediated actin nucleation; integrin-mediated cell adhesion; compound eye morphogenesis;
12	CG4977	Kekkon-2	Integral component of plasma membrane
13	CG1098	MLF1-adaptor molecule	Protein serine/threonine kinase activity; cell proliferation; cell size
14	CG2096	flapwing	Myosin phosphatase activity; protein serine/threonine phosphatase activity; JNK signaling; regulation of actomyosin contractile ring contraction; cell adhesion
15	CG11397	gluon	DNA binding; mitosis

16	CG32221		Ubiquitin-protein transferase activity; SCF ubiquitin ligase complex
17	CG33213		Nucleic acid binding
18	CG8581	frazzled	Integral component of membrane; netrin receptor activity; axon guidance
19	CG5474	Signal sequence receptor β	Integral component of membrane; signal sequence binding; protein retention in ER lumen;
20	CG5057	Mediator complex subunit 10	RNA polymerase II transcription cofactor activity; mediator complex
21	CG5974	pelle	Protein serine/threonine kinase activity; dorsal/ventral axis specification;
22	CG31633		Ubiquitin-protein transferase activity
23	CG3665	Fasciclin 2	Integral component of membrane; protein binding; cell morphogenesis involved in neuron differentiation;
24	CG8866		Protein serine/threonine kinase activity
25	CG17029		Inositol monophosphate 1-phosphatase activity
26	CG32019	bent	Protein serine/threonine/tyrosine kinase activity; structural constituent of cytoskeleton
27	CG7828	β-Amyloid precursor protein binding protein 1	NEDD8 activating enzyme activity; ubiquitin activating enzyme activity; protein neddylation
28	CG8237		
29	CG6251	Nucleoporin 62kD	Nucleocytoplasmic transporter activity; structural constituent of nuclear pore
30	CG10751	roadblock	Dynein intermediate chain binding; microtubule-based movement; microtubule associated complex
31	CG12031	Mediator complex subunit 14	RNA polymerase II transcription cofactor activity; mediator complex

Table 31: Common hits between the *rap1* and *crumbs*^{intra}-genetic modifier screens

Number	CG number	Gene	Predicted function
1	CG32717	Stardust	Guanylate kinase activity; apical/basal polarity
2	CG9952	Partner of paired	SCF-dependent proteasomal ubiquitin-dependent protein catabolic process
3	CG17436	Verthandi/cohesin	Chromatin binding; mitosis
4	CG5670	Na pump α subunit	Sodium:potassium-exchanging ATPase activity; septate junction assembly
5	CG6625	α Soluble NSF attachment protein	SNARE binding; ER to Golgi vesicle-mediated transport; compound eye morphogenesis
6	CG9238	Glycogen binding subunit 70E	Protein phosphatase 1 binding
7	CG10808	Synaptogyrin	Synaptic vesicle transport
8	CG7627		ATPase activity, coupled to transmembrane movement of substances
9	CG8439	T-complex Chaperonin 5	ATPase activity; unfolded protein binding; mitotic spindle organization; microtubule associated complex
10	CG9355	dusky	Integral component of membrane; genetic interaction with miniature
11	CG6876	Prp31	Poly(A) RNA binding; ribonucleoprotein complex binding; spliceosomal complex; neurogenesis
12	CG14543		Pre-rRNA-processing protein TSR2; neurogenesis
13	CG11561	smoothened	G-protein coupled receptor activity; eye morphogenesis; notch signalling
14	CG13773		RNA polymerase I activity;
15	CG3473		Ubiquitin-protein transferase activity
16	CG17664		Integral component of membrane; transmembrane transport
17	CG33213		Nucleic acid binding
18	CG5057	Mediator complex subunit 10	RNA polymerase II transcription cofactor activity; mediator complex
19	CG10369	Inwardly rectifying potassium channel 3	Integral component of membrane; inward rectifier potassium channel activity
20	CG11190	attachment of GPI	

		anchor to protein	
21	CG3665	Fasciclin 2	Integral component of membrane; protein binding; cell morphogenesis involved in neuron differentiation;
22	CG10281	Transcription factor IIFα	TFIIF-class transcription factor binding; neurogenesis
23	CG8866		Protein serine/threonine kinase activity
24	CG8237		
25	CG6251	Nucleoporin 62kD	Nucleocytoplasmic transporter activity; structural constituent of nuclear pore
26	CG33196	dumpy	Extracellular matrix structural constituent; lateral inhibition
27	CG9153	SUMO-related HECT repeat protein for Toll pathway activation	Ubiquitin-protein transferase activity
28	CG4032	Abl tyrosine kinase	Non-membrane spanning protein tyrosine kinase activity; compound eye development; dorsal closure; epithelial cell morphogenesis
29	CG10751	roadblock	Dynein intermediate chain binding; microtubule-based movement; microtubule associated complex
30	CG12031	Mediator complex subunit 14	RNA polymerase II transcription cofactor activity; mediator complex
31	CG5794	puffyeye	Thiol-dependent ubiquitin-specific protease activity;
32	CG12396	Nnp-1	rRNA metabolic process; mitotic spindle elongation;
33	CG2009	Bip2	Chromatin binding; transcription factor binding; positive regulation of transcription from RNA polymerase II promoter
34	CG8759	Nascent polypeptide associated complex protein alpha subunit	Protein binding; regulation of pole plasm oskar mRNA localization; neurogenesis
35	CG3018	lesswright	SUMO ligase activity; ubiquitin activating enzyme binding; dorsal closure
36	CG5179	Cyclin-dependent kinase 9	Cyclin-dependent protein serine/threonine kinase activity; cell adhesion
37	CG3269	Rab2	Protein binding; GTPase activity (structural similarity to Rab11); Rab protein signal transduction
38	CG1064	Snf5-related 1	Protein binding; regulation of transcription from RNA polymerase II promoter
39	CG4869	β-Tubulin at 97EF	Structural constituent of cytoskeleton; GTPase activity;
40	CG5884	Par6	Protein binding; apical protein localization; establishment or maintenance of epithelial cell apical/basal polarity
41	CG6033	downstream of	Ras protein signal transduction; protein binding; sevenless signalling; Torso signaling; SH3/SH2 adaptor activity; actin

		receptor kinase	filament organization; EGFR signaling
42	CG13281	CAS/CSE1 segregation protein	Ran GTPase binding; protein export from nucleus

Table 32: Common hits between the *rap1*, *aPKC* and *crumbs*-genetic modifier screens

Number	CG number	Gene	Predicted function
1	CG6121	Tat interactive protein 60kDa	Histone acetyltransferase activity;
2	CG7507	Dynein heavy chain 64C	Microtubule motor activity; establishment of epithelial cell apical/basal polarity; mitosis
3	CG7850	puckered	JUN kinase phosphatase activity; MAP kinase tyrosine/serine/threonine phosphatase; actin filament organization; cell shape; dorsal closure
4	CG6876	Prp31	Poly(A) RNA binding; ribonucleoprotein complex binding; spliceosomal complex; neurogenesis
5	CG33213		Nucleic acid binding
6	CG3665	Fasciclin 2	Integral component of membrane; protein binding; cell morphogenesis involved in neuron differentiation;
7	CG8866		Protein serine/threonine kinase activity
8	CG8237		
9	CG12031	Mediator complex subunit 14	RNA polymerase II transcription cofactor activity; mediator complex
10	CG5055	bazooka	Protein binding; apical protein localization; establishment of apical/basal cell polarity; *zonula adherens* assembly
11	CG42611	Megalin	Low-density lipoprotein receptor activity; regulation of endocytosis
12	CG31997		Single domain Von Willebrand factor type C domain
13	CG3980	Cep97	Protein phosphatase type 1 regulator activity; centriole replication
14	CG31962	Scavenger receptor class C, type III	Scavenger receptor activity
15	CG31020	Sanpodo	Integral component of membrane; Notch signalling; protein binding; cell division;
16	CG7664	Cropped	Myosin binding; sequence-specific DNA binding
17	CG43224	Glial cell line-derived neurotrophic	Cell adhesion molecule binding; anchored component of external side of plasma membrane

		family receptor-like	

Table 33: Common hits between the *rap1*-genetic modifier screen and the DE-Cad S2 cell adhesion screen

Number	CG number	Gene	Predicted function
1	CG8978	Actin-related protein 2/3 complex, subunit 1	Actin binding; structural constituent of cytoskeleton; Arp2/3 complex-mediated actin nucleation; integrin-mediated cell adhesion; compound eye morphogenesis
2	CG4977	Kekkon-2	Integral component of plasma membrane
3	CG1404	Ran	GTPase activity; actin filament organization; cell adhesion; mitosis
4	CG34099	MAP kinase-specific phosphatase	MAP kinase tyrosine/serine/threonine phosphatase activity
5	CG42312	Canoe	*Adherens junction* morphogenesis; Rap1 binding; actin binding;
6		Stardust	Guanylate kinase activity; apical/basal polarity
7		shotgun	
8	CG1109		Neuron projection morphogenesis
9	CG12019	Cdc37	Protein tyrosine kinase; ERK signaling
10	CG9423	karyopherin α3	Myosin binding; contain Armadillo repeats
11	CG1913	α-Tubulin at 84B	GTPase activity; mitotic spindle organization
12	CG10800	Regulator of cyclin A1	Ubiquitin-protein transferase activity; lateral inhibition; mitosis
13	CG4254	twinstar	Actin filament organization; compound eye development; genetic interaction with *mbt*

14	CG6625	α Soluble NSF attachment protein	SNARE binding; ER to Golgi vesicle-mediated transport; compound eye morphogenesis
15	CG8439	T-complex Chaperonin 5	ATPase activity; unfolded protein binding; mitotic spindle organization; microtubule associated complex
16	CG5844		Dodecenoyl-CoA delta-isomerase activity; phagocytosis
17	CG7000	Sensory neuron membrane protein 1	Integral component of plasma membrane; scavenger receptor activity; cell adhesion
18	CG8385	ADP ribosylation factor at 79F	GTPase activity; cell adhesion; compound eye development; endocytosis
19	CG10369	Inwardly rectifying potassium channel 3	Integral component of membrane; inward rectifier potassium channel activity
20	CG3644	bicaudal	Intracellular mRNA localization involved in anterior/posterior axis specification; microtubule associated complex
21	CG3938	Cyclin E	Cyclin-dependent protein serine/threonine kinase regulator activity; cell adhesion; cell proliferation involved in compound eye morphogenesis;
22	CG3983	Nucleostemin 1	GTPase activity; insulin signaling; mitotic spindle assembly; ribosome biogenesis
23	CG4869	β-Tubulin at 97EF	Structural constituent of cytoskeleton; GTPase activity;
24	CG17090	Homeodomain interacting protein kinase	Protein serine/threonine kinase activity; compound eye development; hippo signaling; wnt signalling
25	CG13281	CAS/CSE1 segregation protein	Ran GTPase binding; protein export from nucleus
26	CG4166	Non-stop	Thiol-dependent ubiquitin-specific protease activity; axon guidance; transcription regulation
27	CG2092	Scraps	Actin/microtubule binding; cell division;

References:

Araújo, S.J. and Tear, G. 2003. Axon guidance mechanisms and molecules: lessons from invertebrates. *Nature Reviews. Neuroscience* 4(11), pp. 910–922.

Asha, H., de Ruiter, N.D., Wang, M.G. and Hariharan, I.K. 1999. The Rap1 GTPase functions as a regulator of morphogenesis in vivo. *The EMBO Journal* 18(3), pp. 605–615.

Bachmann, A., Schneider, M., Theilenberg, E., Grawe, F. and Knust, E. 2001. Drosophila Stardust is a partner of Crumbs in the control of epithelial cell polarity. *Nature* 414(6864), pp. 638–643.

Bahri, S.M., Yang, X. and Chia, W. 1997. The Drosophila bifocal gene encodes a novel protein which colocalizes with actin and is necessary for photoreceptor morphogenesis. *Molecular and Cellular Biology* 17(9), pp. 5521–5529.

Baril, C., Lefrançois, M., Sahmi, M., Knævelsrud, H. and Therrien, M. 2014. Apical accumulation of the Sevenless receptor tyrosine kinase during Drosophila eye development is promoted by the small GTPase Rap1. *Genetics* 197(4), pp. 1237–1250.

Beers, M. and Kemphues, K. 2006. Depletion of the co-chaperone CDC-37 reveals two modes of PAR-6 cortical association in C. elegans embryos. *Development* 133(19), pp. 3745–3754.

Bender, A. and Pringle, J. 1989. Multicopy suppression of the cdc24 budding defect in yeast by CDC42 and three newly identified genes including the ras-related gene RSRI. *Proc. Natl. Acad. Sci. USA*.

Benton, R. and St Johnston, D. 2003. Drosophila PAR-1 and 14-3-3 inhibit Bazooka/PAR-3 to establish complementary cortical domains in polarized cells. *Cell* 115(6), pp. 691–704.

Bergstralh, D.T. and St Johnston, D. 2012. Epithelial cell polarity: what flies can teach us about cancer. *Essays in biochemistry* 53, pp. 129–140.

Bernadskaya, Y.Y., Patel, F.B., Hsu, H.-T. and Soto, M.C. 2011. Arp2/3 promotes junction formation and maintenance in the Caenorhabditis elegans intestine by regulating membrane association of apical proteins. *Molecular Biology of the Cell* 22(16), pp. 2886–2899.

Bhattacharya, A. and Baker, N.E. 2009. The HLH protein Extramacrochaetae is required for R7 cell and cone cell fates in the Drosophila eye. *Developmental Biology* 327(2), pp. 288–300.

Bilder, D. 2004. Epithelial polarity and proliferation control: links from the Drosophila neoplastic tumor suppressors. *Genes & Development* 18(16), pp. 1909–1925.

Bilder, D. and Perrimon, N. 2000. Localization of apical epithelial determinants by the basolateral PDZ protein Scribble. *Nature* 403(6770), pp. 676–680.

Boettner, B. and Van Aelst, L. 2007. The Rap GTPase activator Drosophila PDZ-GEF regulates cell shape in epithelial migration and morphogenesis. *Molecular and Cellular Biology* 27(22), pp. 7966–7980.
Boettner, B., Govek, E.E., Cross, J. and Van Aelst, L. 2000. The junctional multidomain protein AF-6 is a binding partner of the Rap1A GTPase and associates with the actin cytoskeletal regulator profilin. *Proceedings of the National Academy of Sciences of the United States of America* 97(16), pp. 9064–9069.
Boettner, B., Harjes, P., Ishimaru, S., Heke, M., Fan, H.Q., Qin, Y., Van Aelst, L. and Gaul, U. 2003. The AF-6 homolog canoe acts as a Rap1 effector during dorsal closure of the Drosophila embryo. *Genetics* 165(1), pp. 159–169.
Bos, J.L., de Bruyn, K., Enserink, J., Kuiperij, B., Rangarajan, S., Rehmann, H., Riedl, J., de Rooij, J., van Mansfeld, F. and Zwartkruis, F. 2003. The role of Rap1 in integrin-mediated cell adhesion. *Biochemical Society Transactions* 31(Pt 1), pp. 83–86.
Braga, V.M., Betson, M., Li, X. and Lamarche-Vane, N. 2000. Activation of the small GTPase Rac is sufficient to disrupt cadherin-dependent cell-cell adhesion in normal human keratinocytes. *Molecular Biology of the Cell* 11(11), pp. 3703–3721.
Braga, V.M., Machesky, L.M., Hall, A. and Hotchin, N.A. 1997. The small GTPases Rho and Rac are required for the establishment of cadherin-dependent cell-cell contacts. *The Journal of Cell Biology* 137(6), pp. 1421–1431.
Brand, A.H. and Perrimon, N. 1993. Targeted gene expression as a means of altering cell fates and generating dominant phenotypes. *Development* 118(2), pp. 401–415.
Brennan, C.A., Li, T.R., Bender, M., Hsiung, F. and Moses, K. 2001. Broad-complex, but not ecdysone receptor, is required for progression of the morphogenetic furrow in the Drosophila eye. *Development* 128(1), pp. 1–11.
Brown, K.E., Baonza, A. and Freeman, M. 2006. Epithelial cell adhesion in the developing Drosophila retina is regulated by Atonal and the EGF receptor pathway. *Developmental Biology* 300(2), pp. 710–721.
Bulgakova, N.A., Grigoriev, I., Yap, A.S., Akhmanova, A. and Brown, N.H. 2013. Dynamic microtubules produce an asymmetric E-cadherin-Bazooka complex to maintain segment boundaries. *The Journal of Cell Biology* 201(6), pp. 887–901.
Campbell, K., Knust, E. and Skaer, H. 2009. Crumbs stabilises epithelial polarity during tissue remodelling. *Journal of Cell Science* 122(Pt 15), pp. 2604–2612.
Campbell, K., Whissell, G., Franch-Marro, X., Batlle, E. and Casanova, J. 2011. Specific GATA factors act as conserved inducers of an

endodermal-EMT. *Developmental Cell* 21(6), pp. 1051–1061.
Carmena, A., Makarova, A. and Speicher, S. 2011. The Rap1-Rgl-Ral signaling network regulates neuroblast cortical polarity and spindle orientation. *The Journal of Cell Biology* 195(4), pp. 553–562.
Cereijido, M., Contreras, R.G. and Shoshani, L. 2004. Cell adhesion, polarity, and epithelia in the dawn of metazoans. *Physiological Reviews* 84(4), pp. 1229–1262.
Chanet, S. and Schweisguth, F. 2012. Regulation of epithelial polarity by the E3 ubiquitin ligase Neuralized and the Bearded inhibitors in Drosophila. *Nature Cell Biology* 14(5), pp. 467–476.
Chen, F., Barkett, M., Ram, K.T., Quintanilla, A. and Hariharan, I.K. 1997. Biological characterization of Drosophila Rapgap1, a GTPase activating protein for Rap1. *Proceedings of the National Academy of Sciences of the United States of America* 94(23), pp. 12485–12490.
Chen, X., Kojima, S., Borisy, G.G. and Green, K.J. 2003. p120 catenin associates with kinesin and facilitates the transport of cadherin-catenin complexes to intercellular junctions. *The Journal of Cell Biology* 163(3), pp. 547–557.
Chen, Y.T., Stewart, D.B. and Nelson, W.J. 1999. Coupling assembly of the E-cadherin/beta-catenin complex to efficient endoplasmic reticulum exit and basal-lateral membrane targeting of E-cadherin in polarized MDCK cells. *The Journal of Cell Biology* 144(4), pp. 687–699.
Choi, W., Harris, N.J., Sumigray, K.D. and Peifer, M. 2013. Rap1 and Canoe/afadin are essential for establishment of apical-basal polarity in the Drosophila embryo. *Molecular Biology of the Cell* 24(7), pp. 945–963.
Corrigall, D., Walther, R.F., Rodriguez, L., Fichelson, P. and Pichaud, F. 2007. Hedgehog signaling is a principal inducer of Myosin-II-driven cell ingression in Drosophila epithelia. *Developmental Cell* 13(5), pp. 730–742.
Cox, R.T., Kirkpatrick, C. and Peifer, M. 1996. Armadillo is required for adherens junction assembly, cell polarity, and morphogenesis during Drosophila embryogenesis. *The Journal of Cell Biology* 134(1), pp. 133–148.
Davis, M.A., Ireton, R.C. and Reynolds, A.B. 2003. A core function for p120-catenin in cadherin turnover. *The Journal of Cell Biology* 163(3), pp. 525–534.
Delon, I., Chanut-Delalande, H. and Payre, F. 2003. The Ovo/Shavenbaby transcription factor specifies actin remodelling during epidermal differentiation in Drosophila. *Mechanisms of Development* 120(7), pp. 747–758.
Desai, R., Sarpal, R., Ishiyama, N., Pellikka, M., Ikura, M. and Tepass, U. 2013. Monomeric α-catenin links cadherin to the actin cytoskeleton. *Nature Cell Biology* 15(3), pp. 261–273.

Dickson, B. and Hafen, E. 1994. Genetics of signal transduction in invertebrates. *Current Opinion in Genetics & Development* 4(1), pp. 64–70.
Doerflinger, H., Benton, R., Shulman, J.M. and St Johnston, D. 2003. The role of PAR-1 in regulating the polarised microtubule cytoskeleton in the Drosophila follicular epithelium. *Development* 130(17), pp. 3965–3975.
Drees, F., Pokutta, S., Yamada, S., Nelson, W.J. and Weis, W.I. 2005. Alpha-catenin is a molecular switch that binds E-cadherin-beta-catenin and regulates actin-filament assembly. *Cell* 123(5), pp. 903–915.
Le Droguen, P.-M., Claret, S., Guichet, A. and Brodu, V. 2015. Microtubule-dependent apical restriction of recycling endosomes sustains adherens junctions during morphogenesis of the Drosophila tracheal system. *Development* 142(2), pp. 363–374.
Dupuy, A.G., L'Hoste, S., Cherfils, J., Camonis, J., Gaudriault, G. and de Gunzburg, J. 2005. Novel Rap1 dominant-negative mutants interfere selectively with C3G and Epac. *Oncogene* 24(28), pp. 4509–4520.
Eden, E., Navon, R., Steinfeld, I., Lipson, D. and Yakhini, Z. 2009. GOrilla: a tool for discovery and visualization of enriched GO terms in ranked gene lists. *BMC Bioinformatics* 10, p. 48.
Eisen, M.B., Spellman, P.T., Brown, P.O. and Botstein, D. 1998. Cluster analysis and display of genome-wide expression patterns. *Proceedings of the National Academy of Sciences of the United States of America* 95(25), pp. 14863–14868.
Ellis, S.J., Goult, B.T., Fairchild, M.J., Harris, N.J., Long, J., Lobo, P., Czerniecki, S., Van Petegem, F., Schöck, F., Peifer, M. and Tanentzapf, G. 2013. Talin autoinhibition is required for morphogenesis. *Current Biology* 23(18), pp. 1825–1833.
Escudero, L.M., Bischoff, M. and Freeman, M. 2007. Myosin II regulates complex cellular arrangement and epithelial architecture in Drosophila. *Developmental Cell* 13(5), pp. 717–729.
Etienne-Manneville, S. and Hall, A. 2002. Rho GTPases in cell biology. *Nature* 420(6916), pp. 629–635.
Farquhar, M.G. and Palade, G.E. 1963. Junctional complexes in various epithelia. *The Journal of Cell Biology* 17, pp. 375–412.
Farr, G.A., Hull, M., Stoops, E.H., Bateson, R. and Caplan, M.J. 2015. Dual pulse-chase microscopy reveals early divergence in the biosynthetic trafficking of the Na,K-ATPase and E-cadherin. *Molecular Biology of the Cell* 26(24), pp. 4401–4411.
Fleming, T.P., Papenbrock, T., Fesenko, I., Hausen, P. and Sheth, B. 2000. Assembly of tight junctions during early vertebrate development. *Seminars in Cell & Developmental Biology* 11(4), pp. 291–299.
Freeman, M. 1996. Reiterative use of the EGF receptor triggers differentiation of all cell types in the Drosophila eye. *Cell* 87(4), pp. 651–

660.
Fu, W. and Noll, M. 1997. The Pax2 homolog sparkling is required for development of cone and pigment cells in the Drosophila eye. *Genes & Development* 11(16), pp. 2066–2078.
Gaengel, K. and Mlodzik, M. 2003. Egfr signaling regulates ommatidial rotation and cell motility in the Drosophila eye via MAPK/Pnt signaling and the Ras effector Canoe/AF6. *Development* 130(22), pp. 5413–5423.
Garvalov, B.K., Flynn, K.C., Neukirchen, D., Meyn, L., Teusch, N., Wu, X., Brakebusch, C., Bamburg, J.R. and Bradke, F. 2007. Cdc42 regulates cofilin during the establishment of neuronal polarity. *The Journal of Neuroscience* 27(48), pp. 13117–13129.
Genova, J.L. and Fehon, R.G. 2003. Neuroglian, Gliotactin, and the Na+/K+ ATPase are essential for septate junction function in Drosophila. *The Journal of Cell Biology* 161(5), pp. 979–989.
Georgiou, M., Marinari, E., Burden, J. and Baum, B. 2008. Cdc42, Par6, and aPKC regulate Arp2/3-mediated endocytosis to control local adherens junction stability. *Current Biology* 18(21), pp. 1631–1638.
Gomez, G.A., McLachlan, R.W., Wu, S.K., Caldwell, B.J., Moussa, E., Verma, S., Bastiani, M., Priya, R., Parton, R.G., Gaus, K., Sap, J. and Yap, A.S. 2015. An RPTPα/Src family kinase/Rap1 signaling module recruits myosin IIB to support contractile tension at apical E-cadherin junctions. *Molecular Biology of the Cell* 26(7), pp. 1249–1262.
Gurudev, N., Yuan, M. and Knust, E. 2014. chaoptin, prominin, eyes shut and crumbs form a genetic network controlling the apical compartment of Drosophila photoreceptor cells. *Biology open* 3(5), pp. 332–341.
Harding, M.J., McGraw, H.F. and Nechiporuk, A. 2014. The roles and regulation of multicellular rosette structures during morphogenesis. *Development* 141(13), pp. 2549–2558.
Hariharan, I.K., Carthew, R.W. and Rubin, G.M. 1991. The Drosophila roughened mutation: activation of a rap homolog disrupts eye development and interferes with cell determination. *Cell* 67(4), pp. 717–722.
Harris, K.P. and Tepass, U. 2008. Cdc42 and Par proteins stabilize dynamic adherens junctions in the Drosophila neuroectoderm through regulation of apical endocytosis. *The Journal of Cell Biology* 183(6), pp. 1129–1143.
Harris, T.J.C. 2012. Adherens junction assembly and function in the Drosophila embryo. *International review of cell and molecular biology* 293, pp. 45–83.
Harris, T.J.C. and Peifer, M. 2004. Adherens junction-dependent and -independent steps in the establishment of epithelial cell polarity in Drosophila. *The Journal of Cell Biology* 167(1), pp. 135–147.
Harris, T.J.C. and Peifer, M. 2005. The positioning and segregation of

apical cues during epithelial polarity establishment in Drosophila. *The Journal of Cell Biology* 170(5), pp. 813–823.
Harris, T.J.C. and Tepass, U. 2010. Adherens junctions: from molecules to morphogenesis. *Nature Reviews. Molecular Cell Biology* 11(7), pp. 502–514.
Hogan, C., Serpente, N., Cogram, P., Hosking, C.R., Bialucha, C.U., Feller, S.M., Braga, V.M.M., Birchmeier, W. and Fujita, Y. 2004. Rap1 regulates the formation of E-cadherin-based cell-cell contacts. *Molecular and Cellular Biology* 24(15), pp. 6690–6700.
Hong, Y., Ackerman, L., Jan, L.Y. and Jan, Y.-N. 2003. Distinct roles of Bazooka and Stardust in the specification of Drosophila photoreceptor membrane architecture. *Proceedings of the National Academy of Sciences of the United States of America* 100(22), pp. 12712–12717.
Hordijk, P.L., Klooster, J.P. ten, van der Kammen, R.A., Michiels, F., Oomen, L.C. and Collard, J.G. 1997. Inhibition of invasion of epithelial cells by Tiam1-Rac signaling. *Science (New York)* 278(5342), pp. 1464–1466.
Horne-Badovinac, S. and Bilder, D. 2008. Dynein regulates epithelial polarity and the apical localization of stardust A mRNA. *PLoS Genetics* 4(1), p. e8.
Hoshino, T., Sakisaka, T., Baba, T., Yamada, T., Kimura, T. and Takai, Y. 2005. Regulation of E-cadherin endocytosis by nectin through afadin, Rap1, and p120ctn. *The Journal of Biological Chemistry* 280(25), pp. 24095–24103.
Huang, R.Y.-J., Guilford, P. and Thiery, J.P. 2012. Early events in cell adhesion and polarity during epithelial-mesenchymal transition. *Journal of Cell Science* 125(Pt 19), pp. 4417–4422.
Huelsmann, S., Hepper, C., Marchese, D., Knöll, C. and Reuter, R. 2006. The PDZ-GEF dizzy regulates cell shape of migrating macrophages via Rap1 and integrins in the Drosophila embryo. *Development* 133(15), pp. 2915–2924.
Ireton, R.C., Davis, M.A., van Hengel, J., Mariner, D.J., Barnes, K., Thoreson, M.A., Anastasiadis, P.Z., Matrisian, L., Bundy, L.M., Sealy, L., Gilbert, B., van Roy, F. and Reynolds, A.B. 2002. A novel role for p120 catenin in E-cadherin function. *The Journal of Cell Biology* 159(3), pp. 465–476.
Ishimaru, S., Williams, R., Clark, E., Hanafusa, H. and Gaul, U. 1999. Activation of the Drosophila C3G leads to cell fate changes and overproliferation during development, mediated by the RAS-MAPK pathway and RAP1. *The EMBO Journal* 18(1), pp. 145–155.
Izaddoost, S., Nam, S.-C., Bhat, M.A., Bellen, H.J. and Choi, K.-W. 2002. Drosophila Crumbs is a positional cue in photoreceptor adherens junctions and rhabdomeres. *Nature* 416(6877), pp. 178–183.

Izumi, Y., Hirose, T., Tamai, Y., Hirai, S., Nagashima, Y., Fujimoto, T., Tabuse, Y., Kemphues, K.J. and Ohno, S. 1998. An atypical PKC directly associates and colocalizes at the epithelial tight junction with ASIP, a mammalian homologue of Caenorhabditis elegans polarity protein PAR-3. *The Journal of Cell Biology* 143(1), pp. 95–106.
Jacinto, A., Woolner, S. and Martin, P. 2002. Dynamic Analysis of Dorsal Closure in Drosophila. *Developmental Cell* 3(1), pp. 9–19.
Jaffe, A.B. and Hall, A. 2005. Rho GTPases: biochemistry and biology. *Annual Review of Cell and Developmental Biology* 21, pp. 247–269.
Jauffred, B. and Bellaiche, Y. 2012. Analyzing frizzled signaling using fixed and live imaging of the asymmetric cell division of the Drosophila sensory organ precursor cell. *Methods in Molecular Biology* 839, pp. 19–25.
Jolliffe, I.T. 2002. *Principal component analysis*. 2nd ed. New York: Springer.
Jones, B.W., Fetter, R.D., Tear, G. and Goodman, C.S. 1995. glial cells missing: a genetic switch that controls glial versus neuronal fate. *Cell* 82(6), pp. 1013–1023.
Kawabe, H., Neeb, A., Dimova, K., Young, S.M., Takeda, M., Katsurabayashi, S., Mitkovski, M., Malakhova, O.A., Zhang, D.-E., Umikawa, M., Kariya, K., Goebbels, S., Nave, K.-A., Rosenmund, C., Jahn, O., Rhee, J. and Brose, N. 2010. Regulation of Rap2A by the ubiquitin ligase Nedd4-1 controls neurite development. *Neuron* 65(3), pp. 358–372.
Kemphues, K.J., Priess, J.R., Morton, D.G. and Cheng, N.S. 1988. Identification of genes required for cytoplasmic localization in early C. elegans embryos. *Cell* 52(3), pp. 311–320.
Kitayama, H., Sugimoto, Y., Matsuzaki, T., Ikawa, Y. and Noda, M. 1989. A ras-related gene with transformation suppressor activity. *Cell* 56(1), pp. 77–84.
Knox, A.L. and Brown, N.H. 2002. Rap1 GTPase regulation of adherens junction positioning and cell adhesion. *Science (New York)* 295(5558), pp. 1285–1288.
Kolodziej, P.A., Timpe, L.C., Mitchell, K.J., Fried, S.R., Goodman, C.S., Jan, L.Y. and Jan, Y.N. 1996. frazzled encodes a Drosophila member of the DCC immunoglobulin subfamily and is required for CNS and motor axon guidance. *Cell* 87(2), pp. 197–204.
Krahn, M.P., Bückers, J., Kastrup, L. and Wodarz, A. 2010. Formation of a Bazooka-Stardust complex is essential for plasma membrane polarity in epithelia. *The Journal of Cell Biology* 190(5), pp. 751–760.
Krahn, M.P., Egger-Adam, D. and Wodarz, A. 2009. PP2A antagonizes phosphorylation of Bazooka by PAR-1 to control apical-basal polarity in dividing embryonic neuroblasts. *Developmental Cell* 16(6), pp. 901–908.

Krantz, D.E. and Zipursky, S.L. 1990. Drosophila chaoptin, a member of the leucine-rich repeat family, is a photoreceptor cell-specific adhesion molecule. *The EMBO Journal* 9(6), pp. 1969–1977.
Kurita, S., Yamada, T., Rikitsu, E., Ikeda, W. and Takai, Y. 2013. Binding between the junctional proteins afadin and PLEKHA7 and implication in the formation of adherens junction in epithelial cells. *The Journal of Biological Chemistry* 288(41), pp. 29356–29368.
Lamouille, S., Xu, J. and Derynck, R. 2014. Molecular mechanisms of epithelial-mesenchymal transition. *Nature Reviews. Molecular Cell Biology* 15(3), pp. 178–196.
Laprise, P., Lau, K.M., Harris, K.P., Silva-Gagliardi, N.F., Paul, S.M., Beronja, S., Beitel, G.J., McGlade, C.J. and Tepass, U. 2009. Yurt, Coracle, Neurexin IV and the Na(+),K(+)-ATPase form a novel group of epithelial polarity proteins. *Nature* 459(7250), pp. 1141–1145.
Leckband, D. and Sivasankar, S. 2000. Mechanism of homophilic cadherin adhesion. *Current Opinion in Cell Biology* 12(5), pp. 587–592.
Lee, J.H., Cho, K.S., Lee, J., Kim, D., Lee, S.-B., Yoo, J., Cha, G.-H. and Chung, J. 2002. Drosophila PDZ-GEF, a guanine nucleotide exchange factor for Rap1 GTPase, reveals a novel upstream regulatory mechanism in the mitogen-activated protein kinase signaling pathway. *Molecular and Cellular Biology* 22(21), pp. 7658–7666.
Lee, J.-Y. and Harland, R.M. 2010. Endocytosis is required for efficient apical constriction during Xenopus gastrulation. *Current Biology* 20(3), pp. 253–258.
Leibfried, A., Fricke, R., Morgan, M.J., Bogdan, S. and Bellaiche, Y. 2008. Drosophila Cip4 and WASp define a branch of the Cdc42-Par6-aPKC pathway regulating E-cadherin endocytosis. *Current Biology* 18(21), pp. 1639–1648.
Levayer, R., Pelissier-Monier, A. and Lecuit, T. 2011. Spatial regulation of Dia and Myosin-II by RhoGEF2 controls initiation of E-cadherin endocytosis during epithelial morphogenesis. *Nature Cell Biology* 13(5), pp. 529–540.
Lim, H.-Y. and Tomlinson, A. 2006. Organization of the peripheral fly eye: the roles of Snail family transcription factors in peripheral retinal apoptosis. *Development* 133(18), pp. 3529–3537.
Lin, D., Edwards, A.S., Fawcett, J.P., Mbamalu, G., Scott, J.D. and Pawson, T. 2000. A mammalian PAR-3-PAR-6 complex implicated in Cdc42/Rac1 and aPKC signalling and cell polarity. *Nature Cell Biology* 2(8), pp. 540–547.
Linnemann, T., Geyer, M., Jaitner, B.K., Block, C., Kalbitzer, H.R., Wittinghofer, A. and Herrmann, C. 1999. Thermodynamic and kinetic characterization of the interaction between the Ras binding domain of AF6 and members of the Ras subfamily. *The Journal of Biological*

Chemistry 274(19), pp. 13556–13562.
Longley, R.L. and Ready, D.F. 1995. Integrins and the development of three-dimensional structure in the Drosophila compound eye. *Developmental Biology* 171(2), pp. 415–433.
Luo, L., Liao, Y.J., Jan, L.Y. and Jan, Y.N. 1994. Distinct morphogenetic functions of similar small GTPases: Drosophila Drac1 is involved in axonal outgrowth and myoblast fusion. *Genes & Development* 8(15), pp. 1787–1802.
Mack, N.A. and Georgiou, M. 2014. The interdependence of the Rho GTPases and apicobasal cell polarity. *Small GTPases* 5(2), p. 10.
Malliri, A., van Es, S., Huveneers, S. and Collard, J.G. 2004. The Rac exchange factor Tiam1 is required for the establishment and maintenance of cadherin-based adhesions. *The Journal of Biological Chemistry* 279(29), pp. 30092–30098.
Manhire-Heath, R., Golenkina, S., Saint, R. and Murray, M.J. 2013. Netrin-dependent downregulation of Frazzled/DCC is required for the dissociation of the peripodial epithelium in Drosophila. *Nature Communications* 4, p. 2790.
Marston, A.L., Chen, T., Yang, M.C., Belhumeur, P. and Chant, J. 2001. A localized GTPase exchange factor, Bud5, determines the orientation of division axes in yeast. *Current Biology* 11(10), pp. 803–807.
McGill, M.A., McKinley, R.F.A. and Harris, T.J.C. 2009. Independent cadherin-catenin and Bazooka clusters interact to assemble adherens junctions. *The Journal of Cell Biology* 185(5), pp. 787–796.
McKinley, R.F.A. and Harris, T.J.C. 2012. Displacement of basolateral Bazooka/PAR-3 by regulated transport and dispersion during epithelial polarization in Drosophila. *Molecular Biology of the Cell* 23(22), pp. 4465–4471.
Meghana, C., Ramdas, N., Hameed, F.M., Rao, M., Shivashankar, G.V. and Narasimha, M. 2011. Integrin adhesion drives the emergent polarization of active cytoskeletal stresses to pattern cell delamination. *Proceedings of the National Academy of Sciences of the United States of America* 108(22), pp. 9107–9112.
Meng, W., Mushika, Y., Ichii, T. and Takeichi, M. 2008. Anchorage of microtubule minus ends to adherens junctions regulates epithelial cell-cell contacts. *Cell* 135(5), pp. 948–959.
Menzel, N., Melzer, J., Waschke, J., Lenz, C., Wecklein, H., Lochnit, G., Drenckhahn, D. and Raabe, T. 2008. The Drosophila p21-activated kinase Mbt modulates DE-cadherin-mediated cell adhesion by phosphorylation of Armadillo. *The Biochemical Journal* 416(2), pp. 231–241.
Menzel, N., Schneeberger, D. and Raabe, T. 2007. The Drosophila p21 activated kinase Mbt regulates the actin cytoskeleton and adherens

junctions to control photoreceptor cell morphogenesis. *Mechanisms of Development* 124(1), pp. 78–90.
Mével-Ninio, M., Terracol, R. and Kafatos, F.C. 1991. The ovo gene of Drosophila encodes a zinc finger protein required for female germ line development. *The EMBO Journal* 10(8), pp. 2259–2266.
Miles, W.O., Jaffray, E., Campbell, S.G., Takeda, S., Bayston, L.J., Basu, S.P., Li, M., Raftery, L.A., Ashe, M.P., Hay, R.T. and Ashe, H.L. 2008. Medea SUMOylation restricts the signaling range of the Dpp morphogen in the Drosophila embryo. *Genes & Development* 22(18), pp. 2578–2590.
Mochizuki, N., Yamashita, S., Kurokawa, K., Ohba, Y., Nagai, T., Miyawaki, A. and Matsuda, M. 2001. Spatio-temporal images of growth-factor-induced activation of Ras and Rap1. *Nature* 411(6841), pp. 1065–1068.
Mohr, S.E. and Perrimon, N. 2012. RNAi screening: new approaches, understandings, and organisms. *Wiley interdisciplinary reviews. RNA* 3(2), pp. 145–158.
Morais-de-Sá, E., Mirouse, V. and St Johnston, D. 2010. aPKC phosphorylation of Bazooka defines the apical/lateral border in Drosophila epithelial cells. *Cell* 141(3), pp. 509–523.
Müller, H.A. and Wieschaus, E. 1996. armadillo, bazooka, and stardust are critical for early stages in formation of the zonula adherens and maintenance of the polarized blastoderm epithelium in Drosophila. *The Journal of Cell Biology* 134(1), pp. 149–163.
Murray, M.J., Davidson, C.M., Hayward, N.M. and Brand, A.H. 2006. The Fes/Fer non-receptor tyrosine kinase cooperates with Src42A to regulate dorsal closure in Drosophila. *Development* 133(16), pp. 3063–3073.
Myster, S.H., Cavallo, R., Anderson, C.T., Fox, D.T. and Peifer, M. 2003. Drosophila p120catenin plays a supporting role in cell adhesion but is not an essential adherens junction component. *The Journal of Cell Biology* 160(3), pp. 433–449.
Nagafuchi, A. and Takeichi, M. 1988. Cell binding function of E-cadherin is regulated by the cytoplasmic domain. *The EMBO Journal* 7(12), pp. 3679–3684.
Nagai-Tamai, Y., Mizuno, K., Hirose, T., Suzuki, A. and Ohno, S. 2002. Regulated protein-protein interaction between aPKC and PAR-3 plays an essential role in the polarization of epithelial cells. *Genes To Cells* 7(11), pp. 1161–1171.
Nam, S.-C., Mukhopadhyay, B. and Choi, K.-W. 2007. Antagonistic functions of Par-1 kinase and protein phosphatase 2A are required for localization of Bazooka and photoreceptor morphogenesis in Drosophila. *Developmental Biology* 306(2), pp. 624–635.
Nelson, W.J., Dickinson, D.J. and Weis, W.I. 2013. Roles of cadherins

and catenins in cell-cell adhesion and epithelial cell polarity. *Progress in molecular biology and translational science* 116, pp. 3–23.
Neuman-Silberberg, F.S., Schejter, E., Hoffmann, F.M. and Shilo, B.Z. 1984. The Drosophila ras oncogenes: structure and nucleotide sequence. *Cell* 37(3), pp. 1027–1033.
Newsome, T.P., Asling, B. and Dickson, B.J. 2000. Analysis of Drosophila photoreceptor axon guidance in eye-specific mosaics. *Development* 127(4), pp. 851–860.
Niessen, C.M. and Gottardi, C.J. 2008. Molecular components of the adherens junction. *Biochimica et Biophysica Acta* 1778(3), pp. 562–571.
Nobes, C.D. and Hall, A. 1999. Rho GTPases control polarity, protrusion, and adhesion during cell movement. *The Journal of Cell Biology* 144(6), pp. 1235–1244.
Oda, H. and Tsukita, S. 2001. Real-time imaging of cell-cell adherens junctions reveals that Drosophila mesoderm invagination begins with two phases of apical constriction of cells. *Journal of Cell Science* 114(Pt 3), pp. 493–501.
Oda, H., Uemura, T., Harada, Y., Iwai, Y. and Takeichi, M. 1994. A Drosophila homolog of cadherin associated with armadillo and essential for embryonic cell-cell adhesion. *Developmental Biology* 165(2), pp. 716–726.
O'Keefe, D.D., Gonzalez-Niño, E., Burnett, M., Dylla, L., Lambeth, S.M., Licon, E., Amesoli, C., Edgar, B.A. and Curtiss, J. 2009. Rap1 maintains adhesion between cells to affect Egfr signaling and planar cell polarity in Drosophila. *Developmental Biology* 333(1), pp. 143–160.
Orsulic, S. and Peifer, M. 1996. An in vivo structure-function study of armadillo, the beta-catenin homologue, reveals both separate and overlapping regions of the protein required for cell adhesion and for wingless signaling. *The Journal of Cell Biology* 134(5), pp. 1283–1300.
Oyama, T., Kanai, Y., Ochiai, A., Akimoto, S., Oda, T., Yanagihara, K., Nagafuchi, A., Tsukita, S., Shibamoto, S. and Ito, F. 1994. A truncated beta-catenin disrupts the interaction between E-cadherin and alpha-catenin: a cause of loss of intercellular adhesiveness in human cancer cell lines. *Cancer Research* 54(23), pp. 6282–6287.
Ozawa, M., Baribault, H. and Kemler, R. 1989. The cytoplasmic domain of the cell adhesion molecule uvomorulin associates with three independent proteins structurally related in different species. *The EMBO Journal* 8(6), pp. 1711–1717.
Ozawa, M., Ringwald, M. and Kemler, R. 1990. Uvomorulin-catenin complex formation is regulated by a specific domain in the cytoplasmic region of the cell adhesion molecule. *Proceedings of the National Academy of Sciences of the United States of America* 87(11), pp. 4246–4250.

Pacquelet, A., Lin, L. and Rorth, P. 2003. Binding site for p120/delta-catenin is not required for Drosophila E-cadherin function in vivo. *The Journal of Cell Biology* 160(3), pp. 313–319.
Pappas, D.J. and Rimm, D.L. 2006. Direct interaction of the C-terminal domain of alpha-catenin and F-actin is necessary for stabilized cell-cell adhesion. *Cell communication & adhesion* 13(3), pp. 151–170.
Pellikka, M., Tanentzapf, G., Pinto, M., Smith, C., McGlade, C.J., Ready, D.F. and Tepass, U. 2002. Crumbs, the Drosophila homologue of human CRB1/RP12, is essential for photoreceptor morphogenesis. *Nature* 416(6877), pp. 143–149.
Petronczki, M. and Knoblich, J.A. 2001. DmPAR-6 directs epithelial polarity and asymmetric cell division of neuroblasts in Drosophila. *Nature Cell Biology* 3(1), pp. 43–49.
Pichaud, F. 2014. Transcriptional regulation of tissue organization and cell morphogenesis: the fly retina as a case study. *Developmental Biology* 385(2), pp. 168–178.
Pinheiro, E.M. and Montell, D.J. 2004. Requirement for Par-6 and Bazooka in Drosophila border cell migration. *Development* 131(21), pp. 5243–5251.
Pizon, V., Chardin, P., Lerosey, I., Olofsson, B. and Tavitian, A. 1988. Human cDNAs rap1 and rap2 homologous to the Drosophila gene Dras3 encode proteins closely related to ras in the “effector” region. *Oncogene* 3(2), pp. 201–204.
Plutoni, C., Bazellieres, E., Le Borgne-Rochet, M., Comunale, F., Brugues, A., Séveno, M., Planchon, D., Thuault, S., Morin, N., Bodin, S., Trepat, X. and Gauthier-Rouvière, C. 2016. P-cadherin promotes collective cell migration via a Cdc42-mediated increase in mechanical forces. *The Journal of Cell Biology* 212(2), pp. 199–217.
Pokutta, S., Drees, F., Takai, Y., Nelson, W.J. and Weis, W.I. 2002. Biochemical and structural definition of the l-afadin- and actin-binding sites of alpha-catenin. *The Journal of Biological Chemistry* 277(21), pp. 18868–18874.
Pokutta, S. and Weis, W.I. 2000. Structure of the Dimerization and β-Catenin- Binding Region of α-Catenin. *Molecular cell* 5(3), pp. 533–543.
Qin, Y., Capaldo, C., Gumbiner, B.M. and Macara, I.G. 2005. The mammalian Scribble polarity protein regulates epithelial cell adhesion and migration through E-cadherin. *The Journal of Cell Biology* 171(6), pp. 1061–1071.
Rapsomaniki, M.A., Kotsantis, P., Symeonidou, I.-E., Giakoumakis, N.-N., Taraviras, S. and Lygerou, Z. 2012. easyFRAP: an interactive, easy-to-use tool for qualitative and quantitative analysis of FRAP data. *Bioinformatics* 28(13), pp. 1800–1801.
Ready, D.F. 1989. A multifaceted approach to neural development.

Trends in Neurosciences 12(3), pp. 102–110.
Ready, D.F., Hanson, T.E. and Benzer, S. 1976. Development of the Drosophila retina, a neurocrystalline lattice. *Developmental Biology* 53(2), pp. 217–240.
Reuter, R. 1994. The gene serpent has homeotic properties and specifies endoderm versus ectoderm within the Drosophila gut. *Development* 120(5), pp. 1123–1135.
Reynolds, A.B., Daniel, J., McCrea, P.D., Wheelock, M.J., Wu, J. and Zhang, Z. 1994. Identification of a new catenin: the tyrosine kinase substrate p120cas associates with E-cadherin complexes. *Molecular and Cellular Biology* 14(12), pp. 8333–8342.
Rimm, D.L., Koslov, E.R., Kebriaei, P., Cianci, C.D. and Morrow, J.S. 1995. Alpha 1(E)-catenin is an actin-binding and -bundling protein mediating the attachment of F-actin to the membrane adhesion complex. *Proceedings of the National Academy of Sciences of the United States of America* 92(19), pp. 8813–8817.
Robbins, S.M., Khosla, M., Thiery, R., Weeks, G. and Spiegelman, G.B. 1991. Ras-related genes in Dictyostelium discoideum. *Developmental genetics* 12(1-2), pp. 147–153.
Robertson, F., Pinal, N., Fichelson, P. and Pichaud, F. 2012. Atonal and EGFR signalling orchestrate rok- and Drak-dependent adherens junction remodelling during ommatidia morphogenesis. *Development* 139(18), pp. 3432–3441.
Roegiers, F., Younger-Shepherd, S., Jan, L.Y. and Jan, Y.N. 2001. Bazooka is required for localization of determinants and controlling proliferation in the sensory organ precursor cell lineage in Drosophila. *Proceedings of the National Academy of Sciences of the United States of America* 98(25), pp. 14469–14474.
Rørth, P. 1996. A modular misexpression screen in Drosophila detecting tissue-specific phenotypes. *Proceedings of the National Academy of Sciences of the United States of America* 93(22), pp. 12418–12422.
Ruggieri, R., Bender, A., Matsui, Y., Powers, S., Takai, Y., Pringle, J. and Matsumoto, K. 1992. RSRJ, a ras-Like Gene Homologous to Krev-1 (smg21AIraplA): Role in the Development of Cell Polarity and Interactions with the Ras Pathway in Saccharomyces cerevisiae. *MOLECULAR AND CELLULAR BIOLOGY,*.
Ruohola, H., Bremer, K.A., Baker, D., Swedlow, J.R., Jan, L.Y. and Jan, Y.N. 1991. Role of neurogenic genes in establishment of follicle cell fate and oocyte polarity during oogenesis in Drosophila. *Cell* 66(3), pp. 433–449.
Sawyer, J.K., Choi, W., Jung, K.-C., He, L., Harris, N.J. and Peifer, M. 2011. A contractile actomyosin network linked to adherens junctions by Canoe/afadin helps drive convergent extension. *Molecular Biology of the*

Cell 22(14), pp. 2491–2508.
Sawyer, J.K., Harris, N.J., Slep, K.C., Gaul, U. and Peifer, M. 2009. The Drosophila afadin homologue Canoe regulates linkage of the actin cytoskeleton to adherens junctions during apical constriction. *The Journal of Cell Biology* 186(1), pp. 57–73.
Schindelin, J., Arganda-Carreras, I., Frise, E., Kaynig, V., Longair, M., Pietzsch, T., Preibisch, S., Rueden, C., Saalfeld, S., Schmid, B., Tinevez, J.-Y., White, D.J., Hartenstein, V., Eliceiri, K., Tomancak, P. and Cardona, A. 2012. Fiji: an open-source platform for biological-image analysis. *Nature Methods* 9(7), pp. 676–682.
Schneeberger, D. and Raabe, T. 2003. Mbt, a Drosophila PAK protein, combines with Cdc42 to regulate photoreceptor cell morphogenesis. *Development* 130(3), pp. 427–437.
Schwamborn, J.C. and Püschel, A.W. 2004. The sequential activity of the GTPases Rap1B and Cdc42 determines neuronal polarity. *Nature Neuroscience* 7(9), pp. 923–929.
Severson, E.A., Lee, W.Y., Capaldo, C.T., Nusrat, A. and Parkos, C.A. 2009. Junctional adhesion molecule A interacts with Afadin and PDZ-GEF2 to activate Rap1A, regulate beta1 integrin levels, and enhance cell migration. *Molecular Biology of the Cell* 20(7), pp. 1916–1925.
Shao, W., Wu, J., Chen, J., Lee, D.M., Tishkina, A. and Harris, T.J.C. 2010. A modifier screen for Bazooka/PAR-3 interacting genes in the Drosophila embryo epithelium. *Plos One* 5(4), p. e9938.
Shibamoto, S., Hayakawa, M., Takeuchi, K., Hori, T., Miyazawa, K., Kitamura, N., Johnson, K.R., Wheelock, M.J., Matsuyoshi, N. and Takeichi, M. 1995. Association of p120, a tyrosine kinase substrate, with E-cadherin/catenin complexes. *The Journal of Cell Biology* 128(5), pp. 949–957.
Smallhorn, M., Murray, M.J. and Saint, R. 2004. The epithelial-mesenchymal transition of the Drosophila mesoderm requires the Rho GTP exchange factor Pebble. *Development* 131(11), pp. 2641–2651.
Snow, P.M., Bieber, A.J. and Goodman, C.S. 1989. Fasciclin III: a novel homophilic adhesion molecule in Drosophila. *Cell* 59(2), pp. 313–323.
Spahn, P., Ott, A. and Reuter, R. 2012. The PDZ-GEF protein Dizzy regulates the establishment of adherens junctions required for ventral furrow formation in Drosophila. *Journal of Cell Science* 125(Pt 16), pp. 3801–3812.
Spindler, S.R. and Hartenstein, V. 2011. Bazooka mediates secondary axon morphology in Drosophila brain lineages. *Neural Development* 6, p. 16.
Szafranski, P. and Goode, S. 2004. A Fasciclin 2 morphogenetic switch organizes epithelial cell cluster polarity and motility. *Development* 131(9), pp. 2023–2036.

Tachibana, K., Nakanishi, H., Mandai, K., Ozaki, K., Ikeda, W., Yamamoto, Y., Nagafuchi, A., Tsukita, S. and Takai, Y. 2000. Two cell adhesion molecules, nectin and cadherin, interact through their cytoplasmic domain-associated proteins. *The Journal of Cell Biology* 150(5), pp. 1161–1176.
Takahashi, K., Matsuo, T., Katsube, T., Ueda, R. and Yamamoto, D. 1998. Direct binding between two PDZ domain proteins Canoe and ZO-1 and their roles in regulation of the Jun N-terminal kinase pathway in Drosophila morphogenesis. *Mechanisms of Development* 78(1-2), pp. 97–111.
Takahashi, K., Nakanishi, H., Miyahara, M., Mandai, K., Satoh, K., Satoh, A., Nishioka, H., Aoki, J., Nomoto, A., Mizoguchi, A. and Takai, Y. 1999. Nectin/PRR: an immunoglobulin-like cell adhesion molecule recruited to cadherin-based adherens junctions through interaction with Afadin, a PDZ domain-containing protein. *The Journal of Cell Biology* 145(3), pp. 539–549.
Tanaka-Okamoto, M., Itoh, Y., Miyoshi, J., Mizoguchi, A., Mizutani, K., Takai, Y. and Inoue, M. 2014. Genetic ablation of afadin causes mislocalization and deformation of Paneth cells in the mouse small intestinal epithelium. *Plos One* 9(10), p. e110549.
Tepass, U. 2012. The apical polarity protein network in Drosophila epithelial cells: regulation of polarity, junctions, morphogenesis, cell growth, and survival. *Annual Review of Cell and Developmental Biology* 28, pp. 655–685.
Tepass, U. and Harris, K.P. 2007. Adherens junctions in Drosophila retinal morphogenesis. *Trends in Cell Biology* 17(1), pp. 26–35.
Tepass, U. and Hartenstein, V. 1994a. Epithelium formation in the Drosophila midgut depends on the interaction of endoderm and mesoderm. *Development* 120(3), pp. 579–590.
Tepass, U. and Hartenstein, V. 1994b. The development of cellular junctions in the Drosophila embryo. *Developmental Biology* 161(2), pp. 563–596.
Tepass, U., Tanentzapf, G., Ward, R. and Fehon, R. 2001. Epithelial cell polarity and cell junctions in Drosophila. *Annual Review of Genetics* 35, pp. 747–784.
Tepass, U., Theres, C. and Knust, E. 1990. crumbs encodes an EGF-like protein expressed on apical membranes of Drosophila epithelial cells and required for organization of epithelia. *Cell* 61(5), pp. 787–799.
Thompson, B.J., Pichaud, F. and Röper, K. 2013. Sticking together the Crumbs - an unexpected function for an old friend. *Nature Reviews. Molecular Cell Biology* 14(5), pp. 307–314.
Tian, Y., Lei, L. and Minden, A. 2011. A key role for Pak4 in proliferation and differentiation of neural progenitor cells. *Developmental*

Biology 353(2), pp. 206–216.
Toret, C.P., Ambrosio, M.V. D', Vale, R.D., Simon, M.A. and Nelson, W.J. 2014. A genome-wide screen identifies conserved protein hubs required for cadherin-mediated cell-cell adhesion. *The Journal of Cell Biology* 204(2), pp. 265–279.
Vaccari, T., Rabouille, C. and Ephrussi, A. 2005. The Drosophila PAR-1 spacer domain is required for lateral membrane association and for polarization of follicular epithelial cells. *Current Biology* 15(3), pp. 255–261.
Vogler, G., Liu, J., Iafe, T.W., Migh, E., Mihály, J. and Bodmer, R. 2014. Cdc42 and formin activity control non-muscle myosin dynamics during Drosophila heart morphogenesis. *The Journal of Cell Biology* 206(7), pp. 909–922.
Wallace, S.W., Durgan, J., Jin, D. and Hall, A. 2010. Cdc42 regulates apical junction formation in human bronchial epithelial cells through PAK4 and Par6B. *Molecular Biology of the Cell* 21(17), pp. 2996–3006.
Walther, R.F., Nunes de Almeida, F., Vlassaks, E., Burden, J.J. and Pichaud, F. 2016. Pak4 Is Required during Epithelial Polarity Remodeling through Regulating AJ Stability and Bazooka Retention at the ZA. *Cell reports* 15(1), pp. 45–53.
Walther, R.F. and Pichaud, F. 2010. Crumbs/DaPKC-dependent apical exclusion of Bazooka promotes photoreceptor polarity remodeling. *Current Biology* 20(12), pp. 1065–1074.
Walther, R.F. and Pichaud, F. 2006. Immunofluorescent staining and imaging of the pupal and adult Drosophila visual system. *Nature Protocols* 1(6), pp. 2635–2642.
Wang, Y.-C., Khan, Z. and Wieschaus, E.F. 2013. Distinct Rap1 activity states control the extent of epithelial invagination via α-catenin. *Developmental Cell* 25(3), pp. 299–309.
Warner, S.J., Yashiro, H. and Longmore, G.D. 2010. The Cdc42/Par6/aPKC polarity complex regulates apoptosis-induced compensatory proliferation in epithelia. *Current Biology* 20(8), pp. 677–686.
Wee, B., Johnston, C.A., Prehoda, K.E. and Doe, C.Q. 2011. Canoe binds RanGTP to promote Pins(TPR)/Mud-mediated spindle orientation. *The Journal of Cell Biology* 195(3), pp. 369–376.
Wei, S.-Y., Escudero, L.M., Yu, F., Chang, L.-H., Chen, L.-Y., Ho, Y.-H., Lin, C.-M., Chou, C.-S., Chia, W., Modolell, J. and Hsu, J.-C. 2005. Echinoid is a component of adherens junctions that cooperates with DE-Cadherin to mediate cell adhesion. *Developmental Cell* 8(4), pp. 493–504.
Wolf, A.M., Lyuksyutova, A.I., Fenstermaker, A.G., Shafer, B., Lo, C.G. and Zou, Y. 2008. Phosphatidylinositol-3-kinase-atypical protein kinase

C signaling is required for Wnt attraction and anterior-posterior axon guidance. *The Journal of Neuroscience* 28(13), pp. 3456–3467.
Wolff and Ready, T.D.F. 1993. *Pattern formation in the Drosophila retina. In: The Development of Drosophila melanogaster*. 2nd ed. Cold Spring Harbor Laboratory Press.
Wolff, T. and Ready, D.F. 1991. Cell death in normal and rough eye mutants of Drosophila. *Development* 113(3), pp. 825–839.
Wolff, T. and Rubin, G.M. 1998. Strabismus, a novel gene that regulates tissue polarity and cell fate decisions in Drosophila. *Development* 125(6), pp. 1149–1159.
Woods, D.F., Hough, C., Peel, D., Callaini, G. and Bryant, P.J. 1996. Dlg protein is required for junction structure, cell polarity, and proliferation control in Drosophila epithelia. *The Journal of Cell Biology* 134(6), pp. 1469–1482.
Woods, D.F., Wu, J.W. and Bryant, P.J. 1997. Localization of proteins to the apico-lateral junctions of Drosophila epithelia. *Developmental genetics* 20(2), pp. 111–118.
Xu, G., Craig, A.W.B., Greer, P., Miller, M., Anastasiadis, P.Z., Lilien, J. and Balsamo, J. 2004. Continuous association of cadherin with beta-catenin requires the non-receptor tyrosine-kinase Fer. *Journal of Cell Science* 117(Pt 15), pp. 3207–3219.
Xu, T. and Rubin, G.M. 1993. Analysis of genetic mosaics in developing and adult Drosophila tissues. *Development* 117(4), pp. 1223–1237.
Yamada, S., Pokutta, S., Drees, F., Weis, W.I. and Nelson, W.J. 2005. Deconstructing the cadherin-catenin-actin complex. *Cell* 123(5), pp. 889–901.
Yang, D.-S., Roh, S. and Jeong, S. 2016. The axon guidance function of Rap1 small GTPase is independent of PlexA RasGAP activity in Drosophila. *Developmental Biology* 418(2), pp. 258–267.
Zelhof, A.C., Hardy, R.W., Becker, A. and Zuker, C.S. 2006. Transforming the architecture of compound eyes. *Nature* 443(7112), pp. 696–699.